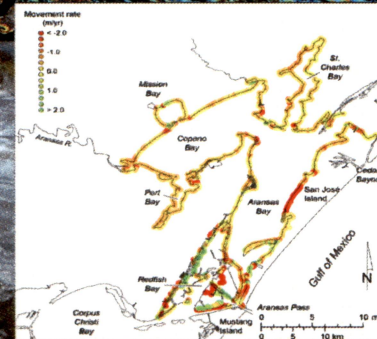
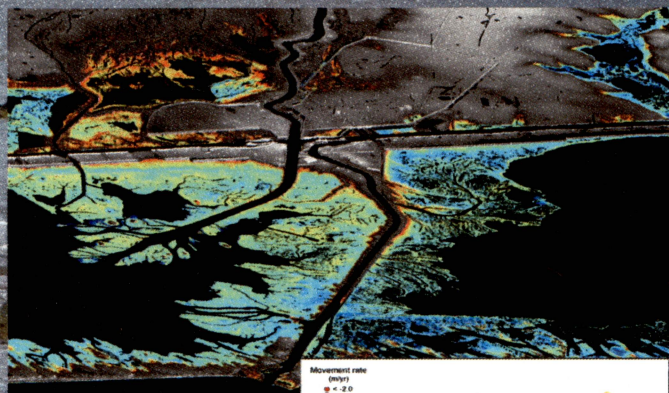


Shoreline Movement in the Copano, San Antonio, and Matagorda Bay Systems, Central Texas Coast, 1930s TO 2010s

Jeffrey G. Paine, Tiffany Caudle, and John Andrews,
with contributions from Aaron Averett, John Hupp, Lucie Costard, and Kutalmis Saylam



Final Report

October 2016

Bureau of Economic Geology

Scott W. Tinker, Director
Jackson School of Geosciences
The University of Texas at Austin
Austin, Texas 78713-8924

A report funded in part by a Financial Assistance Award from the U. S. Department of the Interior, U. S. Fish and Wildlife Service, Coastal Impact Assistance Program. The views expressed herein are those of the authors and do not necessarily reflect the views of the U. S. Fish and Wildlife Service.

Final Report Prepared for the General Land Office under Contract No. 13-258-000-7485.



BUREAU OF
ECONOMIC
GEOLOGY



Page intentionally blank

SHORELINE MOVEMENT IN THE COPANO, SAN ANTONIO, AND
MATAGORDA BAY SYSTEMS, CENTRAL TEXAS COAST, 1930s TO 2010s

by

Jeffrey G. Paine, Tiffany Caudle, and John Andrews
Bureau of Economic Geology
John A. and Katherine G. Jackson School of Geosciences
The University of Texas at Austin
University Station, Box X
Austin, Texas 78713

with contributions from Aaron Averett, Lucie Costard, John Hupp, and Kutalmis Saylam

Corresponding author
jeff.paine@beg.utexas.edu
(512) 471-1260

A report funded in part by a Financial Assistance Award from the U. S. Department of the Interior, U. S. Fish and Wildlife Service, Coastal Impact Assistance Program. The views expressed herein are those of the authors and do not necessarily reflect the views of the U. S. Fish and Wildlife Service.

Final Report Prepared for the General Land Office under Contract No. 13-258-000-7485.

October 31, 2016



JACKSON
SCHOOL OF GEOSCIENCES

Page intentionally blank

CONTENTS

Summary	ix
Introduction	1
Methods	4
Lidar Data Acquisition	4
San Antonio Bay System	5
Copano Bay System	7
Matagorda Bay System	7
Lidar Data Processing	10
Historical Shoreline Mapping	11
Lidar Shoreline Extraction	13
Determining Rates of Shoreline Movement	14
Shoreline Types	15
High and Low Bluffs	17
Sandy Slopes	19
Fan Deltas	24
Spits and Beaches	25
Tidal Passes	25
Flood-tidal Deltas	27
Deltaic Marshes	28
Back-barrier Marshes or Tidal Flats	30
Bay-margin Marshes or Tidal Flats	30
Modified and Protected Shorelines	31
Bay Shoreline Movement on the Central Texas Coast	31
Long-term Shoreline Movement in All Bays, 1930s to 2010s	34
Recent Shoreline Movement in All Bays, 1950s/74/82 to 2010s	34
Shoreline Movement in the Copano Bay System	34
Long-term Shoreline Movement in the Copano Bay System, 1930s to 2014	36
Recent Shoreline Movement in the Copano Bay System, 1982 to 2014	39
Shoreline Movement in the San Antonio Bay System	43
Long-term Shoreline Movement in the San Antonio Bay System, 1930s to 2013	44

Recent Shoreline Movement in the San Antonio Bay System, 1982 to 2013	49
Shoreline Movement in the Matagorda Bay System	49
Long-term Shoreline Movement in the Matagorda Bay System, 1930s to 2015.	51
Recent Shoreline Movement in the Matagorda Bay System, 1950s to 2015.	55
Shoreline Movement by Shoreline Type	57
Long-term Shoreline Movement by Shoreline Type	58
Short-term Shoreline Movement by Shoreline Type	58
Shoreline Classification by Erosion Susceptibility	61
Conclusions	65
Acknowledgments	66
References	66
APPENDIX A: DATA SOURCES	69
APPENDIX B: LIDAR DATA AND GIS FILES	71

FIGURES

1. Map showing the principal Quaternary geologic units on the Texas Coastal Plain and the location of the Copano, San Antonio, and Matagorda Bay study area	2
2. Boundaries of the Copano Bay, San Antonio Bay, and Matagorda Bay systems	3
3. Chiroptera system and the system mounted in a fixed-wing aircraft.	5
4. San Antonio Bay system airborne lidar survey coverage blocks.	6
5. Copano Bay system airborne lidar survey coverage blocks	8
6. Matagorda Bay system airborne lidar survey coverage blocks	9
7. Extracted 0.29- and 0.37-m elevation contours representing shoreline position.	15
8. Extracted 0.29- and 0.37-m elevation contours northwest of the Guadalupe delta	16
9. Distribution of principal shoreline types in the Copano, San Antonio, and Matagorda Bay systems	17
10. Total length and proportion of common shoreline types	19
11. Photographs of (a) high Pleistocene sandy clay bluff, (b) low Pleistocene sandy	

clay bluff, and (c) sandy slope	20
12. Distribution of principal shoreline types in the Copano Bay system.	21
13. Distribution of principal shoreline types in the San Antonio Bay system.	22
14. Distribution of principal shoreline types in the Matagorda Bay system	23
15. Aerial photograph of a fan delta on the northwestern shore of Lavaca Bay	24
16. Photographs of (a) sandy and shelly beach, and (b) sandy and shelly spit	26
17. Aerial photograph of the flood-tidal delta and tidal-pass shorelines	27
18. Photographs of (a) back-barrier marsh and tidal flat, (b) bay-margin marsh and tidal flat, and (c) deltaic marsh.	29
19. Photographs of shorelines protected by (a) low seawall, (b) riprap and a low concrete bulkhead, and (c) a low bulkhead and vegetation	32
20. Net long-term and more recent shoreline movement rates in the Copano, San Antonio, and Matagorda Bay systems	33
21. Distribution of longer-term and more recent shoreline movement rates in central Texas bay systems	36
22. Net long-term shoreline movement rates in the Copano Bay system	38
23. Distribution of longer-term and more recent shoreline movement rates in Aransas Bay, Copano Bay, and St. Charles Bay	40
24. Digital elevation model (DEM) perspective of Mission Bay	41
25. Representative profiles from bluff and marsh shorelines around Mission Bay and northern Copano Bay	42
26. Net recent shoreline movement rates in the Copano Bay system, 1982 to 2014.	43
27. Net long-term shoreline movement rates in the San Antonio Bay system, 1930s to 2013.	45
28. Distribution of longer-term and more recent shoreline movement rates in Mesquite Bay, San Antonio Bay, and Espiritu Santo Bay	46
29. Perspective view of a lidar-derived DEM of the southwestern shoreline of San Antonio Bay	47
30. Representative profiles across shoreline types along the southwestern shoreline of San Antonio Bay	48
31. Net recent shoreline movement rates in the San Antonio Bay system, 1982 to 2013	50
32. Net long-term shoreline movement rates in the Matagorda Bay system, 1930s to 2015 .52	52

33. Distribution of longer-term and more recent shoreline movement rates in Matagorda Bay, Lavaca Bay, and East Matagorda Bay.	53
34. Shoreline position in the 1930s and in 2015 at the Colorado River delta	54
35. Net recent shoreline movement rates in the Matagorda Bay system, 1950s to 2015	56
36. Average (a) long-term and (b) more recent net shoreline movement rates for common bay shoreline types.	59
37. Average (a) long-term and (b) more recent area change rate for common bay shoreline types	60
38. Shoreline types classified by susceptibility to retreat associated with relative sea-level rise.	62
39. Shoreline types classified by susceptibility to erosion associated with storm surge and storm wave action	63
40. Shoreline types classified by susceptibility to retreat associated with wave action	64

TABLES

1. Airborne topographic lidar survey parameters, Matagorda Bay system	9
2. Average water level and mean higher high water (MHHW) level	13
3. Common bay shoreline types and their environmental, elevation, slope, and material characteristics	18
4. Common bay shoreline types and their relative susceptibility to relative sea-level rise, storm surge and waves, and non-storm wave action	23
5. Long-term (1930s to 2010s) shoreline movement statistics in the Copano, San Antonio, and Matagorda Bay systems, central Texas coast	35
6. Recent (1950s, 1974, or 1982 to 2010s) shoreline movement statistics in the Copano, San Antonio, and Matagorda Bay systems	37

SUMMARY

Shoreline position and morphology extracted from airborne lidar surveys acquired over the Copano, San Antonio, and Matagorda Bay systems between 2013 and 2015 were used to (1) classify 1,065 km of bay shoreline into 11 common shoreline types, and (2) compare shoreline positions extracted from lidar survey data with previous shoreline positions determined from aerial photographs from the 1930s, 1950s, and 1982 to determine shoreline-movement and land-loss rates for a long-term (1930s to 2010s) and more recent (1950s or 1982 to 2010s) period. From higher to lower elevation adjacent to the shoreline, the common shoreline types are high and low Pleistocene clayey sand and sandy clay bluffs, Pleistocene sandy slopes, fan deltas, sandy and shelly beaches and spits, tidal passes, flood-tidal delta marshes and tidal flats, deltaic marshes, and back-barrier and bay-margin marshes and tidal flats. The lower-elevation shoreline types (back-barrier and bay-margin marsh and tidal flats) are the most common shoreline types in the three bay systems, together constituting about 50 percent of the total shoreline length.

Shoreline movement was dominantly erosional over both the long-term and more recent periods, with 80 percent of the nearly 10,000 measurement sites retreating between the 1930s and 2010s and 82 percent retreating during the more recent period. Despite the preponderance of sites undergoing shoreline retreat, the net shoreline movement rate for the long-term period was nearly zero because ubiquitous erosion in the Copano, San Antonio, and Matagorda Bay systems was offset by delta progradation across eastern Matagorda Bay when a river logjam on the Colorado River was removed in 1929. During the more recent period, net shoreline retreat averaged -0.60 m/yr for all bay systems, translating to an average land-loss rate of 63.5 ha/yr. Average shoreline retreat rates were highest in Matagorda Bay at -0.64 m/yr, followed by Copano Bay retreat rates at -0.62 m/yr and San Antonio Bay retreat rates at -0.49 m/yr. Shoreline types experiencing the highest rates of retreat between the 1930s and 2010s were the tidal pass (-0.79 m/yr), sandy and shelly spit (-0.72 m/yr), and high bluff (-0.54 m/yr) shorelines. During the more recent period, shoreline retreat rates increased for all shoreline types. Shorelines

retreated most rapidly along tidal passes (-1.67 m/yr), high bluffs (-0.86 m/yr), and spits (-0.84 m/yr) during the most recent period.

Shoreline type properties were used to assess the erosion susceptibility of each type to relative sea-level rise, storm surge and storm-wave action, and normal wave action according to a low-, moderate-, and high-susceptibility scale. Shorelines along most low-elevation shores, including deltaic marshes and back-barrier and bay-margin marshes and tidal flats, are highly susceptible to relative sea-level rise and non-storm wave action, but generally less susceptible to storm surge and waves. Like other low-elevation shoreline types, shorelines along tidal passes and flood-tidal deltas are highly susceptible to retreat caused by relative-sea-level rise and non-storm waves, but are also highly susceptible to retreat caused by flood and ebb currents associated with storm surge. Slightly higher fan delta, beach, and spit shores are highly susceptible to shoreline retreat caused by non-storm wave action and are moderately susceptible to shoreline retreat related to relative sea-level rise and storm surge and waves. Shorelines that front high and low Pleistocene bluffs and sandy slopes are highly susceptible to retreat caused by storm waves elevated by storm surge during tropical cyclone passage and are moderately susceptible to retreat caused by normal wave action, but are relatively insensitive to relative sea-level rise.

INTRODUCTION

Texas coastal shorelines include bay, lagoon, and Gulf of Mexico frontage along geomorphic features such as unconsolidated sandy barrier islands and peninsulas, semiconsolidated muddy marshes and tidal flats, consolidated clayey and sandy bluffs, and sandy and shelly beaches and spits. Common coastal processes such as wind-driven waves, storm surge and storm waves, and relative sea-level rise contribute to the dynamic nature of these coastal boundaries, leading to shoreline advance or retreat through addition or removal of sediment or by submergence and emergence. Because the Texas coastal zone is home to millions of people in urban and rural settings, significant industrial infrastructure, an economically important coastal fishery, and critical habitat for numerous endangered and other critical species, it is important to monitor the movement of these coastal boundaries, determine coastal land loss and gain, and characterize shoreline movement and its potential impact on the varied activities, uses, and functions of coastal land, vegetation, and habitat.

We conducted airborne lidar surveys along the margins of three major bay systems on the central Texas coast: the Copano Bay system, the San Antonio Bay system, and the Matagorda Bay system (figs. 1 and 2). Each bay system includes several smaller bays that were also flown using the airborne lidar system. The purpose of the surveys was to examine detailed bay-margin morphology, identify shoreline types, and determine shoreline position by extracting a common elevation contour that would serve as a shoreline proxy from the digital elevation models (DEMs) produced from the lidar point-cloud data. The San Antonio Bay system was flown in 2013, the Copano Bay system was flown in 2014, and the Matagorda Bay system was flown in 2015. A supplemental survey of the western shore of Matagorda Bay was flown in July 2016 to assess possible effects of Tropical Storm Bill, a tropical cyclone that crossed the central Texas coast in June 2015 (Berg, 2015). Bill was the only tropical cyclone to make landfall in Texas during the 2013 to 2016 study period. We then compared past shoreline positions previously mapped by the Bureau of Economic Geology (BEG) on historical aerial photographs with the

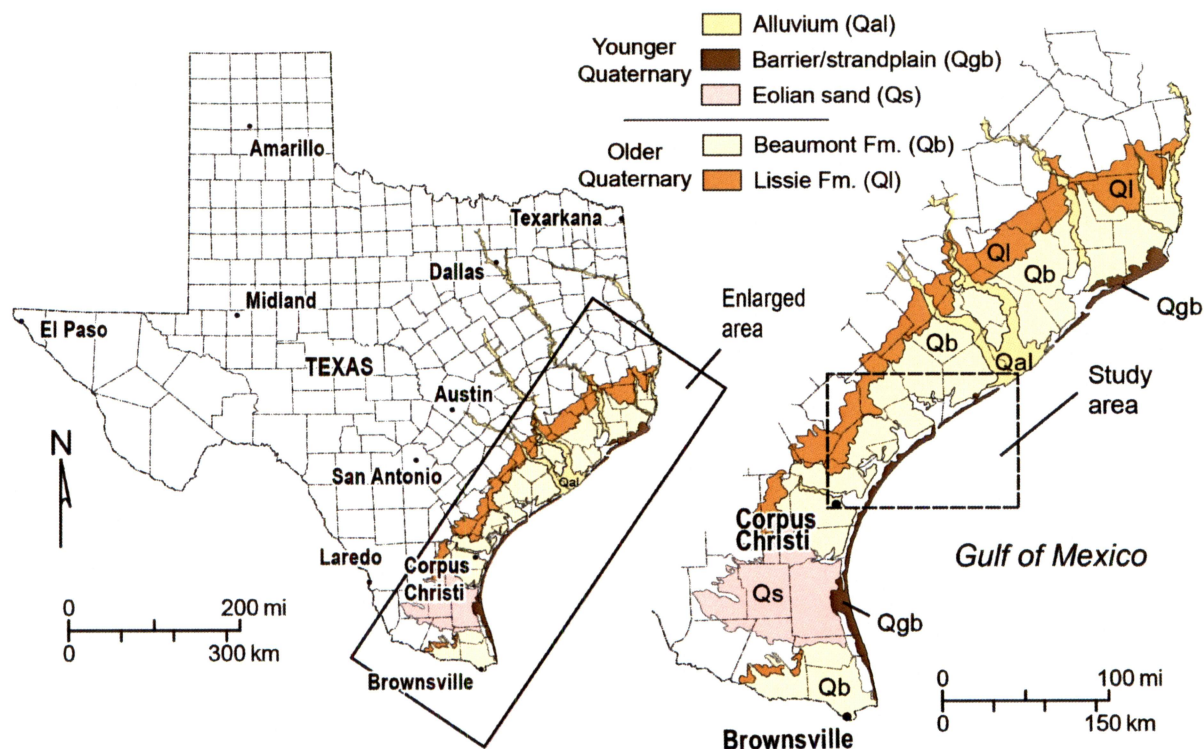


Figure 1. Map showing the principal Quaternary geologic units on the Texas Coastal Plain and the location of the Copano, San Antonio, and Matagorda Bay study area (fig. 2). Map adapted from Bureau of Economic Geology (1992).

shoreline position extracted from the DEMs constructed from the 2013 to 2015 airborne lidar survey data. We determined both a longer-term net movement rate by comparing shoreline positions from the 1930s with those from the lidar surveys, and a more recent net shoreline movement rate by comparing shoreline positions from 1982 (1950s or 1974 in some cases) to those from the lidar survey.

The BEG has conducted several previous studies of historical shoreline movement in Texas bays. These studies have been published in a series of BEG reports and other articles that include the Gulf and bay shorelines of the Matagorda Bay system (McGowen and Brewton, 1975) and the bay shorelines of the Corpus Christi Bay system (Morton and Paine, 1984), the Galveston Bay system (Paine and Morton, 1986, 1991), the San Antonio Bay system (White and Morton, 1987), and the Copano Bay system (Paine and Morton, 1993). These publications focus on historical

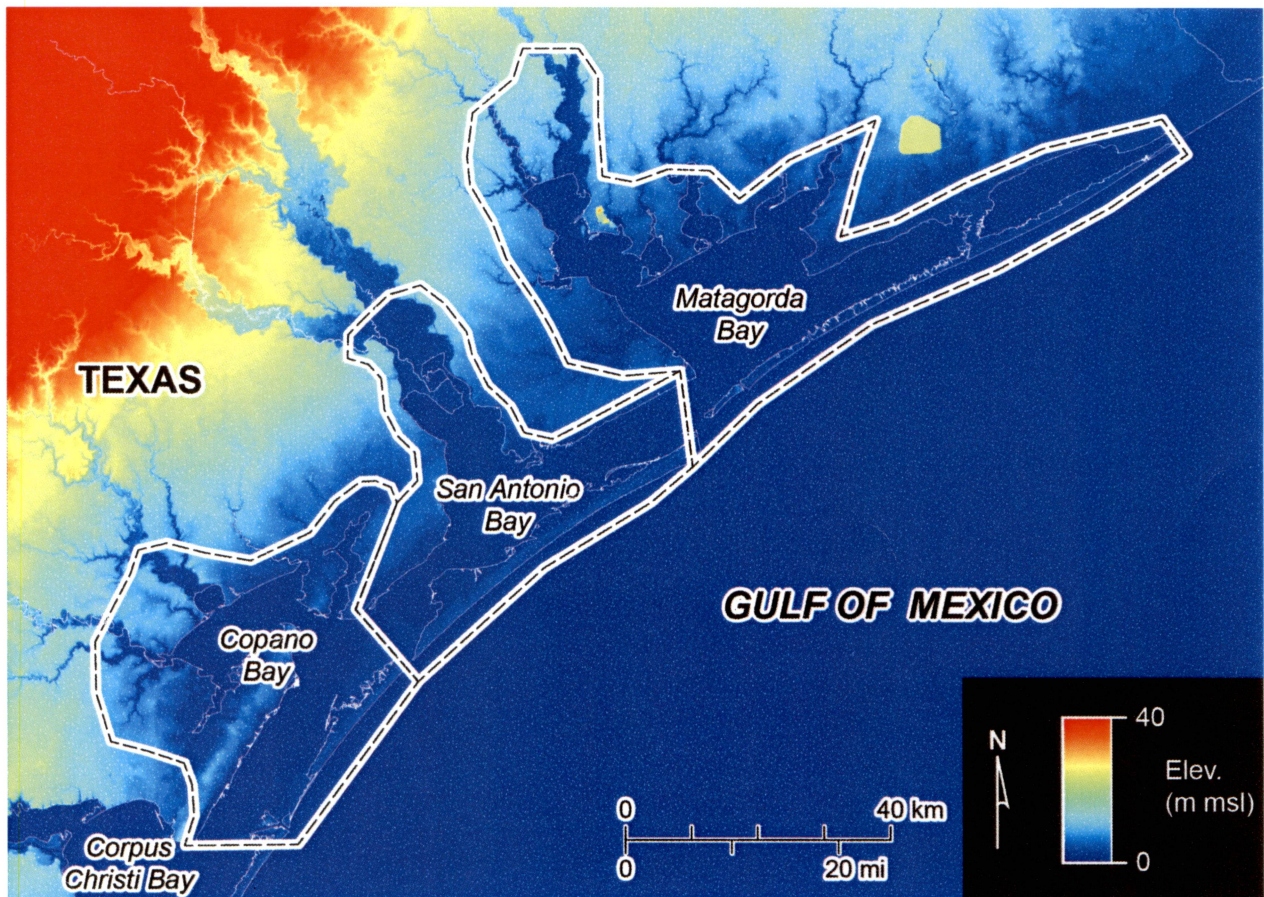


Figure 2. Boundaries of the Copano Bay, San Antonio Bay, and Matagorda Bay systems superimposed on a topographic map of the central Texas coast. Regional topographic data from the U. S. Geological Survey.

shoreline movement determined from mid- to late-1800s topographic charts produced by the U.S. Coast Survey and shoreline position mapped on 1:24, 000-scale aerial photographs taken in the 1930s, 1950s, and 1982 (except for the Matagorda Bay study, which was published before 1982 and used the 1950s photographs as the most recent shoreline). In addition to the data on historical shoreline movement, each of the previous publications contains detailed discussions of the geologic character of the bay systems and the coastal processes that influence shoreline movement, including sediment supply, wave action, tropical cyclones, and relative sea-level.

The shoreline positions determined for the previous Copano, San Antonio, and Matagorda Bay system studies were digitized and georeferenced in this study for use in determining long-term

and more recent shoreline movement between the 1930s and the 2013 to 2015 airborne lidar surveys.

METHODS

We used previously determined shoreline positions from BEG studies of historical shoreline change in the Copano, San Antonio, and Matagorda Bay systems that were based on aerial photographic interpretation and compared those positions with recent shoreline positions extracted from 2013, 2014, and 2015 airborne lidar surveys of the bay systems conducted as part of this project. These shorelines were used to determine long-term (1930s to 2010s) and more recent (1950s or 1982 to 2010s) shoreline change rates for the three major bay systems on the central Texas coast.

Lidar Data Acquisition

BEG researchers acquired lidar data from three Central Texas bay systems between 2013 and 2015. Data were collected using the Chiroptera airborne system (fig. 3) from Airborne Hydrography AB, which collects topographic lidar data, shallow bathymetric lidar data, and natural color or color infrared imagery. The topographic lidar scanner operates at a wavelength of 1 μm , a pulse rate as high as 400 kHz, and an incident angle (from vertical) of 28 to 40 degrees. It can operate to a maximum height of about 1,500 m, allowing the system to be used to rapidly scan large areas with a range accuracy of about 2 cm over a flat target. The bathymetric lidar scanner, used only incidentally in this project, operates at a shorter wavelength (0.515 μm) and a lower pulse rate (36 kHz). The shorter wavelength allows the laser to penetrate water of reasonable clarity to determine water depths. Also mounted in the Chiroptera is a Hasselblad DigiCAM 50 megapixel natural-color (RGB) or color-infrared camera that acquires frame images at a resolution of 8,176 by 6,132 pixels.

Acquisition of topographic lidar data along bay shorelines was a principal objective of this project. Aerial imagery was acquired for reference purposes. Bathymetric lidar data were

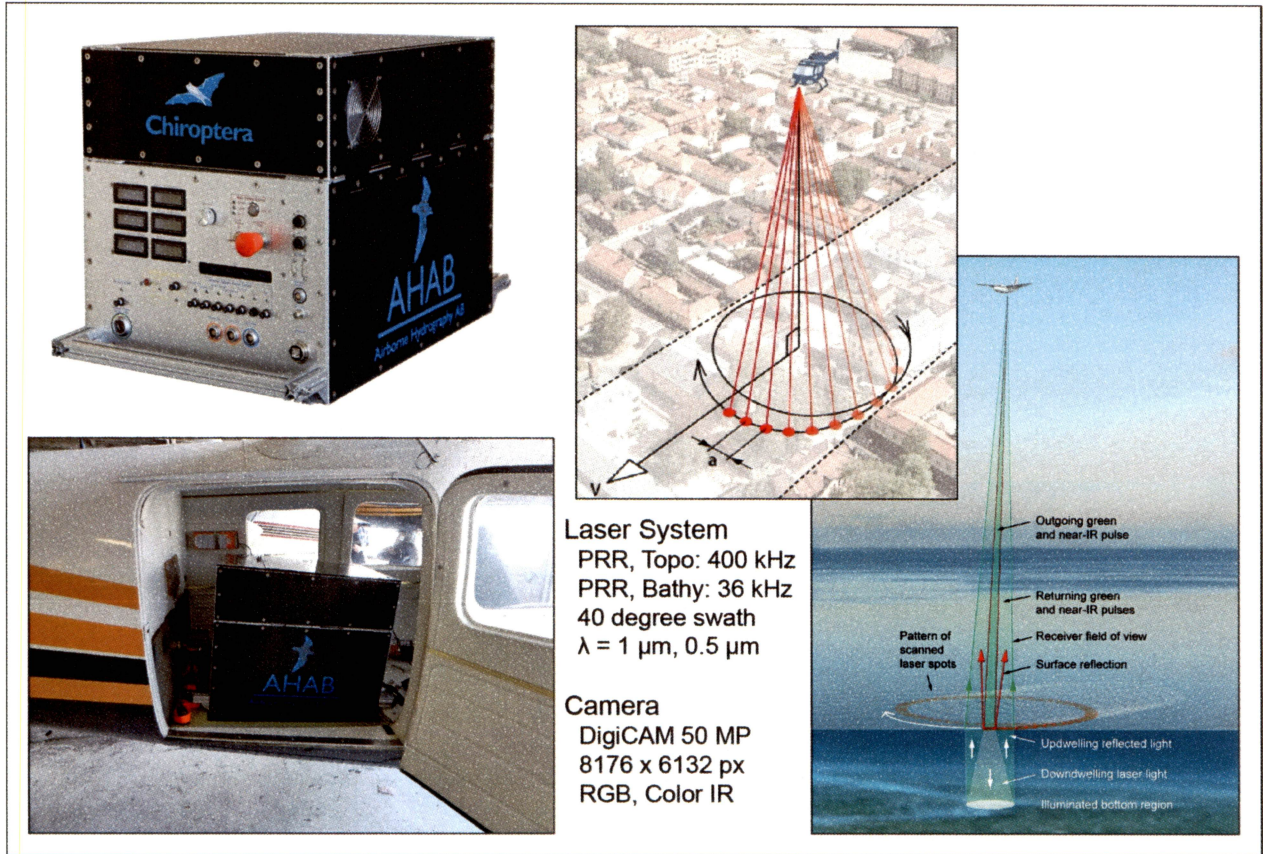


Figure 3. (left) The Chiroptera system and the system mounted in a fixed-wing aircraft. Instruments include topographic and bathymetric lidar and a high-resolution camera. (right) Elliptical (Palmer) scanning pattern employed by the Chiroptera topographic and bathymetric lasers and generalized illustration of water-surface and water-bottom returns.

acquired at a few locations to test system capabilities in murky water. Topographic data were collected for a 1000-m swath landward of the mainland bay shorelines as well as complete coverage of all islands within the bay systems including San José and Matagorda Islands and Matagorda Peninsula.

San Antonio Bay System

We acquired high-resolution airborne lidar data of the San Antonio Bay system, Texas Gulf coast between January and June 2013. Data were acquired in the upper part of San Antonio Bay (Guadalupe delta area, block 1, fig. 4) on January 17, 18, and 19, 2013 using a single-engine Cessna Stationaire 206 aircraft owned and operated by the Texas Department of Transportation,

and flown from Rockport, Texas. Flight elevation was between 440 and 570 m. Topographic laser pulse rate was 200 kHz. A GPS base station (Trimble Net R9) was operated at Seadrift, recording at 1-second interval during each survey.

Airborne lidar data were acquired over shorelines along the lower part of San Antonio Bay, Espiritu Santo Bay, and Ayres Bay (fig. 4) on May 29 (water transects, block 2), June 4 through 7 (blocks 3 through 6), and June 21, 2013 (block 7) using a twin-engine Aero Commander 500

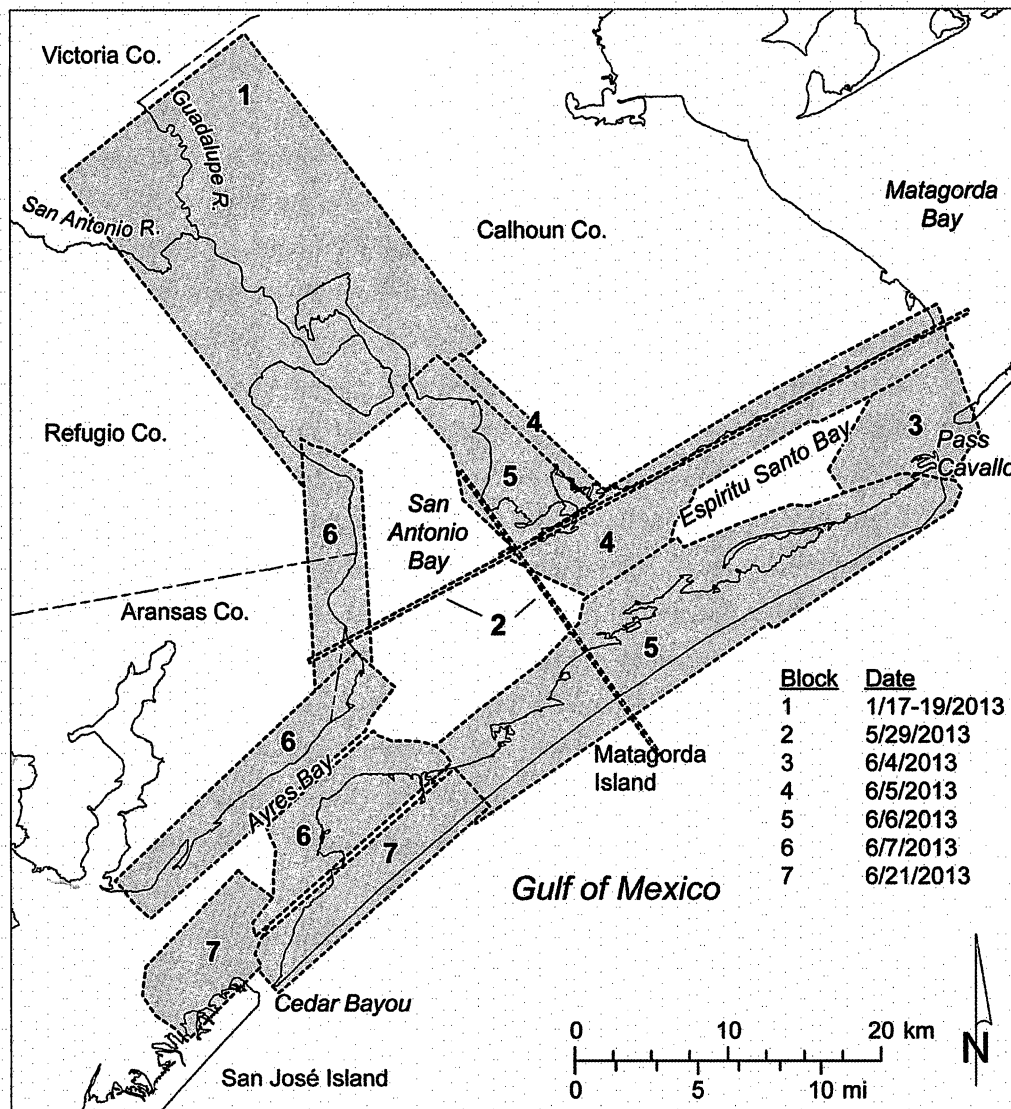


Figure 4. San Antonio Bay system airborne lidar survey coverage blocks acquired in January, May, and June 2013. Topographic lidar data were acquired in all blocks except the narrow corridors (block 2), where only bathymetric lidar data were acquired.

aircraft owned and operated by Aerial Viewpoint, Inc., and flown from the Calhoun County Airport near Port Lavaca, Texas. Flight elevation was 400 m for the open-water transects and 575 to 750 m for the topographic lidar corridors along the bay shoreline. The topographic laser pulse rate was between 180 and 200 kHz. GPS base stations (Trimble Net R9) were operated during each survey flight at two of four locations that included Seadrift, the Aransas National Wildlife Refuge, Shoalwater Flats along Espiritu Santo Bay, and the Rockport airport. GPS base stations recorded at 1-second interval during each survey.

Copano Bay System

Airborne lidar data (fig. 5) were acquired in the Copano Bay system in four deployments (January 29-30, March 30-31, April 22, and April 28-30, 2014) using a twin-engine Aero Commander aircraft (tail number N14AV) owned and operated by Aerial Viewpoint and flown from Rockport, Texas. Flight elevation was between 800 and 900 m. Topographic laser pulse rate was 120 kHz. GPS base stations (Trimble Net R9) were operated at the Aransas County Airport in Rockport and at a temporary benchmark in Bayside recording at a 1-second interval during each survey.

Matagorda Bay System

Airborne lidar data (fig. 6) were acquired in the Matagorda Bay system in one deployment (February 2 to 9, 2015) using a twin-engine Partenavia aircraft owned and operated by Aspen Helicopters, Inc. and flown from the Calhoun County Airport, Port Lavaca, Texas. Survey areas were flown on February 2, 6, 7, 8, and 9. Flight elevation was between 925 and 1018 m for all flights, yielding a single-pass swath width of about 730 m. Topographic laser pulse rate was 100 kHz. GPS base stations (Trimble Net R9) at the Calhoun County Airport near Port Lavaca (PTLV, fig. 6), Palacios (PALA), and the Matagorda Bay Nature Park (IDOL) were recording at a 1-second interval. At least two base stations were operating during each flight.

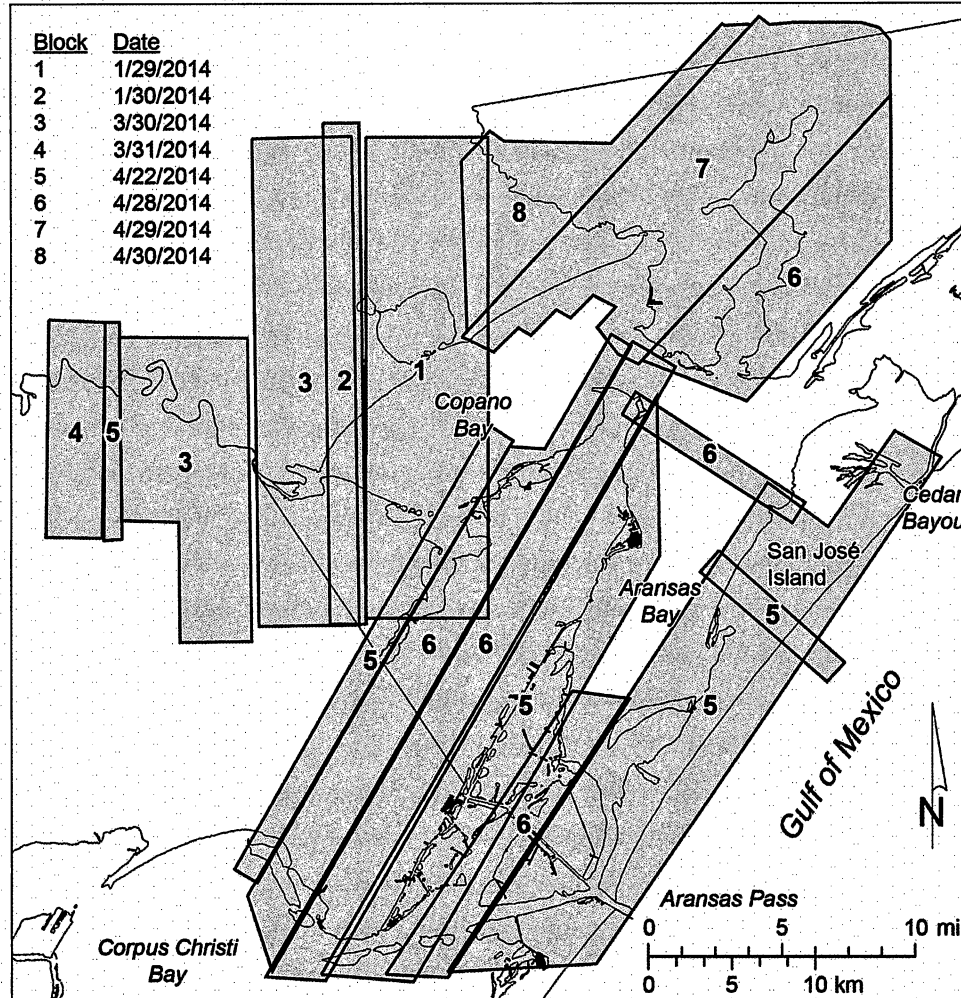


Figure 5. Copano Bay system airborne lidar survey coverage blocks acquired in January, March, and April 2014. Topographic lidar data were acquired in all blocks.

An additional survey of the western shore of Matagorda Bay was flown July 5-8, 2016 to assess possible effects of Tropical Storm Bill, a tropical cyclone that crossed the central Texas coast in June 2015 (Berg, 2015). The equipment was installed in the Cessna Stationaire 206 aircraft owned and operated by the Texas Department of Transportation, and flown from Port Lavaca, Texas. GPS base stations (Trimble Net R9) at the Calhoun County Airport near Port Lavaca and at Powderhorn Ranch near Port O'Connor were recording data at a 1-second interval. Flight elevation was between 450 to 580 m for all flights and topographic laser pulse rate was 240 kHz.

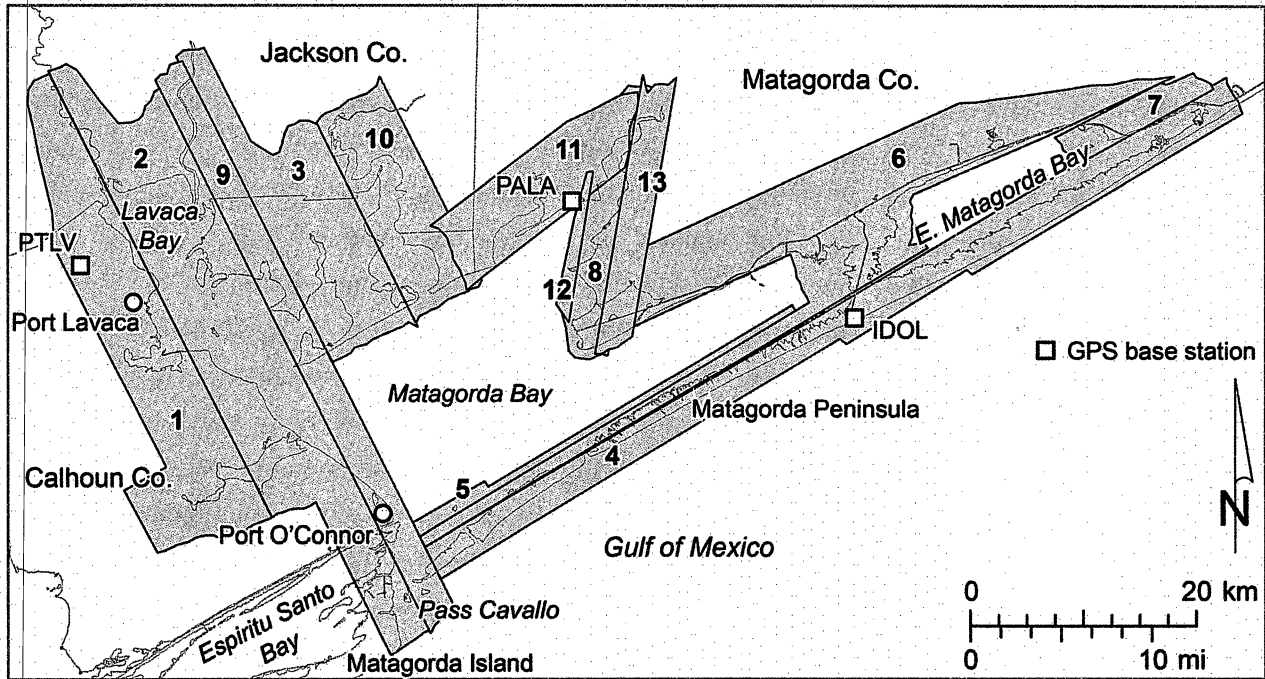


Figure 6. Matagorda Bay system airborne lidar survey coverage blocks acquired in February 2015 (table 1). Topographic lidar data were acquired in all blocks. GPS base stations located at the Calhoun County Airport (PTLV), Palacios (PALA), and at the Matagorda Bay Nature Park (IDOL).

Table 1. Airborne topographic lidar survey parameters, Matagorda Bay system. Blocks are shown on fig. 6.

Block	Date flown	Height (m)	Laser pulse rate (kHz)	Base stations
1, 2	2/2/2015	936-985	100	PALA, PTLV
3	2/6/2015	959-997	100	PTLV, IDOL
4, 5, 6, 7	2/7/2015	939-1009	100	PTLV, PALA, IDOL
8	2/8/2015	925-1010	100	PTLV, PALA, IDOL
9, 10, 11, 12, 13	2/9/2015	969-1018	100	PTLV, PALA

Lidar Data Processing

While in the field, all laser data, raw image files, and positional data are downloaded to a field computer. Preliminary GPS processing is completed by merging base GPS receiver data with the remote (aircraft GPS) data to create an aircraft trajectory. The preliminary trajectory is then combined with attitude information to create a seven-parameter (time, x y, z, roll, pitch, and yaw) navigation file. The navigation solution is used to reference each laser pulse return and then output laser-point-cloud data. The data are examined in the field to determine quality of coverage (such as sufficient overlap of flight lines and point density).

Base-station coordinates are computed using National Geodetic Survey's (NGS) Online Positioning User Service (OPUS). GrafNav software is used to calculate a final aircraft trajectory based upon the known positions of the GPS base stations. The resulting precise trajectories are combined with aircraft attitude information in AEROoffice to create a final precise seven-parameter navigation file.

Laser-point data are generated in AHAB's proprietary processing software Lidar Survey Studio (LSS), combining navigation file information and laser data. During each survey flight, a calibration target is flown with opposing flight lines to correct roll, pitch, and heading errors and adjust elevation bias offsets. A calibration target is a flat, unambiguous surface (road or runway) that has been surveyed using static or kinematic GPS techniques. The ground survey points are estimated to have a vertical accuracy of 0.01 to 0.05 m. The ideal targets are also adjacent to buildings with slanted roofs or parking lots with painted lines. The lidar data points and ground surveyed GPS points are examined for any mismatch between their horizontal and vertical positions. Several iterations of adjustments to the calibration files are made to minimize the errors caused by IMU misalignment.

Laser-point data is output from LSS in LAS v1.2 format (a binary file format) in UTM coordinates. The TerraScan utility MicroStation is used to concatenate flight line segment files and clean the data of miscellaneous returns (such as clouds, reflections, and long returns).

TerraScan is also used to determine bias offsets between lidar point data and the GPS ground reference control points. A lidar data set from the calibration target area is sorted to find data points that fall within 1 m of a ground GPS survey point. The mean elevation difference between the lidar and the ground GPS is used to estimate and remove any elevation bias from the lidar points. Vertical biases are determined for and removed from each flight. The standard deviation of the final elevation differences provides estimates of the lidar point precision. The average RMS value for the Matagorda Bay system survey is 0.048 m, for the Copano Bay system survey is 0.026 m, and for the San Antonio Bay system survey is 0.054m.

LAStools programs are used to perform several functions to prepare the data for final products. Tasks include: parsing the laser point cloud data into 1 x 1 km tiles (including a 20-m buffer), adjusting elevation data from ellipsoidal to orthometric heights (NAVD88) using either GEOID12A or GEOID12B, classifying data as bare ground, and generating all points and bare-earth DEMs. Custom software (gmod) runs a script to fill the small voids in the DEMs, remove surface returns over water bodies, and clip the DEMs to remove the 20-m buffer. The LAS point cloud data and DEMs are delivered as 1 x 1 km files. For each survey area a composite 4-m resolution DEM was created using Global Mapper. From these a composite DEM at 10-m resolution was created in Global Mapper for the entire three-bay system.

Historical Shoreline Mapping

Topographic surveys, aerial photographs, and photomosaics (Appendix A) were used to determine shoreline position and changes prior to the advent of airborne lidar. Accurate topographic charts dating from the 1850s were mapped by the U.S. Coast Survey (now National Ocean Service). Aerial photographs supplemented, and in the early 1930s replaced regional topographic surveys. Aerial photographs show shoreline position—the position of the land-water interface—when the photographs were taken.

The key to detecting shoreline movement is agreement of scale and projection between original data and the selected base map. To achieve this, U.S. Geological Survey 7.5-minute quadrangle topographic maps (at a scale of 1:24,000) were used. Topographic charts and aerial photographs were either enlarged or reduced to the scale of the topographic maps. Shorelines shown on topographic charts and land-water boundaries mapped directly on aerial photographs were optically transferred from the charts and photos onto a common base map. Transferal of shorelines to the base map allowed direct comparison and quantification of changes in shoreline position with time.

For this study, the topographic base maps were scanned at high resolution and georeferenced to the 1927 North American Datum (NAD27) datum of the base map. The historical shorelines recorded on the base maps were digitized in ArcGIS. Shorelines were recorded from the 1850-60s topographic charts and aerial photography from the 1930s, 1950s, 1974, and 1982 (Appendix A). The shorelines were then projected into the 1983 North American Datum (NAD83) to allow for direct comparison with the lidar-derived shorelines from 2013 (San Antonio Bay system), 2014 (Copano Bay system), and 2015 (Matagorda Bay system).

A general statement on the accuracy of the historical shoreline positions is that accuracy improves with advances in technology. There is some inherent uncertainty as to the precision of the data in the original topographic charts that were prepared by the U.S. Coast Survey. For aerial photography, optical resolution, the quality of photographic negatives, and mosaic compilation techniques all improved over time between the earliest photographs in the 1930s and the most recent photographs (1982) used in this study. Another potential source of error is using the land-water interface on aerial photographs because the boundary normally will fall somewhere between high and low tide. This displacement depends on the tidal cycle, slope of the beach, and wind direction when the photo was taken. For this study the 1800s shorelines were not used in the calculation of shoreline movement but they are included in the accompanying GIS dataset (Appendix B).

Lidar Shoreline Extraction

A lidar derived shoreline position is extracted from the digital elevation models to represent the bay shoreline position in the Copano, San Antonio, and Matagorda Bay systems. In previous bay shoreline studies at BEG, shorelines were drawn or digitized on photographs, generally at the boundary between water and land. The position of this boundary can vary due to water level, wave activity, and georeferencing errors. Two elevation contours were selected to represent the position of the bay shoreline based on water-level data from tide gauges located at Port O'Connor, Copano, Rockport, Port Lavaca, and Seadrift. The average water level and mean higher high water (MHHW) level above NAVD88 was determined between 2003 and 2015 (table 2).

The 0.29-m and 0.37-m elevation contours were extracted from the lidar-derived DEM using the “Raster Calculator,” “Reclassify,” and “Raster Domain” functions in ArcGIS. “Raster Calculator” is used to convert the DEM into a raster with all values above the designated elevation contour as a value of 1 and values below the designated contour as 0. “Reclassify” creates a new raster that reclassifies all “0” values to “null.” The “Raster Domain” function creates a polyline footprint of the raster which corresponds to the bay shoreline contour elevation. The extracted files are then smoothed in ArcMap using the “Smooth Line” function

Table 2. Average water level and mean higher high water (MHHW) level between 2003 and 2015 from five tide gauges within the Copano, San Antonio, and Matagorda Bay systems.

Tide gauge	Average water level (NAVD88, m)	Average MHHW level (NAVD88, m)
Port O'Connor	0.25	0.37
Copano	0.29	0.35
Rockport	0.27	0.32
Port Lavaca	0.32	0.45
Seadrift	0.30	0.35
Average	0.29	0.37

(PAEK algorithm with a 2-m smoothing tolerance). The number of vertices in the polyline is reduced by using ET GeoWizards “Generalize Polyline” command with a 0.25-m tolerance. This process retains the shape of the smoothed polyline while reducing the number of vertices. Topology errors, including dangles, self-overlapping lines, and self-intersecting lines, were removed. Adjacent line segments were aggregated using ArcGIS’s “Unsplit Line” function.

Both contour elevations were overlain on National Agriculture Imagery Program (NAIP) aerial imagery from 2014. The elevations were examined to determine which most accurately corresponded with the land and water boundary as depicted on the photographs (fig. 7). The lower elevation contour (0.29 m above NAVD88, the average water level from five tide gauges) was determined to be the most consistent with historical bay shoreline mapping practices. There were a few areas (including the northern shoreline of Hynes Bay) where the land and water boundary as interpreted on aerial photographs was at a higher elevation than the extracted shoreline position (fig. 8). In these instances, the shoreline was hand digitized on the georeferenced NAIP photographs and merged with the lidar-extracted shoreline.

Determining Rates of Shoreline Movement

Shoreline movement was analyzed using ArcGIS geographic information system software. Selected shorelines from 1800s maps, aerial photographs from the 1930s through 1982 (Appendix A), and lidar surveys conducted between 2013 and 2014 were imported into an ArcGIS database. Shoreline movement was quantified using the GIS-based extension software Digital Shoreline Analysis System (DSAS version 4.3; Thieler and others, 2009) following these steps: (1) creating shore-parallel baselines from which shore-perpendicular transects were cast at 100-m intervals along the shoreline; (2) calculating net rates of change and associated statistics for a common long-term period (1930s to 2010s) and a more recent period (1982 to 2013 in the San Antonio Bay system, 1982 to 2014 in the Copano Bay system, and 1950s to 2015 in the Matagorda Bay system) using the transect location and its intersection points with the selected shorelines within DSAS; and (3) creating GIS point files containing the movement rate, shoreline

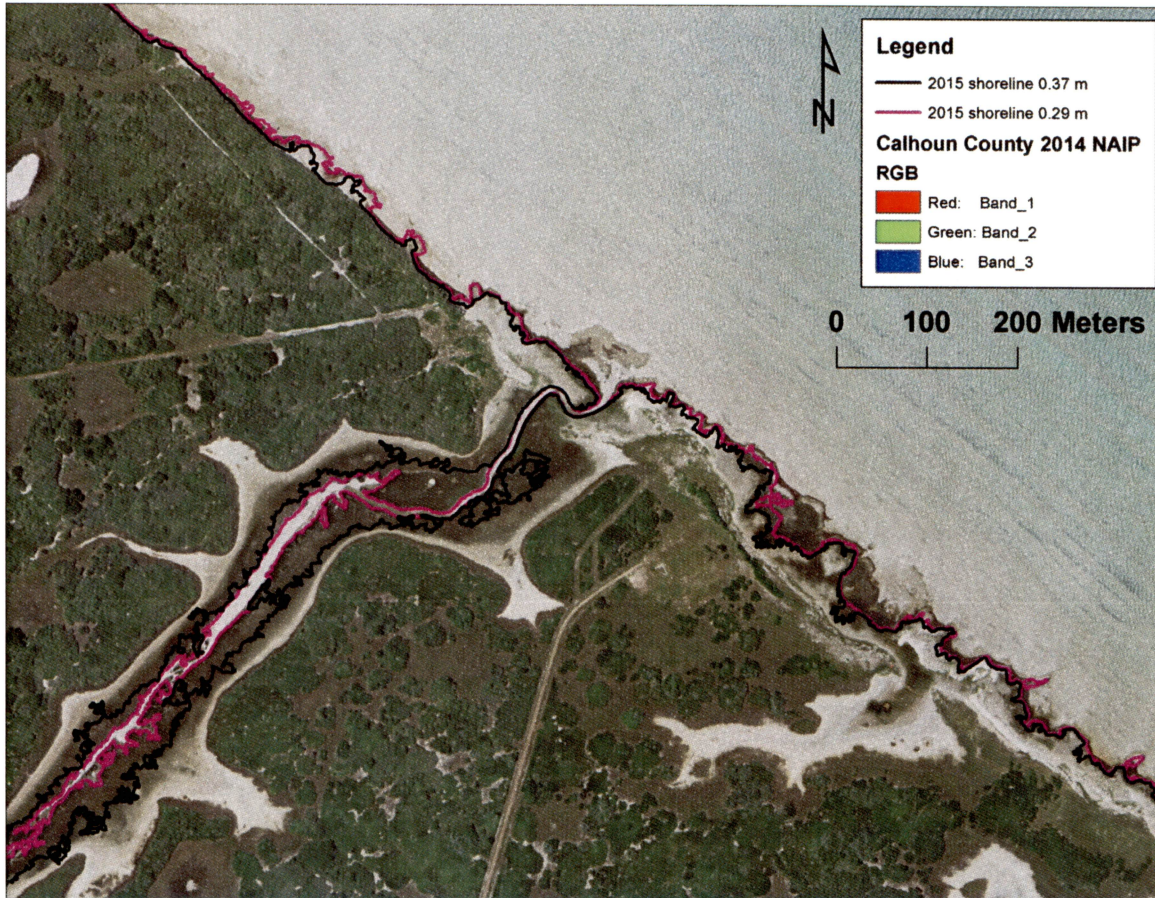


Figure 7. Extracted 0.29- (pink) and 0.37- (black) m NAVD88 elevation contours representing shoreline position northwest of Port O'Connor on Matagorda Bay. The 0.29-m elevation coincides most consistently with the land-water boundary when compared with 2014 NAIP imagery. The boundary between land and water was interpreted as the bay shoreline position on historical aerial photographs.

type, shoreline modification, and susceptibility to retreat related to relative sea-level rise, storm surge and waves, and non-storm waves at each of nearly 10,000 measurement sites for the long-term and more recent monitoring periods. These data served as the basis for the results and analysis presented in this report and the accompanying ArcGIS-format files (Appendix B).

SHORELINE TYPES

We have classified the shorelines that serve as the boundaries of the water bodies within the Copano, San Antonio, and Matagorda Bay systems into 11 types that can be distinguished by

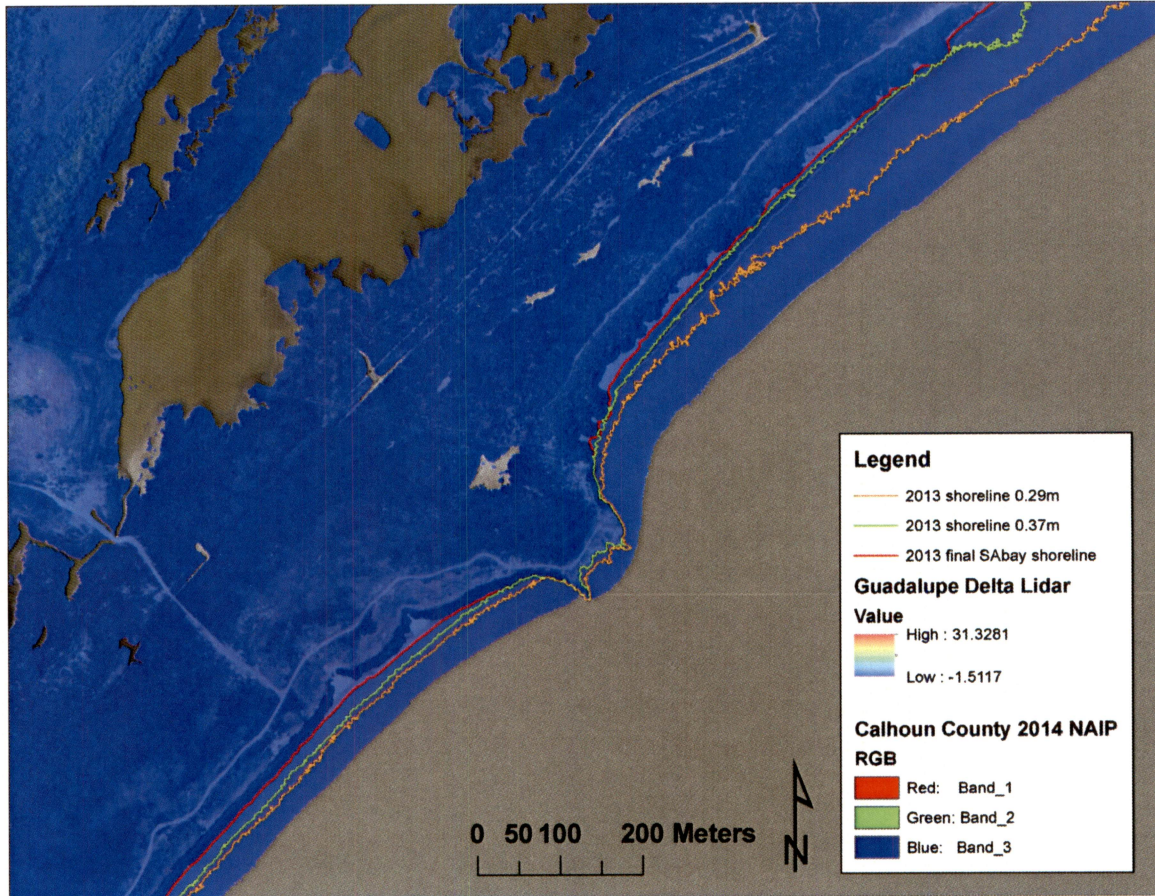


Figure 8. Extracted 0.29- (orange) and 0.37- (green) m NAVD88 elevation contours northwest of the Guadalupe delta. The red line represents the hand-digitized shoreline segment that coincides with the land-water boundary on 2014 NAIP imagery. The hand-digitized segment (at a higher elevation) for this location is more consistent with the shoreline that was mapped on historical aerial photographs.

a combination of elevation, slope, depositional environment, material and consolidation level, and vegetation or habitat (fig. 9; table 3). From highest to lowest elevation, these types are: high and low bluff, sandy slope, fan delta, beach, spit, tidal pass, flood-tidal delta marsh or tidal flat, deltaic marsh, back-barrier marsh or tidal flat, and bay-margin marsh or tidal flat. Together, these shoreline types extend for about 1,065 km among the three central Texas bay systems (fig. 10).

High and Low Bluffs

High (more than about 3 m) and low (less than 3 m) erosional bluffs are formed on Pleistocene Beaumont Formation strata (fig. 1) and are a common shoreline type along the more elevated, inland parts of the bays, constituting 16 percent of the total bay shoreline length in the three bay systems (fig. 10). These consolidated sandy clay or clayey sand strata typically form steep barren bluffs (fig. 11a,b; table 3) that are prone to slope failure. Bluff heights increase landward, following the gentle inland topographic rise characteristic of the Texas coastal plain (fig. 2). These dominantly clay bluffs are common along Port Bay, Mission Bay, and the western shore of Copano Bay in the Copano Bay system (fig. 12); along the eastern and western shores of San Antonio Bay, the southwestern shore of Hynes Bay, the northern and eastern shores of Mission

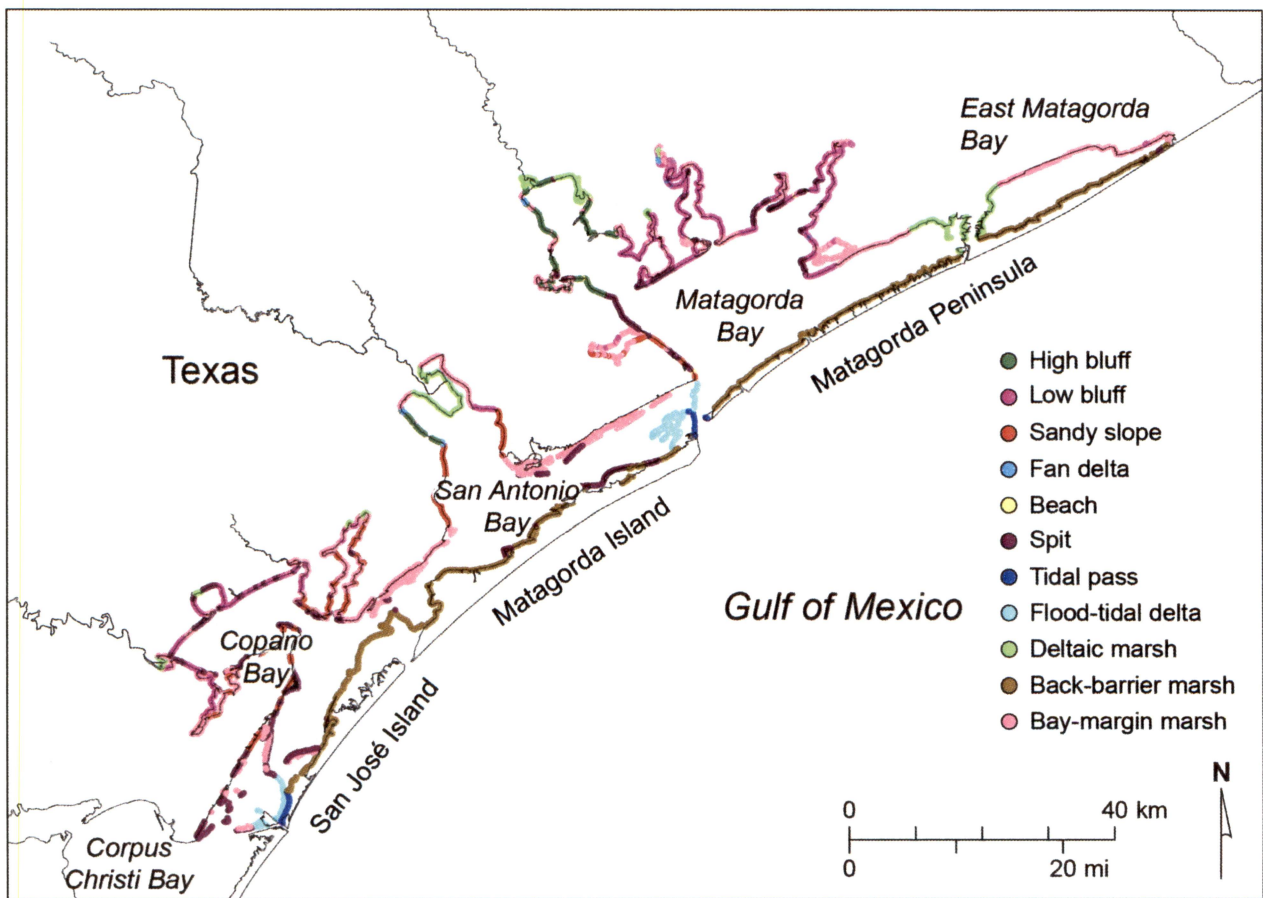


Figure 9. Distribution of principal shoreline types (table 3) in the Copano, San Antonio, and Matagorda Bay systems.

Table 3. Common bay shoreline types and their environmental, elevation, slope, and material characteristics.

Type	Environment	Elevation	Slope	Material
Bluff (high)	Bare or vegetated slope; common slope failure	> 3 m	Steep with minimal fronting beach or marsh	Consolidated silty to sandy clay
Bluff (low)	Bare or vegetated slope; common slope failure	< 3 m	Steep with minimal fronting beach or marsh	Consolidated silty to sandy clay
Sandy slope	Vegetated; moderate slope failure	< 3 m	Moderate with minimal fronting beach or marsh	Sand to muddy sand; semiconsolidated
Fan delta	Vegetated; wetland vegetation common near the shoreline	< 1 m	Minimal	Muddy sand; semiconsolidated
Beach	No or minimal vegetation	< 1 m	Moderate	Sand and shell; unconsolidated
Spit	No or minimal vegetation	< 1 m	Moderate	Sand and shell; unconsolidated
Tidal pass	Wetland vegetation	< 1 m	Minimal	Muddy sand to sandy mud; unconsolidated
Flood-tidal delta	Wetland vegetation to barren algal flats	< 0.5 m	Negligible	Muddy sand to sandy mud; unconsolidated
Deltaic marsh	Wetland vegetation	< 0.5 m	Negligible	Mud to sandy mud; semiconsolidated
Backbarrier marsh or tidal flat	Wetland vegetation to barren algal flats	< 0.5 m	Negligible	Sandy mud to muddy sand; semiconsolidated
Bay-margin marsh or tidal flat	Wetland vegetation to barren algal flats	< 0.5 m	Negligible	Sandy mud to muddy sand; semiconsolidated

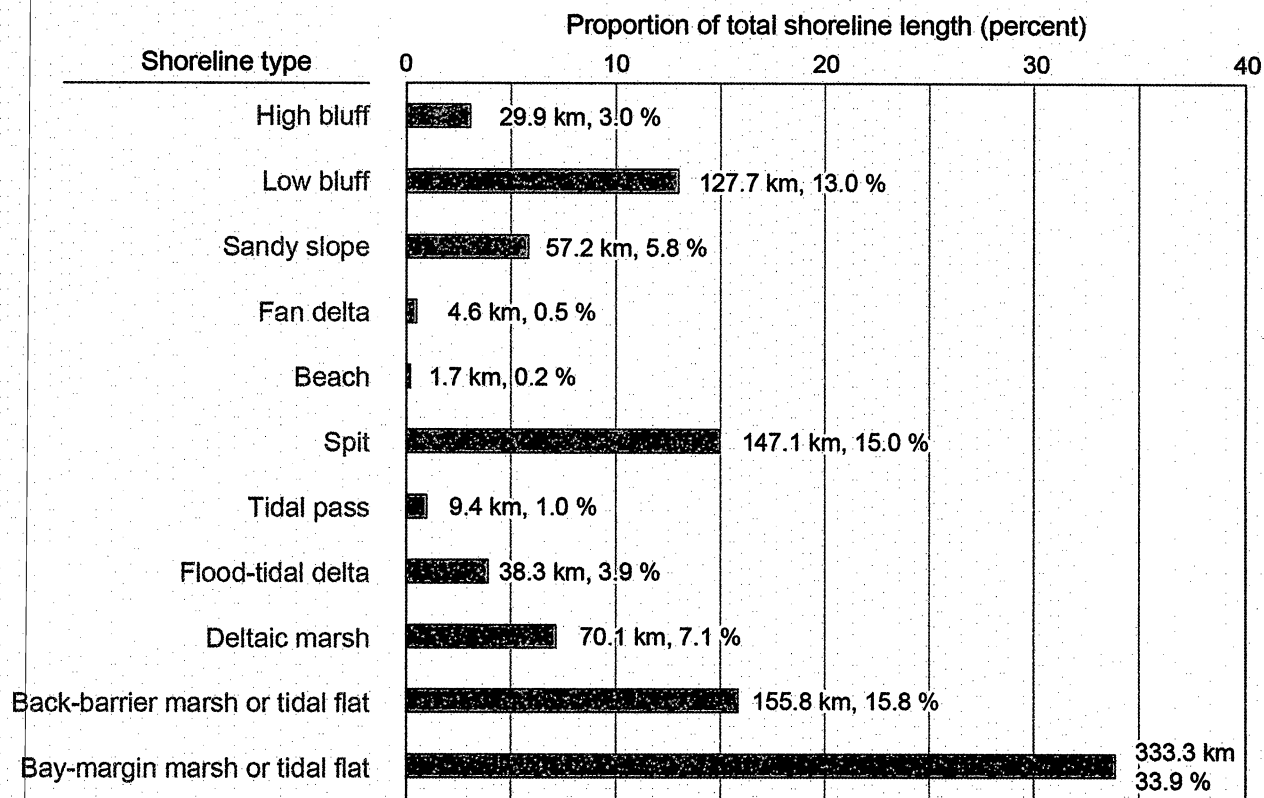


Figure 10. Total length and proportion of common shoreline types (table 3) at 9,845 sites in the Copano, San Antonio, and Matagorda Bay systems. Total shoreline length is approximately 1,065 km.

Lake, and the eastern shore of Guadalupe Bay in the San Antonio Bay system (fig. 13); and along Lavaca Bay, the northern shore of Matagorda Bay, the northern shore of Powderhorn Lake, Chocolate Bay, Cox Bay, Carancahua Bay, Turtle Bay, and Tres Palacios Bay in the Matagorda Bay system (fig. 14). High and low bluffs are highly susceptible to retreat caused by storm surge and storm waves during tropical cyclone passage and are moderately susceptible to retreat caused by non-storm wave action, but are relatively unaffected by relative sea-level rise over the historical record (table 4).

Sandy Slopes

Sandy or clayey sand slopes occur along about 6 percent of the shorelines in all three bay systems (figs. 9 and 10). This shore type slopes gradually bayward from elevations of as much as

(a)



(b)



(c)



Figure 11. Photographs of (a) high Pleistocene sandy clay bluff near Port Lavaca on the southern shore of Lavaca Bay, (b) low Pleistocene sandy clay bluff near Seadrift on the northern shore of San Antonio Bay, and (c) sandy slope near Port O'Connor on the southern shore of Matagorda Bay.

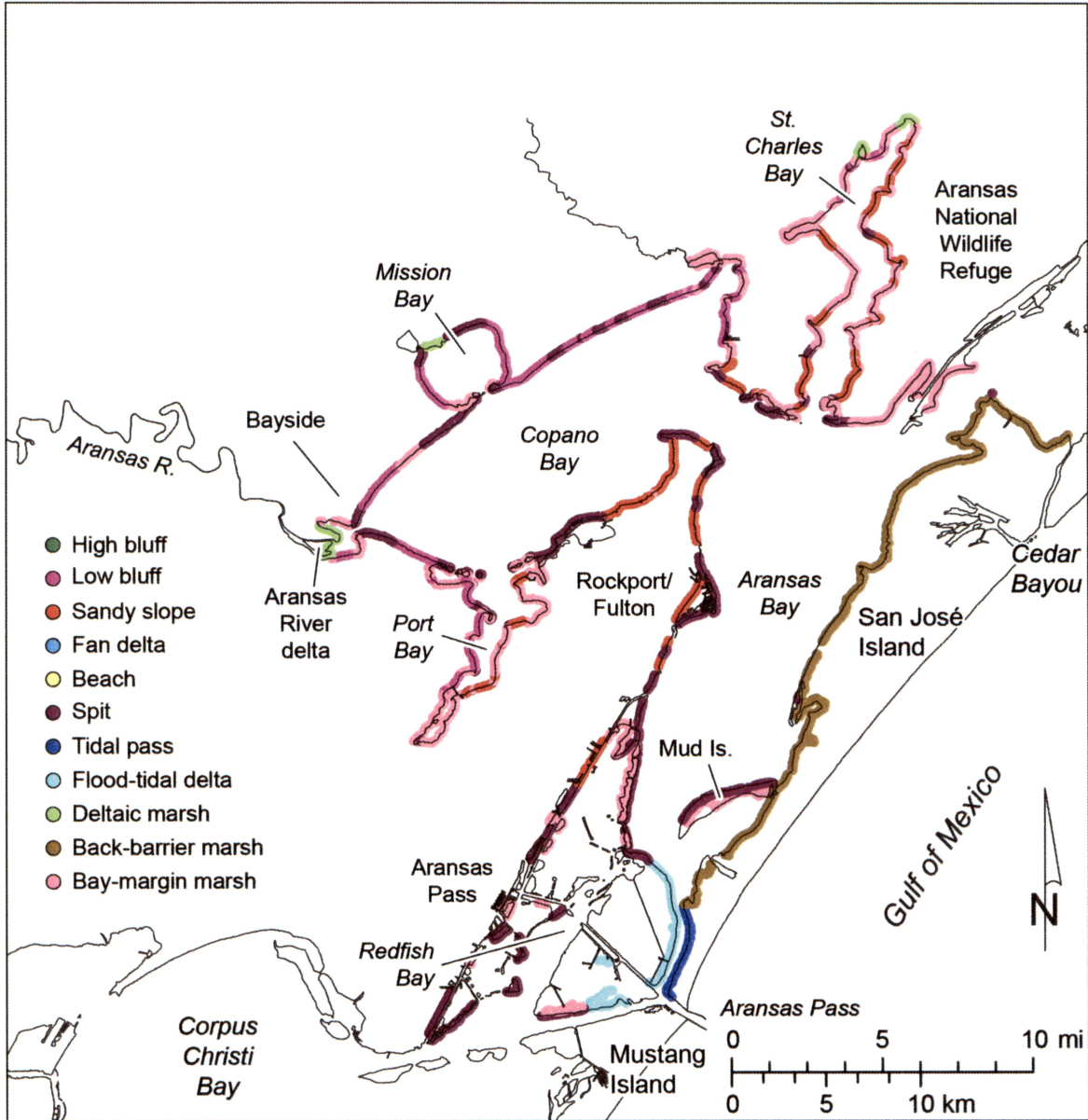


Figure 12. Distribution of principal shoreline types (table 3) in the Copano Bay system.

a few meters and may have a low erosional scarp at the shoreline (fig. 11c). Unconsolidated sand and clayey sand slopes are found where the Pleistocene Ingleside barrier island or strandplain coincides with the modern shoreline and are commonly stabilized by upland grasses and shrubs. In the Copano Bay system, sandy slopes occur along the mainland shore of Redfish and Aransas Bays, the eastern shore of Copano Bay, and the southwestern and eastern shores of St. Charles Bay (fig. 12). In the San Antonio Bay system, sandy slopes occur inland from bay-margin

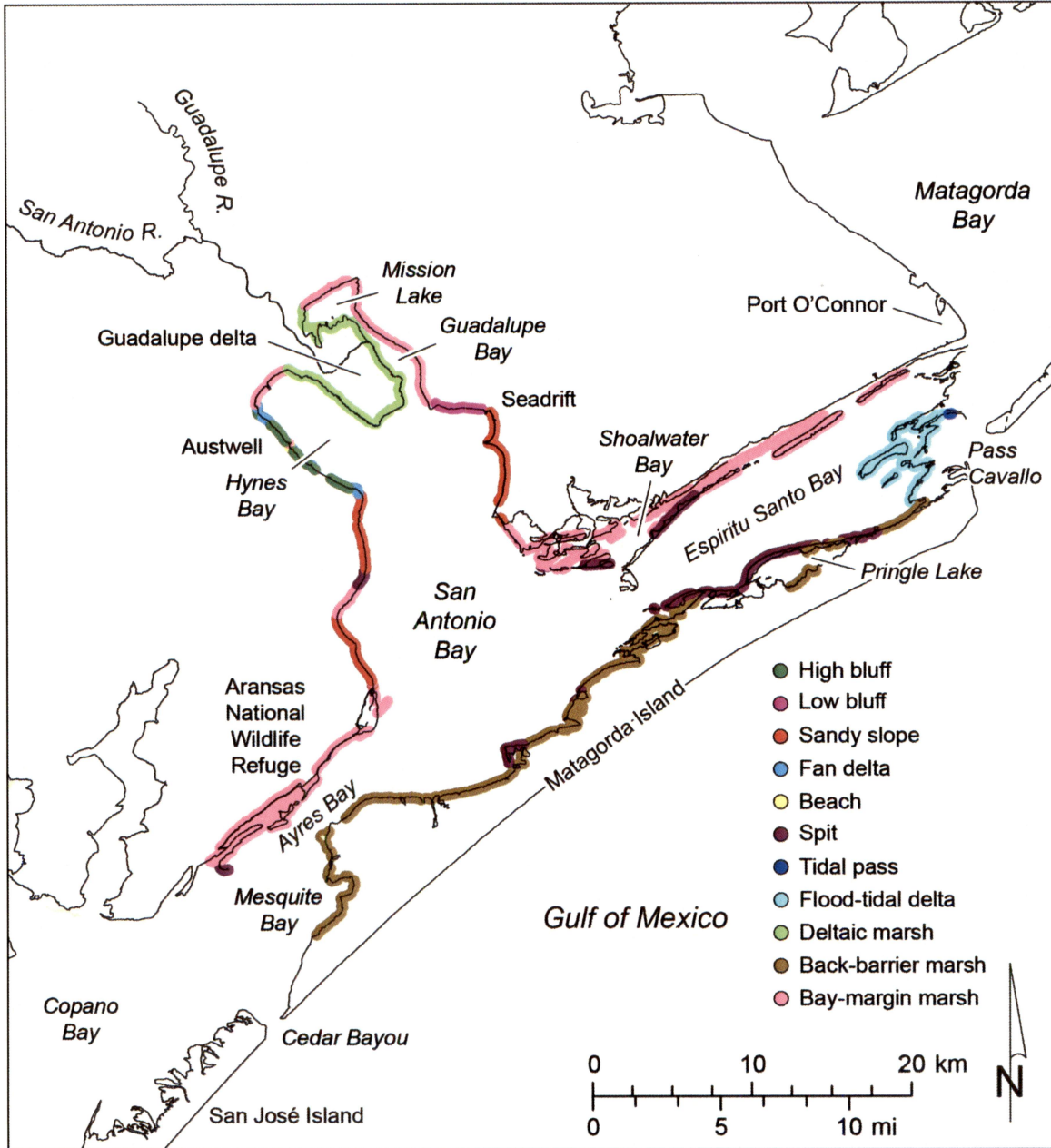


Figure 13. Distribution of principal shoreline types (table 3) in the San Antonio Bay system.

marshes along the western shore of Mesquite, Ayres, San Antonio, and Espiritu Santo Bays (fig. 13). The northeastern limit of sandy slopes is at the easternmost exposure of the Ingleside barrier near Port O'Connor along southwestern Matagorda Bay (fig. 14).

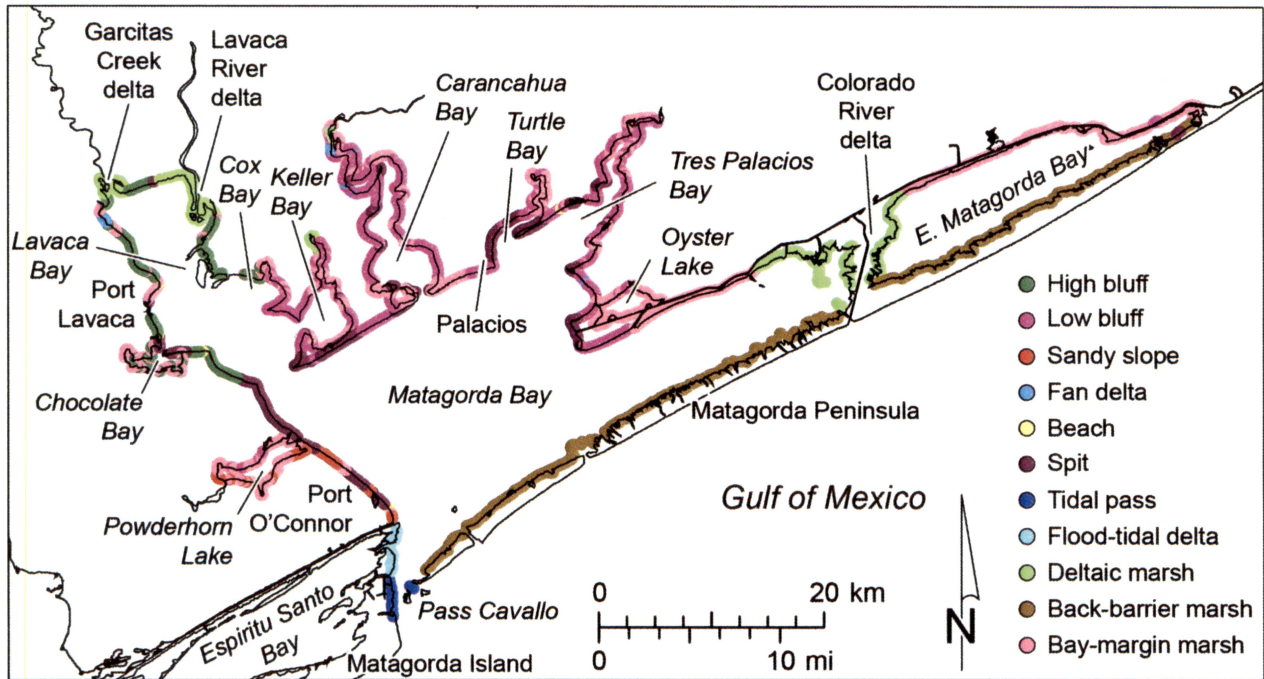


Figure 14. Distribution of principal shoreline types (table 3) in the Matagorda Bay system.

Table 4. Common bay shoreline types (table 3) and their relative susceptibility to relative sea-level rise, storm surge and waves, and non-storm wave action.

Type	Relative sea-level rise	Storm surge and waves	Non-storm wave action
High bluff	Low	High	Moderate
Low bluff	Low	High	Moderate
Sandy slope	Low	High	Moderate
Fan delta	Moderate	Moderate	High
Beach	Moderate	Moderate	High
Spit	Moderate	Moderate	High
Tidal pass	High	High	High
Flood-tidal delta	High	High	High
Deltaic marsh	High	Low	High
Back-barrier marsh or tidal flat	High	Low	High
Bay-margin marsh or tidal flat	High	Low	High

Sandy slopes are highly susceptible to shoreline retreat caused by storm surge and storm waves and moderately susceptible to erosion from normal wave activity, but are relatively insensitive to short-term relative sea-level rise given their typical elevation (table 4).

Fan Deltas

Fan deltas are small geomorphic features formed where local drainages discharge into major or minor bays. They form fan-shaped protrusions into the bays (fig. 15) that may be as much as a few hundred meters across and slope gradually to the shoreline. They compose a small percentage (less than one percent; fig. 10) of the total shoreline frontage in the three bay systems. Fan deltas are composed of semiconsolidated muddy sand or sandy mud and are mostly stabilized by grasses and shrubs at higher elevations and can have wetland vegetation present where elevations are low along the shoreline (table 3). Fan deltas are highly susceptible to retreat caused by non-storm wave activity and are moderately susceptible to retreat caused by relative sea-level rise and storm-related surge and waves (table 4). Several examples can be found along



Figure 15. Aerial photograph of a fan delta on the northwestern shore of Lavaca Bay. Photograph from the 2014 National Agricultural Imagery Program (NAIP).

the western shore of Copano Bay (fig. 12), the western shore of San Antonio Bay (fig. 13), and the western shore of Lavaca Bay (fig. 14).

Spits and Beaches

Small spits and beaches (fig. 16) are relatively common throughout the central Texas bays. About 15 percent of the total bay shoreline is classified as spits (fig. 10), which are low, elongate, and unconsolidated sandy and shelly beaches forming along eroding bay shorelines by longshore drift and lateral migration (fig. 16b; table 3). Beaches are more limited in extent, forming less than one percent of the total bay shoreline length. These typically narrow and low beaches (fig. 16a) are composed of unconsolidated fine sand with some shell; they commonly occur bayward of sandy slopes or bluffs where sufficient sand has been eroded or retained to form a beach. Similar to fan deltas, low-elevation spits and beaches are highly susceptible to erosion from non-storm wave action and are moderately susceptible to retreat caused by relative sea-level rise and storm-related surge and waves (table 4). Prominent spits are found along the eastern shore of Aransas Bay, within Redfish Bay, along western Aransas Bay near Rockport, and across the entrances to minor bays such as Port Bay, Mission Bay, and St. Charles Bay in the Copano Bay system (fig. 12) ; along Matagorda Island on the eastern shores of San Antonio Bay and Espiritu Santo Bay, and adjacent to Shoalwater Bay in the San Antonio Bay system (fig. 13); and along many of the boundaries between Matagorda Bay and smaller bays such as Chocolate Bay, Keller Bay, Carancahua Bay, and Tres Palacios Bay in the Matagorda Bay system (fig. 14).

Tidal Passes

Shorelines along tidal passes represent about one percent of the shoreline in the three bay systems (fig. 10). These shores (fig. 17) have generally low elevations, minimal slopes, and are composed of unconsolidated muddy sand to sandy mud (table 3). Wetland vegetation is common. Because of their low elevation and generally long wave fetch, shores along tidal passes are highly susceptible to erosion from non-storm wave action, tidal currents, and relative sea-level

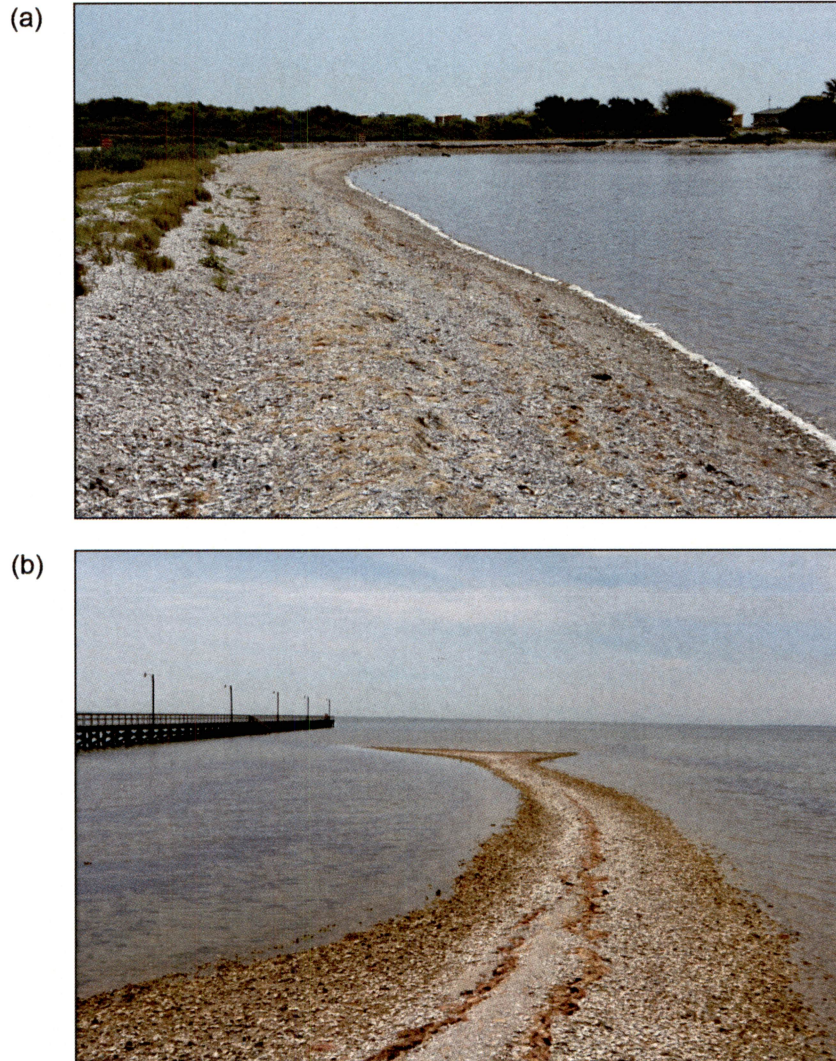


Figure 16. Photographs of (a) sandy and shelly beach, and (b) sandy and shelly spit at Goose Island State Park on the northern shore of Aransas Bay (fig. 12)

rise (table 4). They are also highly susceptible to shoreline movement caused by flood and ebb surge currents during tropical cyclone passage.

Two major tidal passes allow exchange of bay and Gulf water within the three bay systems. Tidal-pass shorelines are associated with Aransas Pass between Mustang and San José Island (fig. 12) and with Pass Cavallo between Matagorda Island and Matagorda Peninsula (fig. 14).

Lesser tidal exchange occurs through Cedar Bayou between San José Island and Matagorda Island.

Flood-tidal Deltas

Closely associated with tidal passes are flood-tidal deltas, which are submerged shoals, emergent landforms, and associated wetlands located on the bayward side of current and former tidal passes (fig. 17). Major flood-tidal deltas are located bayward from Aransas Pass (fig. 12) and Pass Cavallo (fig. 14). Shorelines bounding these features represent about 4 percent of the total shoreline in the three bay systems studied (fig. 10). Flood-tidal deltas have surface elevations below 0.5 m and are composed of unconsolidated muddy sand to sandy mud that may host wetland vegetation or a tidal-flat environment. Because of their low elevation and proximity to tidal passes, they can be highly susceptible to erosion from non-storm wave activity and the effects of relative sea-level rise. Storm waves generated by tropical cyclones generally have little impact on flood-tidal deltas because they flood early during storm passage, but flood-tidal delta



Figure 17. Aerial photograph of the flood-tidal delta and tidal-pass shorelines at Pass Cavallo, Matagorda Bay. Photograph from 2014 NAIP imagery.

shorelines are highly susceptible to movement and reconfiguration caused by storm-generated flood and ebb currents.

Deltaic Marshes

Several rivers and streams flow into the three bay systems. These streams carry sand, silt, and clay to the bays, where those sediments are deposited in low-elevation deltaic environments at the heads and margins of the bays. Several deltas with sizes ranging from quite small to very large have formed in the bays. Shoreline along these deltas makes up about 7 percent of the total bay shoreline (fig. 10).

Marshes and tidal flats commonly occupy low-relief, semiconsolidated, muddy sand and sandy mud substrates (fig. 18c), which are highly susceptible to erosion caused by non-storm wave activity and to land loss related to relative sea-level rise (table 4). Storm surge and storm waves have little impact on deltaic marshes located far from the open Gulf at the head of bays, but heavy rainfall and stream flooding that commonly occurs during tropical cyclone passage can contribute to significant instantaneous advance of the deltas into the bays.

River and stream deltas and associated marsh and other wetlands are found in all three bay systems (fig. 9). The largest of the deltas are (1) the Guadalupe delta, formed by the Guadalupe and San Antonio Rivers at the head of San Antonio Bay (figs. 13 and 18c), and (2) the Colorado River delta that extends from the mainland to Matagorda Peninsula and separates Matagorda and East Matagorda Bays (fig. 14). Other smaller examples include the Aransas and Mission River deltas in Copano and Mission Bays and minor deltas at the head of St. Charles Bay (fig. 12). Smaller deltas also are found where Garcitas Creek and the Lavaca River flow into Lavaca Bay and at the heads of Keller and Carancahua Bays (fig. 14).



Figure 18. Photographs of (a) back-barrier marsh and tidal flat on the southern shore of East Matagorda Bay, (b) bay-margin marsh and tidal flat at Aransas National Wildlife Refuge on Espiritu Santo Bay, and (c) deltaic marsh on the Guadalupe delta in Hynes Bay.

Back-barrier Marshes or Tidal Flats

Marshes and tidal flats are the most common shoreline type on the bay shore of San José Island on Aransas Bay (fig. 12), Matagorda Island on San Antonio and Espiritu Santo Bays (fig. 13), and Matagorda Peninsula on Matagorda and East Matagorda Bays (fig. 14). This shoreline type is the second-most extensive in the three bays, accounting for more than 15 percent of the total shoreline (fig. 10). Semiconsolidated sandy mud to muddy sand substrates support dominant marsh and tidal-flat environments (fig. 18a) that, like other low-elevation types, are highly susceptible to retreat from non-storm waves and land loss from inundation caused by relative sea-level rise. (table 4). Susceptibility to retreat from tropical cyclone surge and waves is low except near tidal passes and washover channels where surge-related flood and ebb currents are concentrated.

Bay-margin Marshes or Tidal Flats

The most extensive shoreline type in the three-bay study area is bay-margin marsh or tidal flat, which constitutes a third of all bay shoreline types by length (fig. 10). This type shares many characteristics with the back-barrier marsh or tidal flat type, including low elevation, minimal slope, muddy sand or sandy mud substrate, and dominant marsh vegetation with interspersed tidal flats (fig. 18b; table 3). It also shares erosion-susceptibility characteristics with the back-barrier type: high susceptibility to erosion by non-storm waves and to land loss related to relative sea level rise, and low susceptibility to erosion related to storm surge and waves (table 4). Because they are not located on barrier islands, bay-margin marshes or tidal flats are not as susceptible to sediment redistribution from flood and ebb currents generated during tropical cyclone passage.

Bay-margin marshes or tidal flats are common in nearly all of the major and minor bays in the Copano (fig. 12), San Antonio (fig. 13), and Matagorda Bay (fig. 14) systems. They are commonly found fronting or adjacent to other shoreline types, including high and low bluffs and

sandy slopes, and are common behind the active sand and shell beaches on many spits such as Mud Island on Aransas Bay (fig. 12).

Modified and Protected Shorelines

About 14 percent of the 1,065 km of bay shoreline in the three-bay system study area has been modified by dredging, cuts, or fills, or armored with shore protection features such as low seawalls (fig. 19a), riprap (fig. 19b), or bulkheads (fig. 19b,c). These modifications have been employed on virtually all natural shoreline types in an attempt to stabilize the shoreline position and protect bayfront property, but are easily overtopped and are prone to damage or failure during storms, can reduce or eliminate the function of the natural habitat, and can increase erosion rates on adjacent unprotected property.

BAY SHORELINE MOVEMENT ON THE CENTRAL TEXAS COAST

Net shoreline movement was determined at nearly 10,000 measurement sites (fig. 20) in the Copano Bay, San Antonio Bay, and Matagorda Bay systems. These sites are spaced at 100 m along the major and minor bay shorelines and include sites along all major shoreline types (fig. 9). Two periods were examined: a long-term period, which begins with shoreline position determined from 1930s aerial photographs and ends with the shoreline extracted from DEMs produced from airborne lidar surveys completed in the 2010s (2013, 2014, or 2015, depending on the bay system), and a more recent period, which begins with shoreline position determined from 1982 aerial photographs and ends with the 2010s lidar-derived shoreline. For the Matagorda Bay system only, the more recent period begins with the 1950s shoreline because that was the most recent shoreline included in the previous study of historical shoreline change in Matagorda Bay (McGowen and Brewton, 1975).



Figure 19. Photographs of shorelines protected by (a) low seawall at Goose Island State Park on the northern shore of Aransas Bay, (b) riprap and a low concrete bulkhead at Seadrift on the northern shore of San Antonio Bay, and (c) a low bulkhead and vegetation at Bayside on the southwestern shore of Copano Bay.

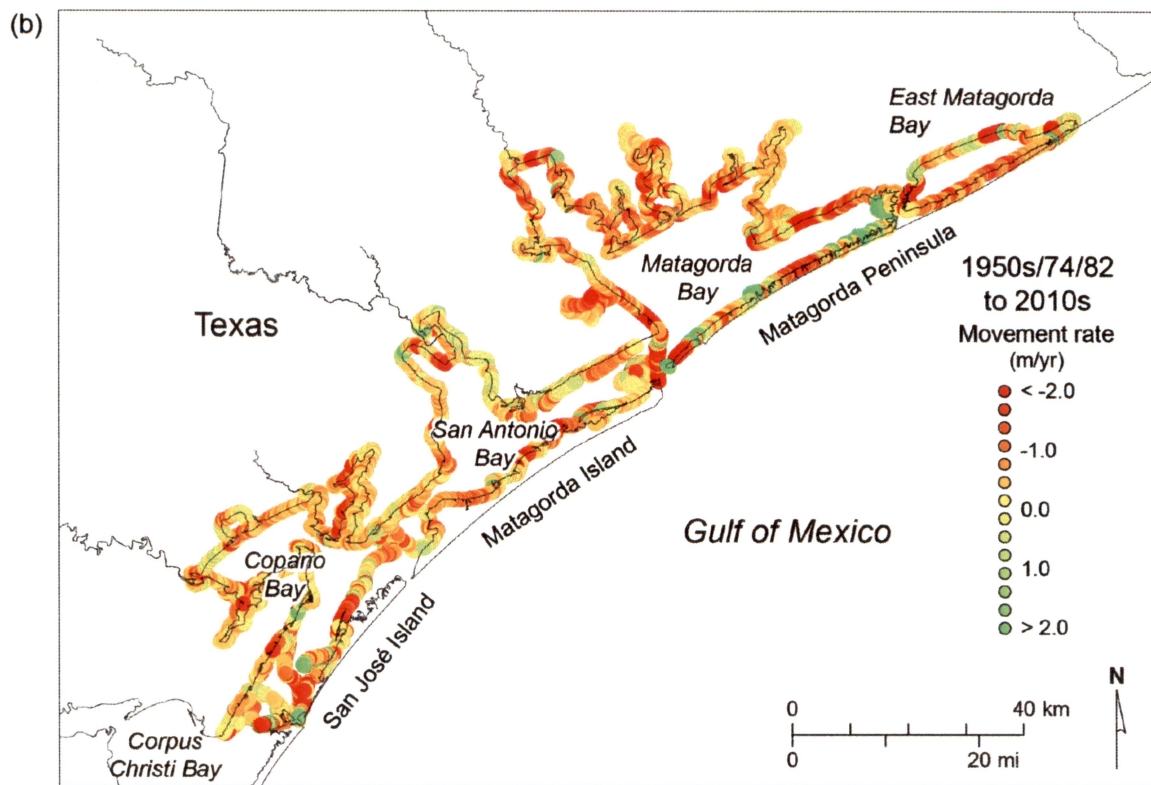
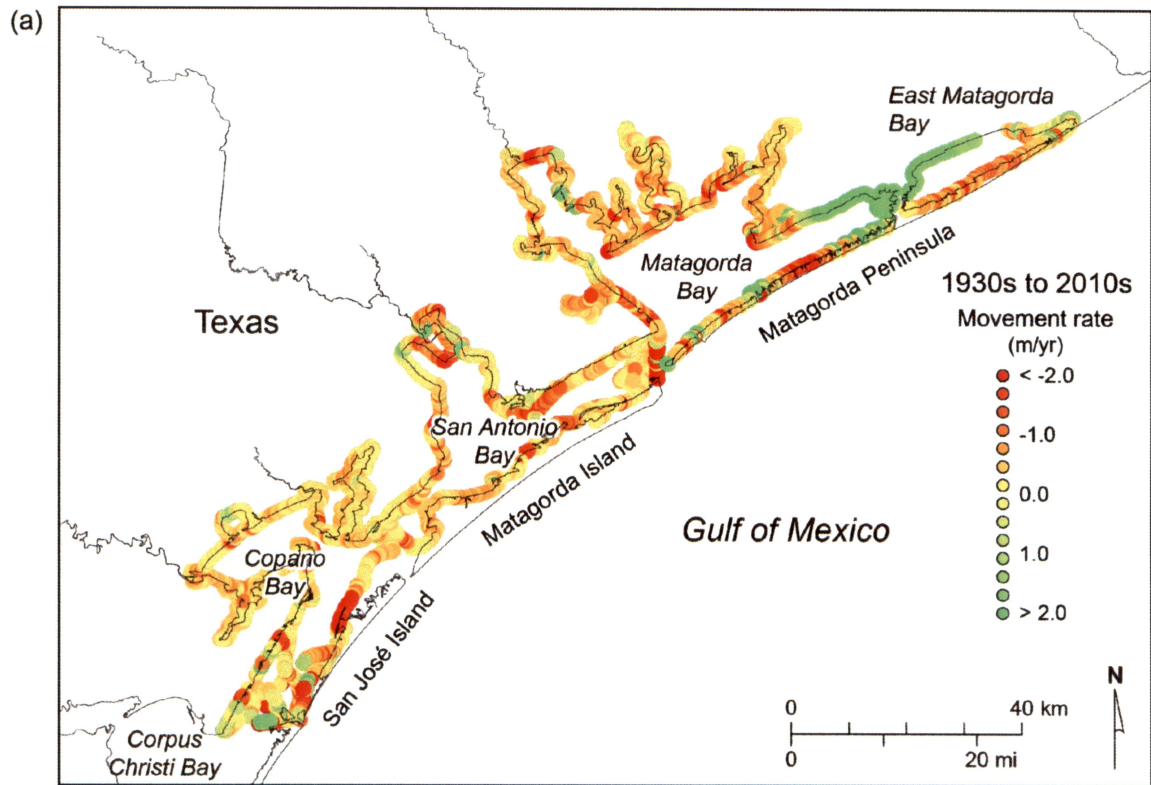


Figure 20. (a) Net long-term (1930s to 2010s) and (b) more recent (1950s, 1974, or 1982 to 2010s) shoreline movement rates in the Copano, San Antonio, and Matagorda Bay systems, central Texas coast.

Long-term Shoreline Movement in All Bays, 1930s to 2010s

Net shoreline movement in all bays between the 1930s and the 2010s, measured at 9,696 sites, was nearly zero (0.01 m/yr, table 5). This does not indicate that the shorelines were stable; rather, that shoreline retreat observed at nearly 80 percent of the sites was almost entirely offset by larger net shoreline advance at 20 percent of the measurement sites. The distribution of long-term shoreline movement rates is weighted toward retreat (fig. 21a), with the most common range being retreat at 0 to -0.3 m/yr (about 30 percent of all sites). This dominant retreat is nearly completely offset by almost 5 percent of the sites that have average advance rates greater than +3 m/yr (fig. 21a). As a result, the standard deviation of the rate distribution is high (4 m/yr, table 5). A map depicting rates of net long-term movement (fig. 20a) shows many areas throughout the bays that retreated, but relatively few, isolated areas where the shoreline advanced. The most prominent of the advancing areas was in eastern Matagorda Bay, where the Colorado River delta advanced across the bay from the mainland to Matagorda Peninsula.

Recent Shoreline Movement in All Bays, 1950s/74/82 to 2010s

More recent net shoreline movement, measured at 9,845 sites around the three bay systems, was more dominantly erosional than it was during the longer-term period, averaging -0.6 m/yr of retreat (fig. 20b; table 6). The shoreline retreated at 82 percent of the sites, with more than 20 percent of the rates falling within the most common range of retreat between -0.3 and -0.7 m/yr (fig. 21b). Combining the average movement rate with the total shoreline length yields an average annual land-loss rate of 64 ha/yr (table 6). Nearly all major shoreline segments in each of the bay systems underwent net retreat (fig. 20b), whereas advancing shorelines were limited to isolated segments in each of the major bay systems.

Shoreline Movement in the Copano Bay System

For the purposes of this report, the Copano Bay system includes Copano Bay proper as well as other large and small bays including Redfish Bay, Aransas Bay, Port Bay, Mission Bay, and St.

Table 5. Long-term (1930s to 2010s) shoreline movement statistics in the Copano, San Antonio, and Matagorda Bay systems, central Texas coast.

Bay Systems	n	Length (km)	Rate (m/yr)	Std. dev. (m/yr)	Area (ha/yr)	Range (m/yr)	Advancing sites (%)	Retreating sites (%)
All bays	9696	1064.6	-0.01	3.97	-1.0	-5.55 to 80.94	19.9%	79.6%
Copano Bay system	3092	337.8	-0.41	0.87	-14.0	-5.9 to 5.91	18.8%	80.6%
San Antonio Bay system	2312	267.9	-0.42	0.92	-11.3	-5.67 to 9.33	19.4%	79.9%
Matagorda Bay system	4292	458.7	0.51	5.84	23.2	-5.55 to 80.94	20.9%	78.7%
Copano Bay System Bays	n	Length (km)	Rate (m/yr)	Std. dev. (m/yr)	Area (ha/yr)	Range (m/yr)	Advancing sites (%)	Retreating sites (%)
Redfish Bay	414	60.8	-0.38	1.80	-2.3	-5.9 to 5.91	37.7%	61.8%
Aransas Bay	1057	110.9	-0.50	0.84	-5.5	-4.65 to 4.35	21.4%	78.3%
Copano Bay	561	57.8	-0.43	0.44	-2.5	-2.62 to 0.57	9.8%	88.9%
Port Bay	332	34.4	-0.41	0.29	-1.4	-1.8 to 0.44	7.2%	92.2%
Aransas River delta	74	7.3	-0.57	0.51	-0.4	-2.13 to 0.46	10.8%	87.8%
Mission Bay	130	13.1	-0.19	0.58	-0.3	-1.5 to 1.61	21.5%	76.9%
St. Charles Bay	524	52.9	-0.31	0.31	-1.6	-1.55 to 0.6	16.2%	83.4%
San Antonio Bay System Bays	n	Length (km)	Rate (m/yr)	Std. dev. (m/yr)	Area (ha/yr)	Range (m/yr)	Advancing sites (%)	Retreating sites (%)
Mesquite Bay	231	32.9	-0.22	0.46	-0.7	-1.58 to 0.99	34.2%	64.1%
Ayres Bay	45	4.9	-0.54	0.43	-0.3	-1.8 to -0.02	0.0%	100.0%
San Antonio Bay	764	81.9	-0.56	0.75	-4.6	-5.67 to 3.06	14.4%	84.3%
Hynes Bay	176	17.9	-0.33	0.80	-0.6	-2.92 to 2.08	31.3%	68.8%
Guadalupe Bay	123	15.0	-0.60	0.98	-0.9	-2.72 to 2.12	17.9%	82.1%
Mission Lake	85	8.4	0.20	3.05	0.2	-3.13 to 9.33	24.7%	75.3%
Shoalwater Bay	156	30.0	0.03	0.76	0.1	-1.8 to 3.76	65.4%	34.6%
Espiritu Santo Bay	689	71.8	-0.51	0.62	-3.7	-3.55 to 1.59	13.2%	86.4%
Pringle Lake	43	4.3	-0.17	0.35	-0.1	-1.16 to 0.32	37.2%	62.8%
Matagorda Bay System Bays	n	Length (km)	Rate (m/yr)	Std. dev. (m/yr)	Area (ha/yr)	Range (m/yr)	Advancing sites (%)	Retreating sites (%)
Matagorda Bay system (except East Matagorda Bay)	3701	389.3	0.32	5.92	12.3	-5.55 to 80.94	17.9%	81.7%
Matagorda Bay proper	1136	122.0	2.01	10.40	24.5	-5.55 to 80.94	32.0%	67.8%
-Western shore	228	23.5	-1.32	1.38	-3.1	-5.36 to 1.42	17.1%	82.9%
-Northern shore	462	46.2	0.10	2.62	0.5	-5.55 to 10.63	26.2%	73.6%
-Colorado delta shore	61	9.1	37.39	22.96	34.0	8.27 to 80.94	100.0%	0.0%
Matagorda Peninsula shore	385	42.9	0.66	3.88	2.8	-3.74 to 23.44	37.1%	62.6%
Powderhorn Lake	193	21.0	-0.56	0.44	-1.2	-1.85 to 1.77	6.2%	93.8%
Lavaca Bay	583	62.0	-0.57	0.74	-3.5	-3.15 to 7.57	11.3%	88.2%
Chocolate Bay	139	14.1	-0.17	0.61	-0.2	-0.96 to 4.37	21.6%	77.0%
Cox Bay	97	9.7	-0.16	1.74	-0.2	-1.61 to 8.01	14.4%	85.6%
Keller Bay	236	23.9	-0.60	0.54	-1.4	-3.85 to 0.38	7.2%	92.8%
Carancahua Bay	558	59.2	-0.43	0.54	-2.5	-3 to 3.4	14.2%	85.3%
Turtle Bay	203	20.9	-0.56	0.56	-1.2	-2.68 to 0.75	7.4%	92.6%
Tres Palacios Bay	411	41.2	-0.50	0.55	-2.1	-3.54 to 0.64	5.8%	93.4%
Oyster Lake	145	14.4	0.49	2.28	0.7	-1.94 to 7.92	29.0%	71.0%
East Matagorda Bay	591	69.3	1.70	5.20	11.8	-3.54 to 29.62	39.9%	59.9%
-Colorado delta shore	33	5.8	16.24	7.66	9.4	2.24 to 29.62	100.0%	0.0%
-Mainland shore	223	29.5	3.15	4.48	9.3	-1.71 to 21.98	76.2%	23.8%
-Matagorda Peninsula shore	335	33.8	-0.71	0.75	-2.4	-3.54 to 3.57	9.9%	89.9%

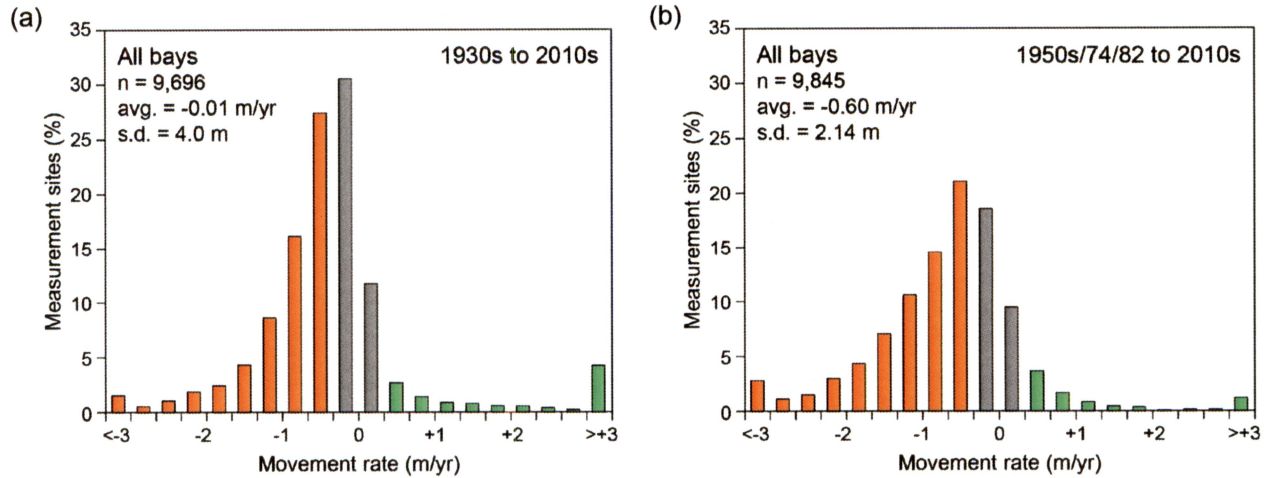


Figure 21. Distribution of longer-term (1930s to 2010s, left column) and more recent (1950s, 1974, or 1982 to 2010s, right column) shoreline movement rates in central Texas coastal bay systems (Copano, San Antonio, and Matagorda Bay systems combined).

Charles Bay (fig. 12). The Copano Bay system has approximately 338 km of bay shoreline that includes all major shoreline types. Notable are extensive back-barrier marshes and tidal flats along the Aransas Bay shoreline of San José Island, flood-tidal delta marshes and tidal flats on Redfish Bay near Aransas Pass, sandy and shelly spits fronting bay-margin marshes and tidal flats in Redfish Bay, sandy slopes adjacent to the Pleistocene Ingleside barrier island deposits along the eastern and part of the western shore of St. Charles Bay and the eastern shore of Copano Bay, high and low bluffs and bay-margin marshes on the western and southern shores of Copano Bay, Mission Bay, and Port Bay, and deltaic marshes at the Aransas River and Mission River deltas (fig. 12).

Long-term Shoreline Movement in the Copano Bay System, 1930s to 2014

Comparison of Copano Bay system shoreline positions in the 1930s with those extracted from the 2014 lidar survey reveals that the shoreline retreated at 81 percent of the 3,092 measurement sites (fig. 22; table 5). The average rate of long-term shoreline movement was retreat at -0.41 m/yr, the lowest net rate of the three major bay systems during the period (table 5). That

Table 6. Recent (1950s, 1974, or 1982 to 2010s) shoreline movement statistics in the Copano, San Antonio, and Matagorda Bay systems.

Bay Systems	n	Length (km)	Rate (m/yr)	Std. dev. (m/yr)	Area (ha/yr)	Range (m/yr)	Advancing sites (%)	Retreating sites (%)
All bays	9845	1064.6	-0.60	2.14	-63.5	-16.5 to 62.14	17.5%	82.1%
Copano Bay system	3157	337.8	-0.62	1.41	-21.0	-16.5 to 12.93	18.1%	81.4%
San Antonio Bay system	2338	267.9	-0.49	0.96	-13.0	-6.94 to 8.48	24.9%	74.9%
Matagorda Bay system	4350	458.7	-0.64	2.90	-29.3	-8.24 to 62.14	13.2%	86.5%
Copano Bay System Bays								
	n	Length (km)	Rate (m/yr)	Std. dev. (m/yr)	Area (ha/yr)	Range (m/yr)	Advancing sites (%)	Retreating sites (%)
Redfish Bay	453	60.8	-0.49	1.24	-3.0	-5.7 to 6.01	28.3%	70.9%
Aransas Bay	1109	110.9	-0.57	2.03	-6.3	-16.5 to 12.93	21.2%	78.4%
Copano Bay	557	57.8	-0.64	0.84	-3.7	-6.98 to 1.25	14.7%	84.9%
Port Bay	328	34.4	-0.67	0.55	-2.3	-4.26 to 1.27	6.4%	93.0%
Aransas River delta	67	7.3	-0.77	1.03	-0.6	-4.73 to 1.17	20.9%	79.1%
Mission Bay	129	13.1	-0.51	0.74	-0.7	-3.63 to 1.6	18.6%	80.6%
St. Charles Bay	514	52.9	-0.81	0.85	-4.3	-4.65 to 0.79	12.8%	86.4%
San Antonio Bay System Bays								
	n	Length (km)	Rate (m/yr)	Std. dev. (m/yr)	Area (ha/yr)	Range (m/yr)	Advancing sites (%)	Retreating sites (%)
Mesquite Bay	325	32.9	-0.37	0.53	-1.2	-1.86 to 1.23	25.2%	74.5%
Ayres Bay	40	4.9	-0.73	0.64	-0.4	-2.1 to 0.66	7.5%	92.5%
San Antonio Bay	768	81.9	-0.68	0.89	-5.6	-6.41 to 1.69	20.4%	79.2%
Hynes Bay	165	17.9	-0.35	1.02	-0.6	-3.22 to 3.03	25.5%	74.5%
Guadalupe Bay	135	15.0	-0.32	0.90	-0.5	-6.94 to 1.67	31.9%	68.1%
Mission Lake	84	8.4	0.19	1.81	0.2	-2.41 to 7.4	40.5%	59.5%
Shoalwater Bay	271	30.0	-0.20	1.05	-0.6	-4.36 to 8.48	32.1%	67.5%
Espiritu Santo Bay	517	71.8	-0.62	0.94	-4.4	-3.78 to 7.01	22.1%	77.8%
Pringle Lake	33	4.3	-0.03	0.85	0.0	-2.1 to 2.22	57.6%	42.4%
Matagorda Bay System Bays								
	n	Length (km)	Rate (m/yr)	Std. dev. (m/yr)	Area (ha/yr)	Range (m/yr)	Advancing sites (%)	Retreating sites (%)
Matagorda Bay system (all except East Matagorda Bay)	3709	389.3	-0.59	3.08	-23.0	-8.24 to 62.14	12.4%	87.3%
Matagorda Bay proper	1140	122.0	-0.27	5.43	-3.3	-8.24 to 62.14	18.9%	80.8%
-Western shore	233	23.5	-1.70	1.79	-4.0	-8.24 to 2.73	9.0%	91.0%
-Northern shore	457	46.2	-1.21	0.97	-5.6	-5.78 to 1.28	7.7%	92.1%
-Colorado delta shore	89	9.1	6.03	16.44	5.5	-2.36 to 62.14	28.1%	71.9%
Matagorda Peninsula shore	361	42.9	0.29	3.26	1.2	-6.75 to 19.58	37.4%	62.0%
Powderhorn Lake	196	21.0	-1.00	0.92	-2.1	-7.6 to 0.13	1.5%	98.0%
Lavaca Bay	598	62.0	-0.83	0.83	-5.1	-6.17 to 1.69	12.7%	87.3%
Chocolate Bay	131	14.1	-0.26	0.81	-0.4	-1.43 to 5.53	14.5%	84.7%
Cox Bay	86	9.7	-1.03	0.45	-1.0	-2.16 to -0.13	0.0%	100.0%
Keller Bay	231	23.9	-0.72	0.66	-1.7	-2.83 to 1.17	13.9%	85.7%
Carancahua Bay	576	59.2	-0.72	0.70	-4.3	-3.44 to 1.71	10.8%	89.1%
Turtle Bay	203	20.9	-0.69	0.68	-1.4	-3.66 to 0.47	7.9%	92.1%
Tres Palacios Bay	404	41.2	-0.61	0.66	-2.5	-4.49 to 0.98	4.2%	95.5%
Oyster Lake	144	14.4	-0.67	0.59	-1.0	-2.25 to 1	13.2%	86.1%
East Matagorda Bay	641	69.3	-0.92	1.39	-6.4	-6.89 to 10.17	17.6%	81.9%
-Colorado delta shore	55	5.8	-2.84	1.67	-1.6	-6.89 to 2.14	3.6%	94.5%
-Mainland shore	274	29.5	-0.58	1.36	-1.7	-4.04 to 1.99	32.1%	67.5%
-Matagorda Peninsula shore	312	33.8	-0.88	1.06	-3.0	-3.77 to 10.17	7.4%	92.3%

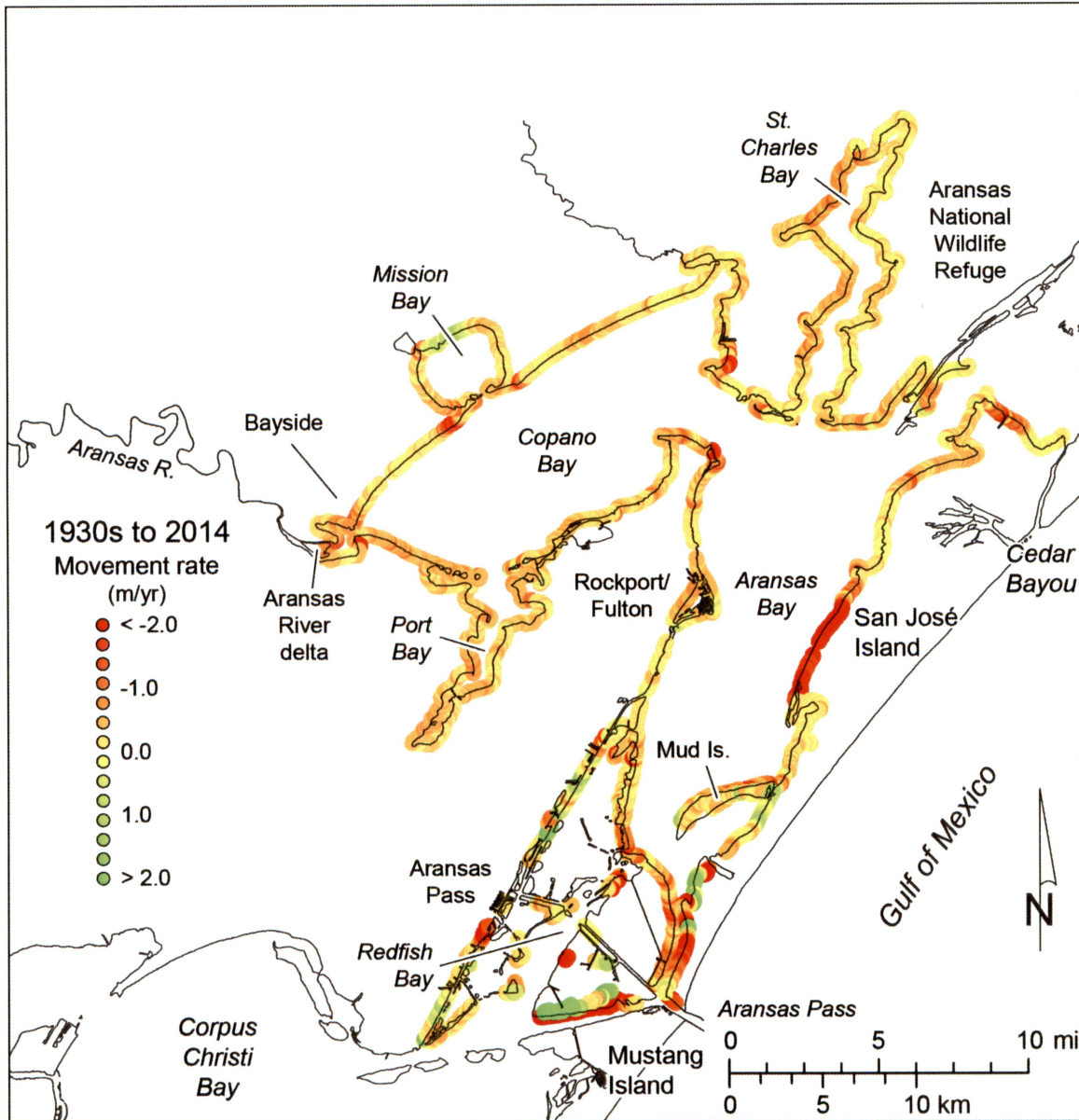


Figure 22. Net long-term shoreline movement rates in the Copano Bay system, 1930s to 2014.

average movement rate translates to an average annual land loss of 14 ha/yr in the Copano Bay system (table 5).

All the bays included within the Copano Bay system experienced net shoreline retreat at rates ranging from -0.19 to -0.57 m/yr (table 5). Among the component bays, the highest average rates of net retreat were along the Aransas River delta (-0.57 m/yr) and Aransas Bay (-0.50 m/yr). Copano Bay (-0.43 m/yr), Port Bay (-0.41 m/yr), Redfish Bay (-0.38 m/yr), and St. Charles Bay

(-0.31 m/yr) had slightly lower rates of net retreat. The distribution of shoreline movement rates in the three bays with the longest shoreline (Aransas, Copano, and St. Charles Bays, fig. 23) illustrates the dominance of retreating shorelines in these bays, but also indicates that the largest fraction falls within the lowest retreat-rate category (0 to -0.3 m/yr). Considering the length of bay shoreline, the average land loss rate was greatest in Aransas Bay (5.5 ha/yr), followed by Copano (2.5 ha/yr) and Redfish Bays (2.3 ha/yr).

Mission Bay, the most protected of the component bays, had the lowest average retreat rate (-0.19 m/yr, table 5). Here the Mission River has built a low delta that has partly filled a valley surrounded by Pleistocene bluffs, spits, and bay-margin marshes (figs. 24 and 25).

Extensive areas of net retreat include the back-barrier marshes and tidal-pass shoreline along San José Island and spits along the Corpus Christi Ship Channel on Redfish Bay and the southern shore of Aransas Bay (fig. 22). Limited areas of shoreline advance occurred along bay-margin marshes (1) backing spits along the Corpus Christi Ship Channel in Redfish Bay, (2) behind Mud Island in Aransas Bay, and (3) along the mainland shore of Redfish Bay. The deltaic and bay-margin marshes fronting the Mission River delta in Mission Bay also advanced during this period.

Recent Shoreline Movement in the Copano Bay System, 1982 to 2014

Recent shoreline movement (1982 to 2014) in the Copano Bay system is more erosional than the long-term movement (fig. 26; table 6). Shorelines in the Copano Bay system retreated at 81 percent of 3,157 measurement sites at an average rate of -0.62 m/yr, a 50-percent increase over long-term rates. Average land-loss rate for the bay system since 1982 is 21 ha/yr.

All of the component bays showed increases in net retreat rates as well; rates ranged from -0.49 to -0.81 m/yr. The highest retreat rates were measured around St. Charles Bay (-0.81 m/yr), the Aransas River delta (-0.77 m/yr), Port Bay (-0.64 m/yr), and Copano Bay (-0.64 m/yr). Considering the length of its shoreline, Aransas Bay had the highest rate of land loss at 6.3 ha/yr.

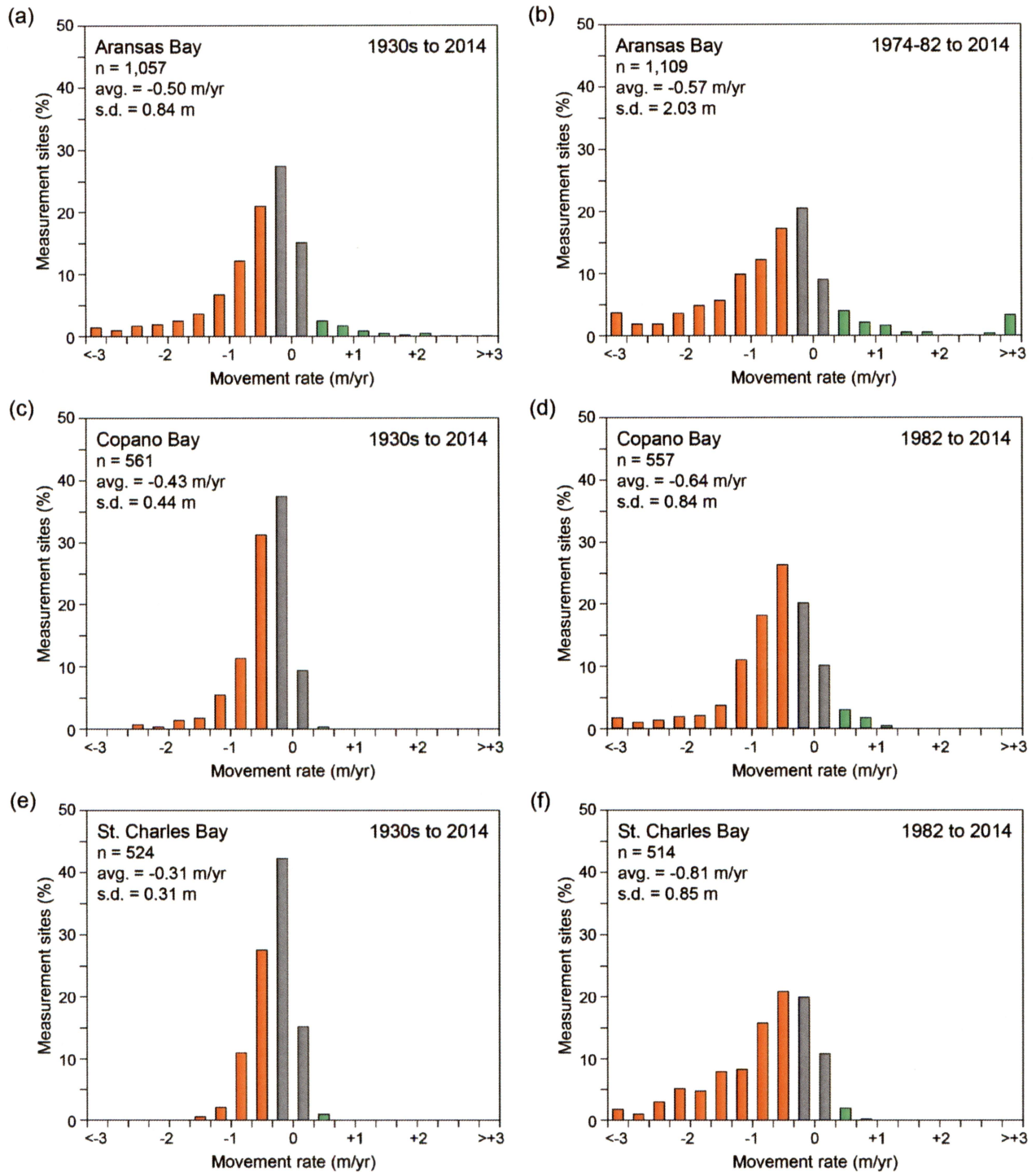


Figure 23. Distribution of longer-term (1930s to 2014, left column) and more recent (1982 to 2014, right column) shoreline movement rates in Aransas Bay, Copano Bay, and St. Charles Bay within the Copano Bay system.

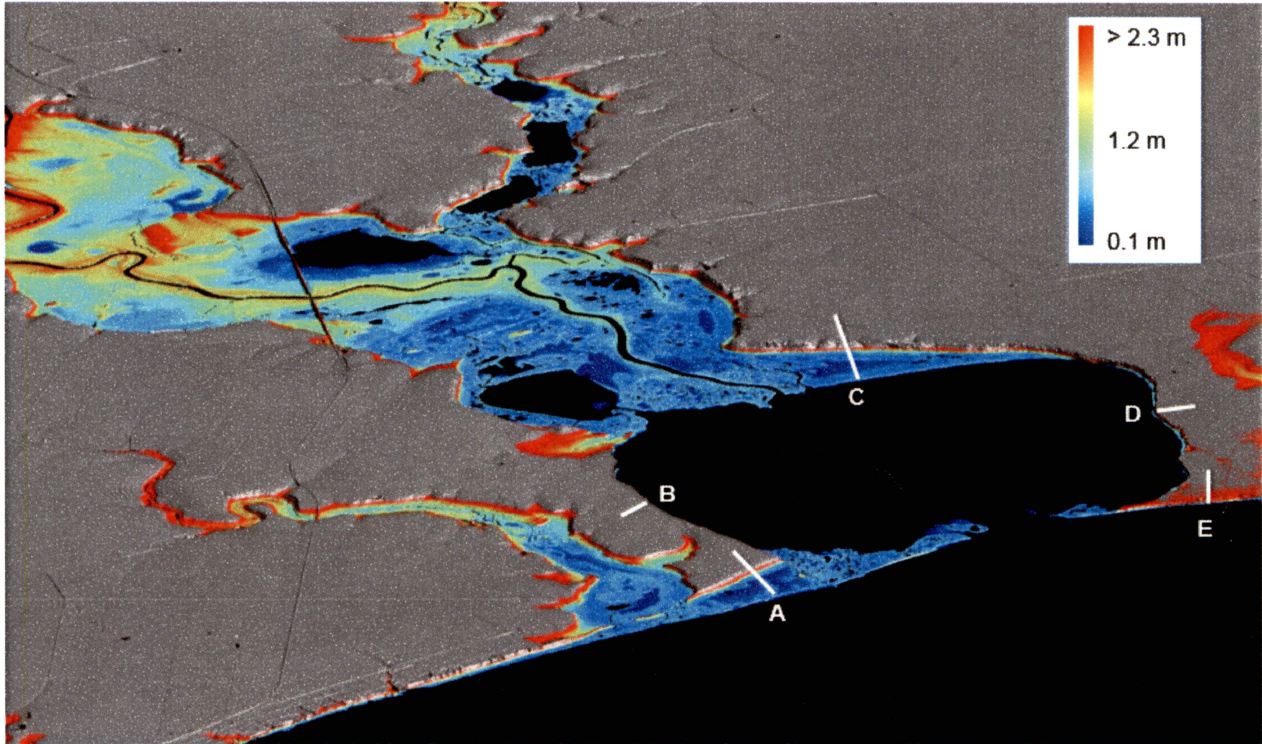


Figure 24. Digital elevation model (DEM) perspective of Mission Bay and the northern shoreline of Copano Bay. All elevations above 3.75 meters have been grayed to emphasize topography in the low-lying marsh and river valley adjacent to the Mission River.

Distribution of shoreline retreat rates in the three bays with the longest shoreline illustrate an increasing frequency of higher net retreat rates compared to the long-term distributions. The most common retreat rates for Copano and Aransas Bay shorelines increased from the 0 to -0.3 m/yr category to the -0.3 to -0.7 m/yr category (fig. 23b,d,f).

More extensive areas of significant erosion are evident in the more recent period (fig. 26). These include bay-margin marshes and sandy slopes fronting St. Charles Bay, back-island marshes and tidal flats on San José Island, tidal-pass shorelines and spits in southern Aransas Bay and Redfish Bay, and deltaic marshes along the Aransas River and Mission River deltas. Shoreline advance in the more recent period occurred in isolated, small areas around the bay system, including on bay-margin marshes behind migrating spits on Mud Island, some segments of tidal-pass shoreline at Aransas Pass, the nourished beach at Rockport, and the bay-margin marsh behind spits along the Corpus Christi Ship Channel in Redfish Bay.

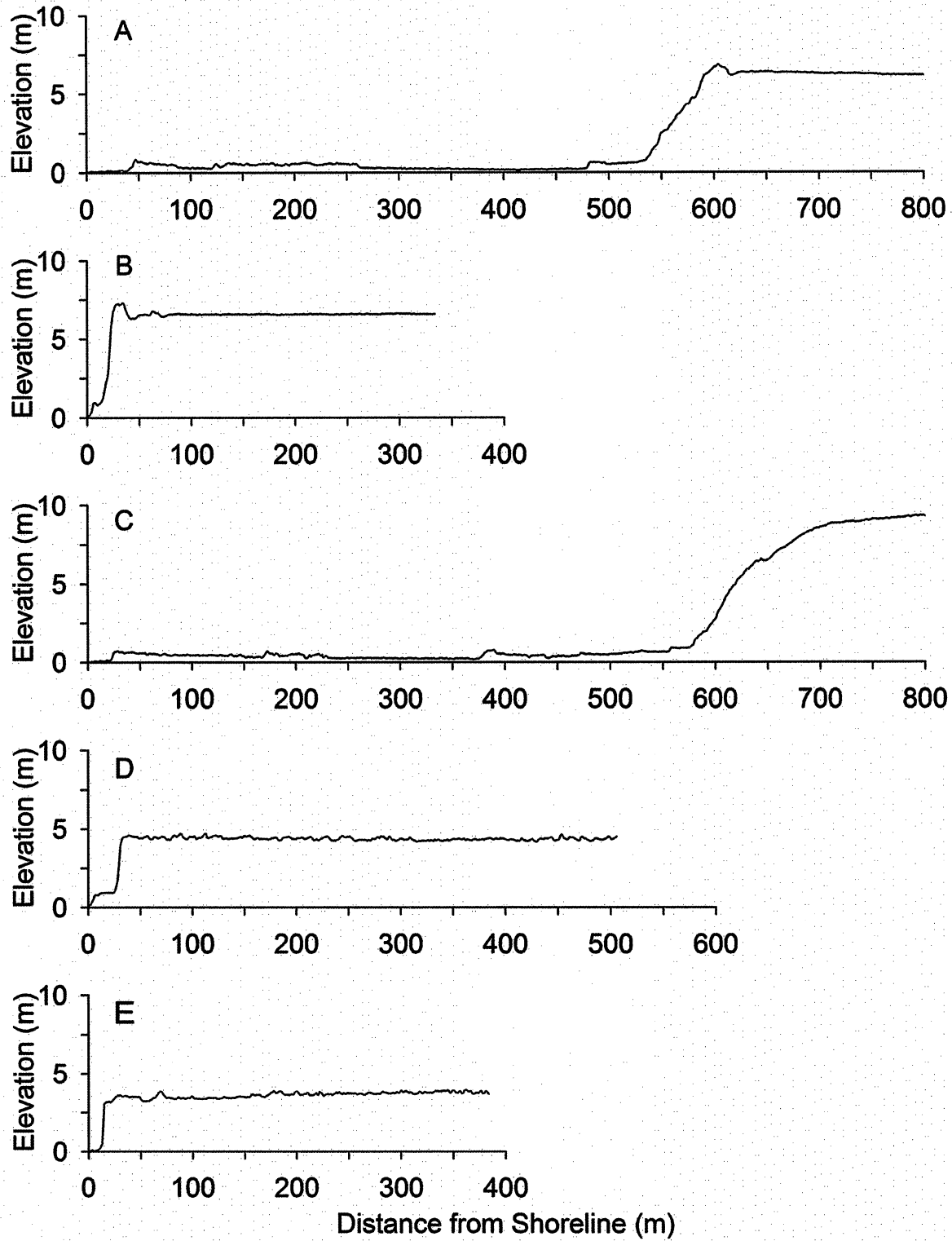


Figure 25. Representative profiles from bluff and marsh shorelines around Mission Bay and northern Copano Bay. Vertical exaggeration of the profiles is 15 to 1. Profile locations are shown on Figure 24.

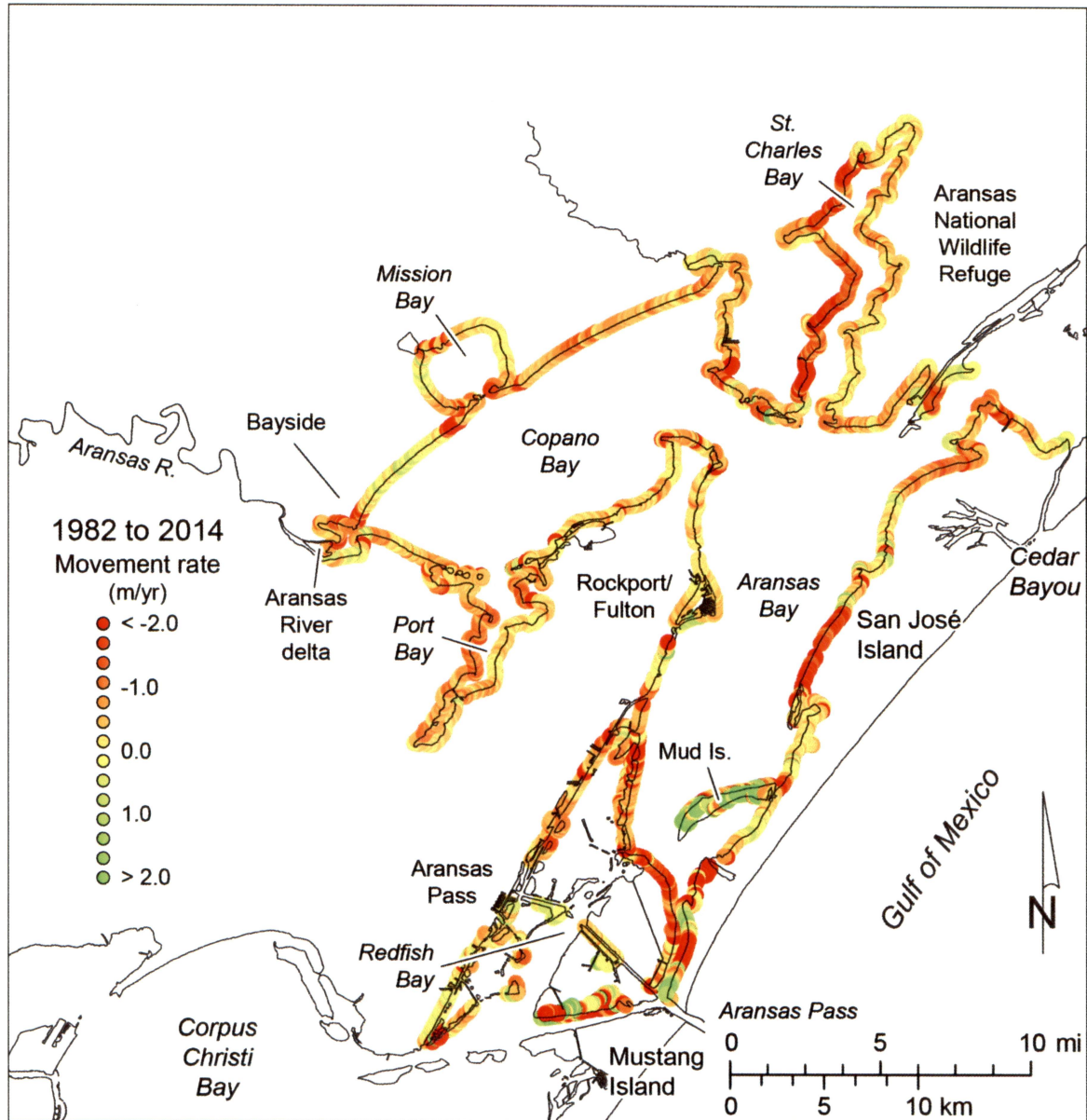


Figure 26. Net recent shoreline movement rates in the Copano Bay system, 1982 to 2014.

Shoreline Movement in the San Antonio Bay System

The San Antonio Bay system (fig. 13) includes San Antonio Bay, Mesquite Bay, Ayres Bay, Hynes Bay, Mission Lake, Guadalupe Bay, Shoalwater Bay, and Espiritu Santo Bay and has the least total shoreline length (about 268 km) of the three major bay systems (table 5). The bay system is separated from the Gulf of Mexico by Matagorda Island, a sandy barrier

island bounded by tidal passes at Pass Cavallo to the north and Cedar Bayou to the south. The Guadalupe delta, built by the San Antonio and Guadalupe Rivers, is a prominent geological feature at the head of San Antonio Bay.

Common shoreline types in the San Antonio Bay system (fig. 13) include extensive back-barrier marshes, tidal flats, and spits on the Matagorda Island shores of Mesquite Bay, Ayres Bay, and Espiritu Santo Bay; bay-margin marshes, tidal flats, and spits along the mainland shores of Mesquite, Ayres, Shoalwater, and Espiritu Santo Bays; flood-tidal delta marsh and tidal-pass shorelines on Espiritu Santo Bay at Pass Cavallo; sandy slopes and low and high bluffs on the western and eastern shores of San Antonio Bay; bay-margin marshes along Guadalupe Bay and Mission Lake; and extensive deltaic marshes on the Guadalupe delta on Hynes Bay, upper San Antonio Bay, Guadalupe Bay, and Mission Lake.

Long-Term Shoreline Movement in the San Antonio Bay System, 1930s to 2013

Of the 2,312 measurement sites around the San Antonio Bay system, 80 percent retreated between the 1930s and 2013 (fig. 27; table 5). The average shoreline retreat was -0.42 m/yr, similar to the rate for the same period in the Copano Bay system. Average land-loss rates in the bay system were 11.3 ha/yr.

Rate histograms for the three bays with the longest shorelines (fig. 28a,c,e) illustrate that retreating sites predominate in Mesquite Bay, San Antonio Bay, and Espiritu Santo Bay. The most common rates for each of these bay systems fall within the 0 to -0.3 m/yr category, which is slightly lower than the average rate of retreat. The highest average rates of retreat were measured in Guadalupe Bay (-0.56 m/yr), Ayres Bay (-0.54 m/yr), and Espiritu Santo Bay (-0.51 m/yr). Only Mission Lake (+0.20 m/yr) and Shoalwater Bay (+0.03 m/yr) underwent net shoreline advance for the period. The highest rates of land loss were measured in San Antonio Bay (4.6 ha/yr) and Espiritu Santo Bay (3.7 ha/yr).

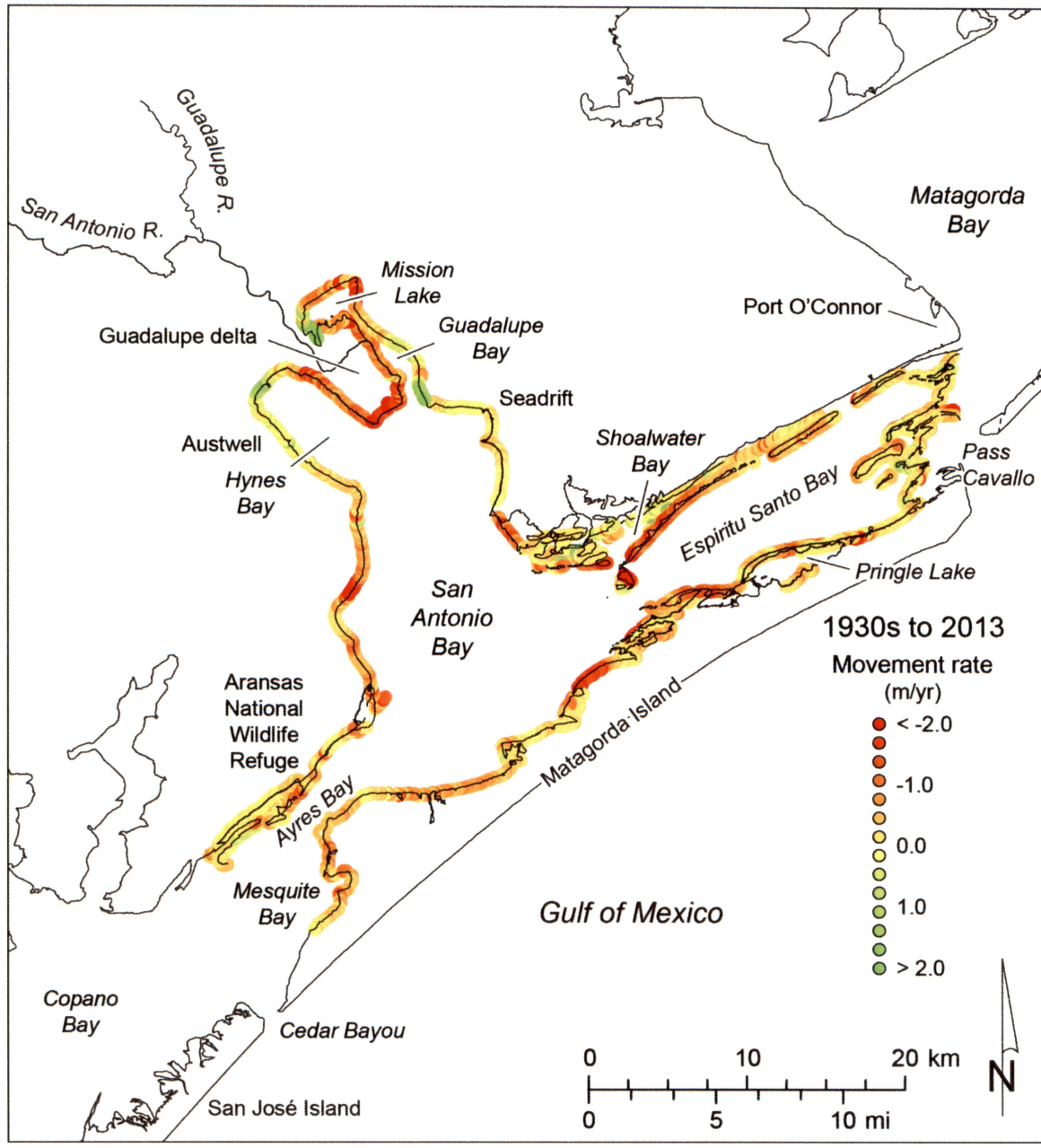


Figure 27. Net long-term shoreline movement rates in the San Antonio Bay system, 1930s to 2013.

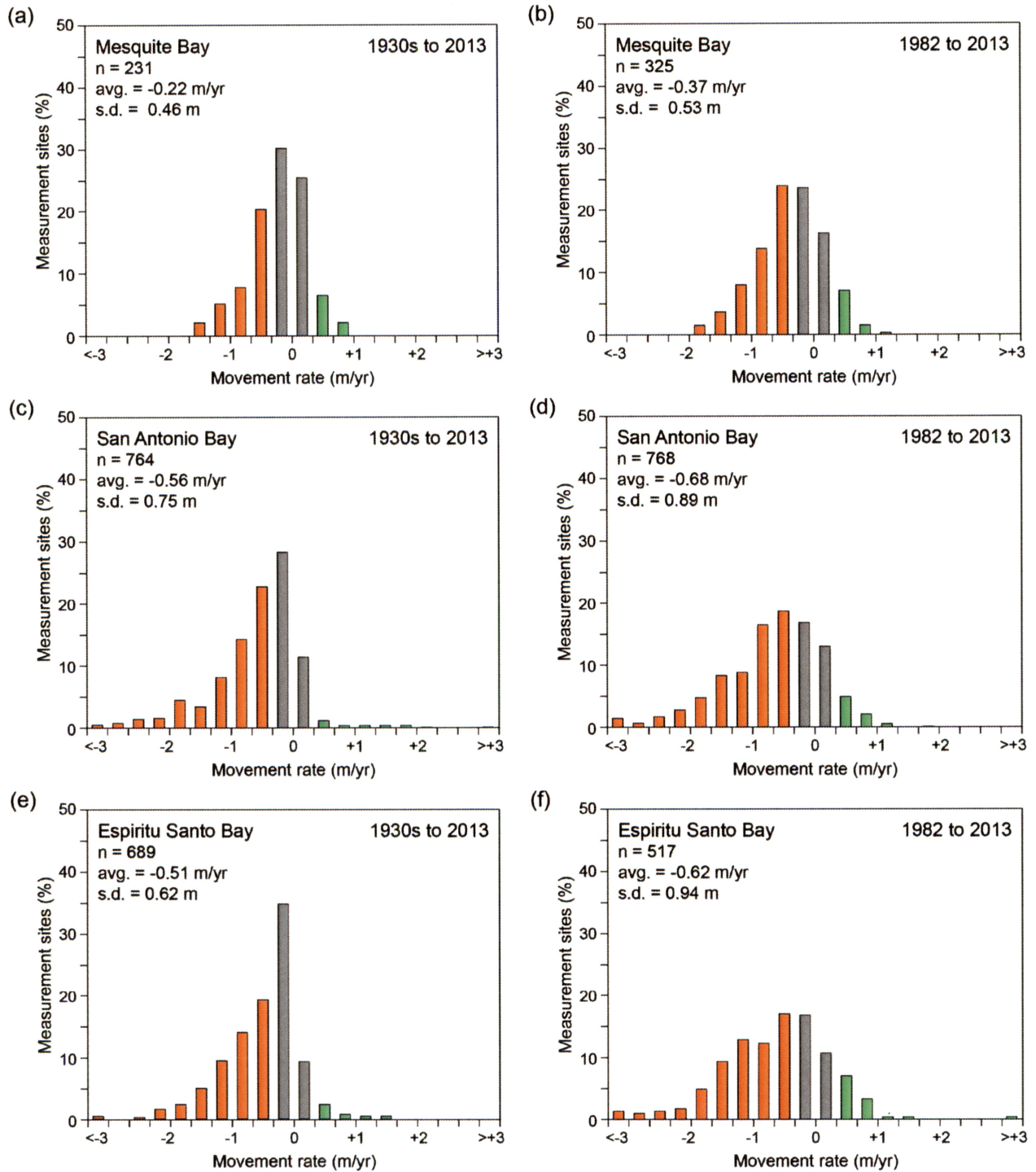


Figure 28. Distribution of longer-term (1930s to 2013, left column) and more recent (1982 to 2013, right column) shoreline movement rates in Mesquite Bay, San Antonio Bay, and Espiritu Santo Bay within the San Antonio Bay system.

Notable shoreline retreat occurred along the back-barrier marshes, tidal flats, and spits on the San Antonio and Espiritu Santo Bay shores of Matagorda Island; spits on the flood-tidal delta at Pass Cavallo; sandy slopes, spits, and bay-margin marshes on the western and eastern shores of San Antonio Bay; bay-margin marshes along Mission Lake; and most of the deltaic marsh shoreline around the Guadalupe delta (fig. 27). Retreat was also measured along the bay-margin marshes, sandy and shelly berm ridges, and sandy slopes on the northeastern margin of the Aransas National Wildlife Refuge in southwestern San Antonio Bay (figs. 29 and 30). The only significant advance was associated with Guadalupe delta progradation into Mission Lake, bay-margin advance at a sediment accumulation zone on the northwestern shore of Hynes Bay, and bay-margin marshes on Guadalupe Bay near the Guadalupe delta terminus.

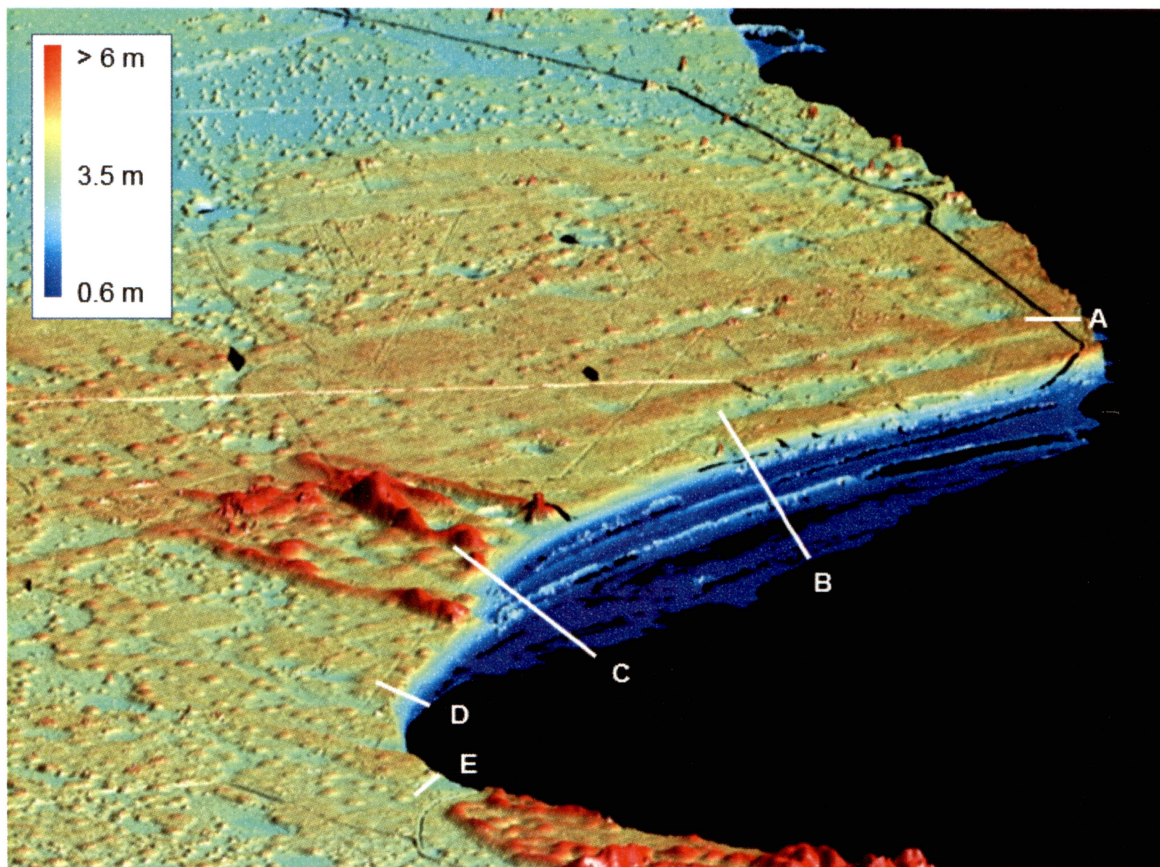


Figure 29. Perspective view of a lidar-derived DEM of the southwestern shoreline of San Antonio Bay at the Aransas National Wildlife Refuge. Dominant shoreline types are Pleistocene sandy slopes and bay-margin marshes. Bayward of the sandy slopes, shell-berm ridges are separated by swales that are filled with brackish- to fresh-water marshes. Elevation profiles A through E are shown on fig. 30.

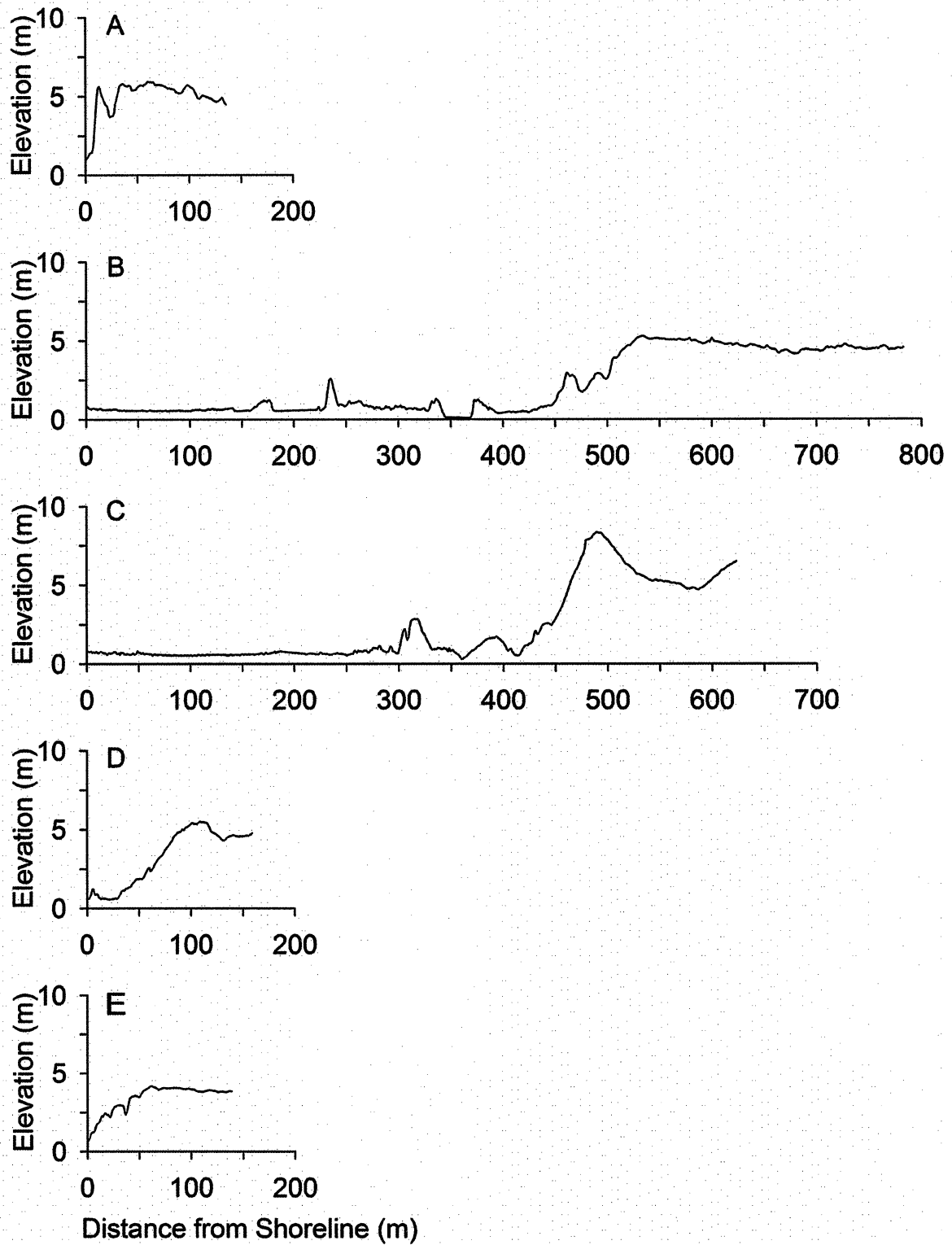


Figure 30. Representative profiles across shoreline types along the southwestern shoreline of San Antonio Bay. Vertical exaggeration of the profiles is 15 to 1. Profile locations are shown on fig. 29.

Recent Shoreline Movement in the San Antonio Bay System, 1982 to 2013

During the more recent period between 1982 and 2013, the proportion of measurement sites where the shoreline retreated decreased to 75 percent, but the average rate of retreat increased to -0.49 m/yr. Resulting land-loss rates for the bay system also increased 15 percent to 13 ha/yr (fig. 31; table 6). In addition, shorelines in all component bays except Mission Lake underwent retreat. The three bays with the longest shorelines (Mesquite, San Antonio, and Espiritu Santo Bays) each had significant increase in average retreat rates from the long-term rates. The highest-frequency rate category shifted from the 0 to -0.3 m/yr category between the 1930s and 2013 to the -0.3 to -0.7 m/yr category in the more recent period (fig. 28).

The highest average rates of retreat were measured for shorelines in Ayres Bay (-0.73 m/yr), San Antonio Bay (-0.68 m/yr), and Espiritu Santo Bay (-0.62 m/yr). Rates of land loss were highest for shorelines along San Antonio Bay (5.6 ha/yr) and Espiritu Santo Bay (4.4 ha/yr).

Overall patterns of shoreline movement in the more recent period were similar to the long-term pattern. The only areas of significant shoreline advance were along bay-margin marshes at the sediment accumulation zone at the head of Hynes Bay and the marsh prograding into Mission Bay at the Guadalupe delta (fig. 31). Extensive erosion continued on the back-barrier marshes, tidal flats, and spits on Matagorda Island, the deltaic marshes on the Guadalupe delta along Hynes, San Antonio, and Guadalupe Bay, and along the bay-margin marshes and sandy slopes on the western and eastern shores of San Antonio Bay.

Shoreline Movement in the Matagorda Bay System

The Matagorda Bay system is the largest of the three major bay systems on the central Texas coast. Bay shorelines within this system have a total length of more than 459 km, constituting nearly half of the total shoreline length in the three bay systems (table 5). Its numerous bays are separated from the Gulf of Mexico by Matagorda Peninsula, a sandy barrier peninsula that has

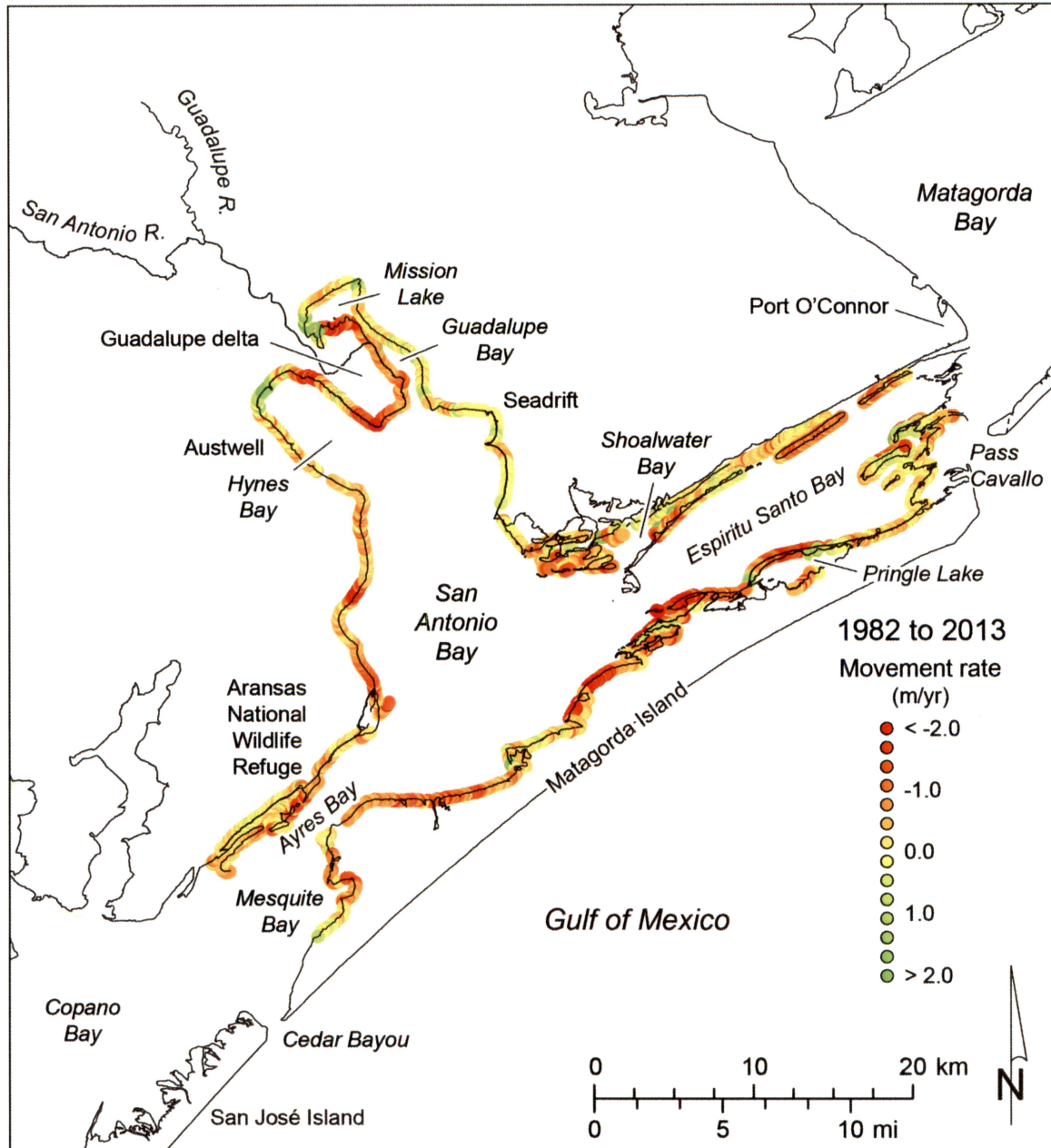


Figure 31. Net recent shoreline movement rates in the San Antonio Bay system, 1982 to 2013.

migrated southwestward by longshore drift from the fluvial and deltaic headland constructed by the Brazos and Colorado Rivers (fig. 14).

The component bays with the longest shoreline are Matagorda Bay (122 km on its southwestern, northern, Colorado delta, and Matagorda Peninsula shorelines), East Matagorda Bay (69 km on the northern mainland, Matagorda Peninsula, and Colorado delta shorelines), and Lavaca Bay (69 km on its southwestern, northern, and northeastern shores). Other significant water bodies in the system are Powderhorn and Oyster Lake and Chocolate, Cox, Keller, Carancahua, Turtle, and Tres Palacios Bays (fig. 14).

Relatively extensive shoreline types (table 3) found around the bay system are (a) back-barrier marsh, tidal flats, and sand and shell spits fringing Matagorda Peninsula on Matagorda and East Matagorda Bays; (b) deltaic marshes on the Colorado River delta in Matagorda and East Matagorda Bays, at the Garcitas Creek and Lavaca River deltas at the head of Lavaca Bay, and in small areas at the heads of Keller and Carancahua Bays; (c) bay-margin marshes and tidal flats along parts of Powderhorn and Oyster Lakes and Chocolate, Cox, Keller, Carancahua, Turtle, and Tres Palacios Bays; (d) sandy slopes of the Ingleside barrier island on the southwestern mainland shore of Matagorda Bay near Port O'Connor and the southeastern shore of Powderhorn Lake; (e) sandy and shelly spits at the intersections of bays along the mainland shores of Matagorda and Lavaca Bays; and (f) low and high bluffs on the mainland shore of northern Matagorda Bay and parts of Lavaca, Cox, Keller, Carancahua, Turtle, and Tres Palacios Bays.

Long-term Shoreline Movement in the Matagorda Bay System, 1930s to 2015

Comparisons of shoreline positions in the 1930s with those determined from the 2015 lidar survey at 4,292 sites distributed around the Matagorda Bay system (fig. 32) reveal that the shoreline has retreated at 79 percent of the sites and that the most common shoreline movement rate in two of the three largest component bays is -0.7 to -1.0 m/yr for Matagorda Bay and -0.3 to -0.7 m/yr for Lavaca Bay (fig. 33a,c). Nevertheless, the average rate of shoreline movement

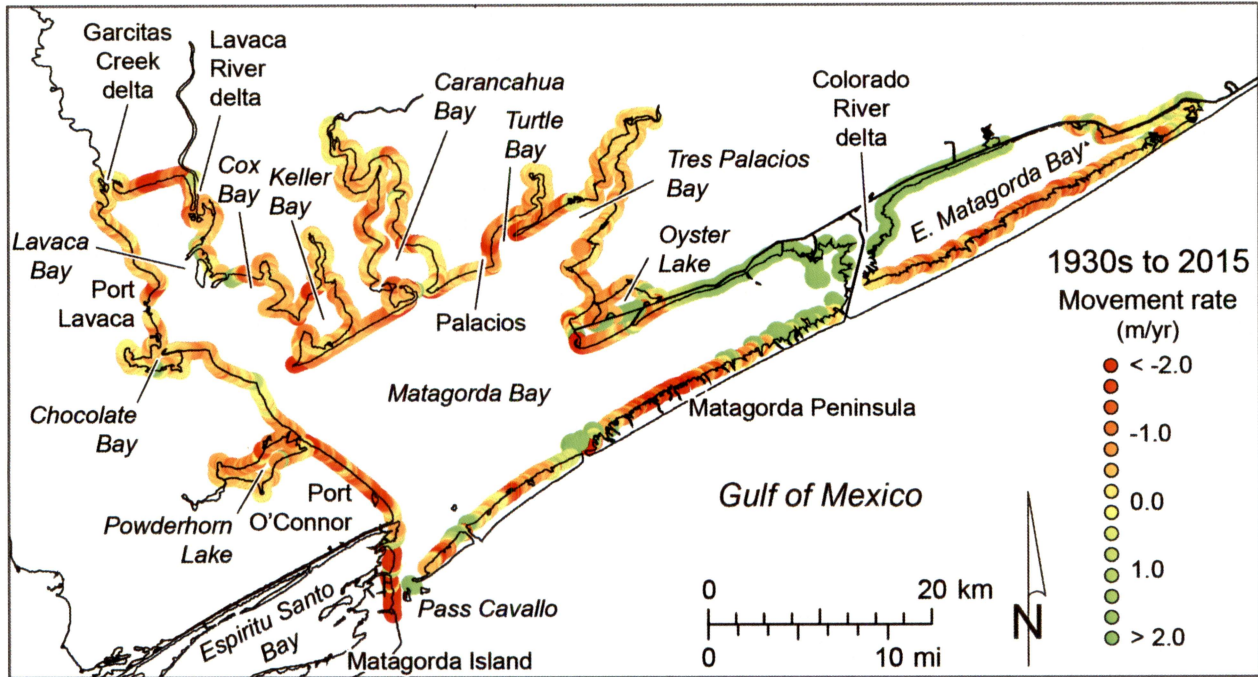


Figure 32. Net long-term shoreline movement rates in the Matagorda Bay system, 1930s to 2015.

in the Matagorda Bay system is net advance at $+0.51$ m/yr, translating to an average land gain of 23.2 ha/yr between the 1930s and 2015 (table 5). Although the shoreline retreated at the large majority of measurement sites, significant shoreline advance in East Matagorda Bay (the most common rate of change in this bay is advance at greater than $+3$ m/yr, fig. 33e) offsets dominant retreat in the rest of the bay system, resulting in net land gain since the 1930s.

Unlike other bay systems, component bays in the Matagorda Bay system exhibit two modes of movement. Shorelines along most bay components dominantly retreated. Average retreat rates in these bays were similar to those in other bay systems (table 5). Highest average rates of retreat were measured along the western shore of Matagorda Bay (-1.32 m/yr) and in Keller Bay (-0.60 m/yr), Lavaca Bay (-0.57 m/yr), Powderhorn Lake (-0.56 m/yr), Turtle Bay (-0.56 m/yr), and Tres Palacios Bay (-0.50 m/yr). Most of the other bays have lower average retreat rates. Conversely, several bay shoreline segments show advance at high average rates that are not present in other bay systems. These high average advance rates are found along the Colorado River delta shore in Matagorda Bay (advance at $+37.4$ m/yr) and East Matagorda Bay

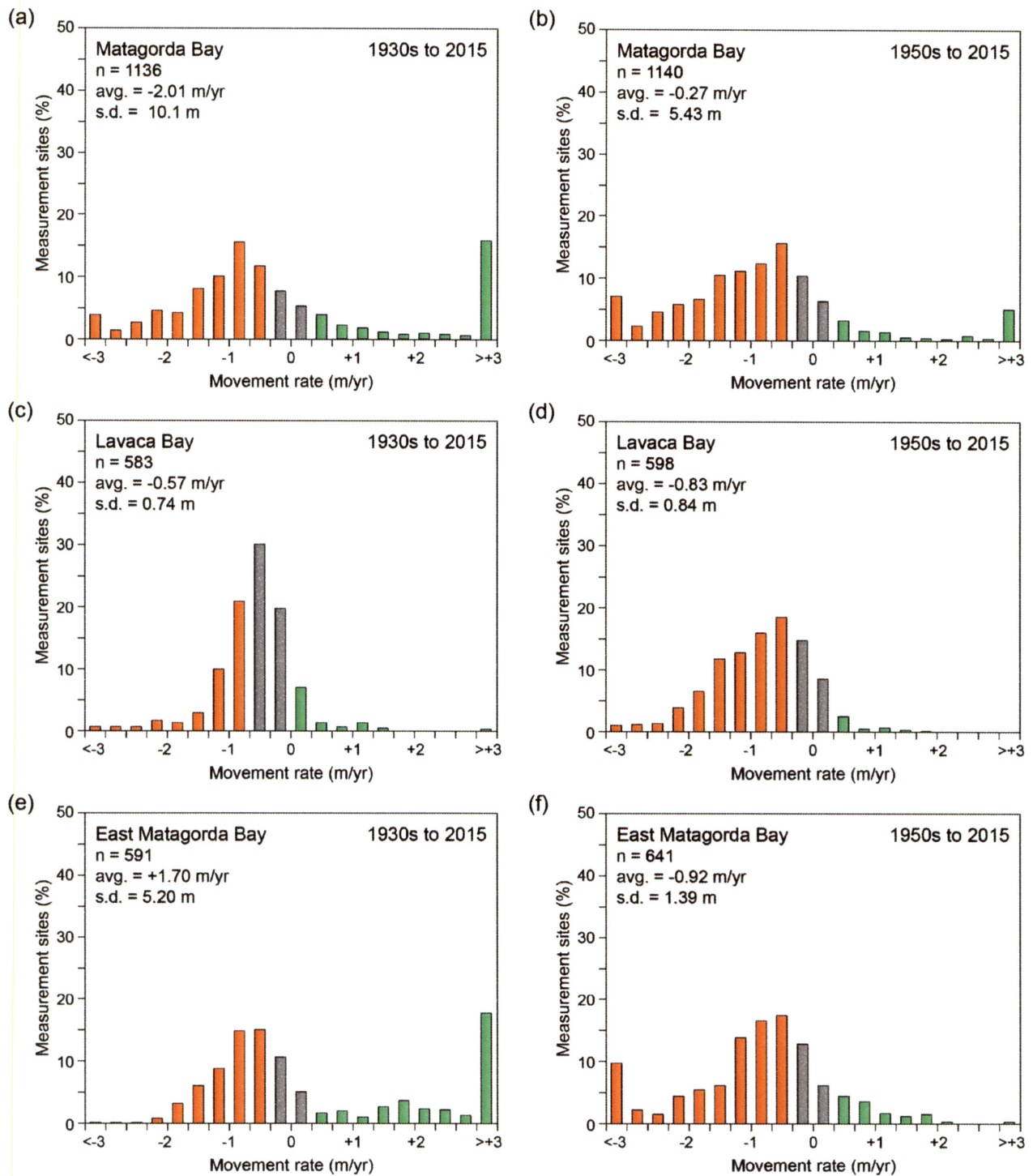


Figure 33. Distribution of longer-term (1930s to 2015, left column) and more recent (1950s to 2015, right column) shoreline movement rates in Matagorda Bay, Lavaca Bay, and East Matagorda Bay within the Matagorda Bay system.

(+16.2 m/yr). The elevated advance rates of the Colorado River delta are associated with its rapid progradation across the eastern arm of Matagorda Bay following the clearing of a logjam on the Colorado River in 1929 (McGowen and Brewton, 1975) and the subsequent diversion into Matagorda Bay (fig. 34). Net rates of land gain on the Colorado delta shoreline in Matagorda and East Matagorda Bays is 43.4 ha/yr (table 5). Elsewhere in the bay system, the highest rates of net land loss are along shorelines in Lavaca Bay (3.5 ha/yr), the western shore of Matagorda Bay (3.1 ha/yr), and Carancahua Bay (2.5 ha/yr).

In addition to the dominant land gain along the deltaic marshes of the Colorado River delta and adjacent mainland shore in Matagorda and East Matagorda Bays (fig. 32), areas of shoreline

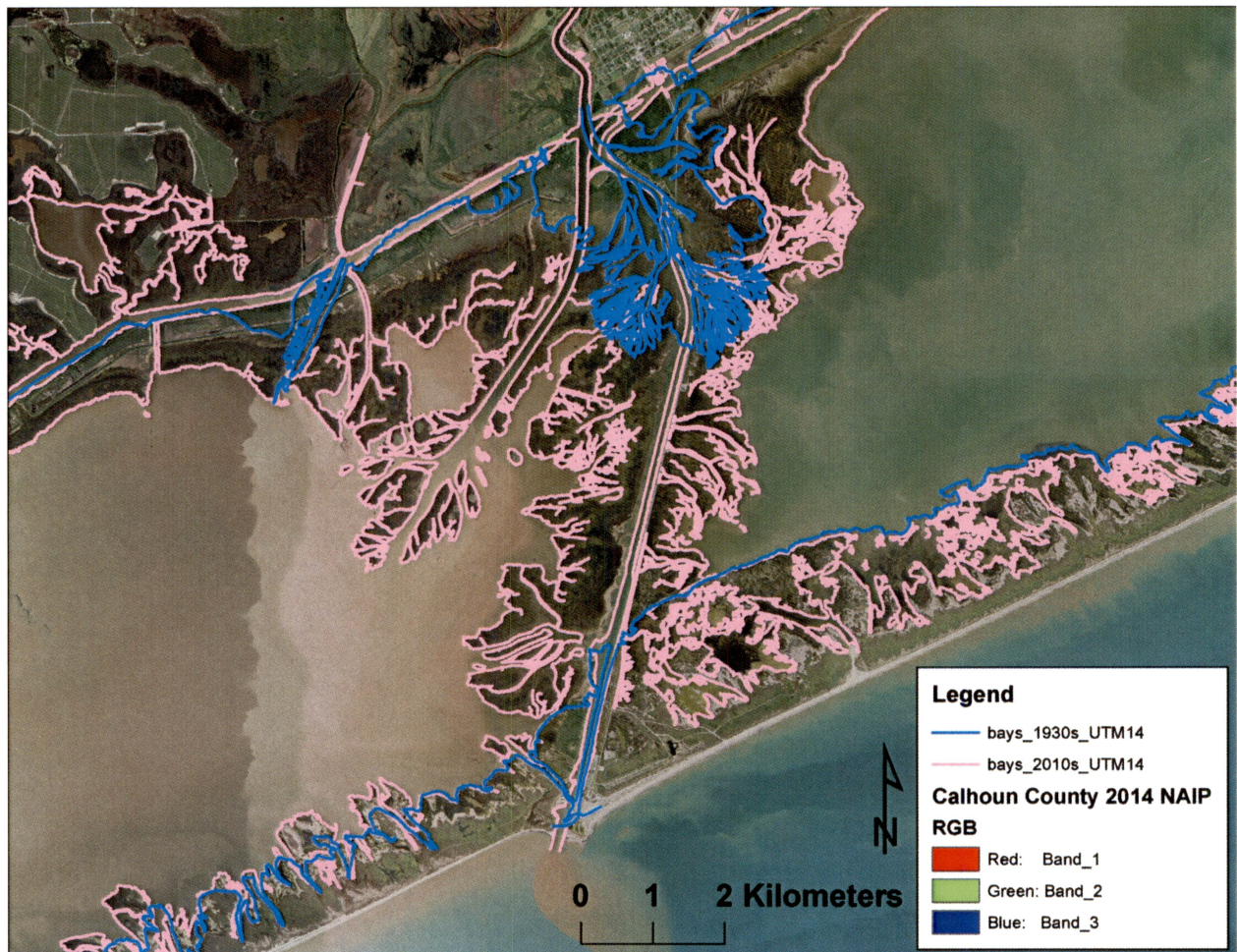


Figure 34. Shoreline position in the 1930s (blue) and in 2015 (pink) at the Colorado River delta in Matagorda Bay.

advance were located along the back-barrier marshes, tidal flats, and spits on Matagorda Peninsula on Matagorda Bay. These local areas of advance are related to shoreline progradation into the bay at breaches that are periodically opened through Matagorda Peninsula during storms. Storm-surge flood currents transport sediment bayward across the peninsula at these preferred washover sites, serving to migrate the island bayward.

Significant retreating shoreline segments were located on the back-barrier marsh, tidal flat, and spit shorelines on Matagorda Peninsula in Matagorda and East Matagorda Bays. Bay-margin marshes retreated along the northwestern shore of Powderhorn Lake, Chocolate Bay, and parts of Cox and Keller Bays and the mainland shore of East Matagorda Bay. Tidal-pass, flood-tidal delta marsh, sandy slope, and spit shorelines along western Matagorda Bay had high net rates of retreat, as did spit shorelines on northern Matagorda Bay at Keller and Carancahua Bays, Tres Palacios and Turtle Bays, and fronting Oyster Lake. Significant net retreat also occurred along bluffs and deltaic marshes on Lavaca Bay near Garcitas Creek (fig. 32).

Recent Shoreline Movement in the Matagorda Bay System, 1950s to 2015

The most recent shoreline position examined in the original analysis of Matagorda Bay system shoreline movement (McGowen and Brewton, 1975) was determined from 1950s aerial photographs. We used that shoreline to assess recent shoreline movement by comparing its position with the 2015 lidar-derived shoreline. For this period of approximately 60 years, Matagorda Bay shorelines retreated at more than 86 percent of 4,350 measurement sites, which is an increase over the longer-term period and is the highest percentage of retreating shorelines among the bay systems of the central Texas coast (fig. 35; table 6). Average rates of retreat were -0.64 m/yr, the highest average retreat rate of the bay systems and significantly changed from long-term net advance. This rate translates to an average land-loss rate of 29.3 ha/yr, nearly half of the total recent land-loss rate estimated for the combined bay systems (63.5 ha/yr).

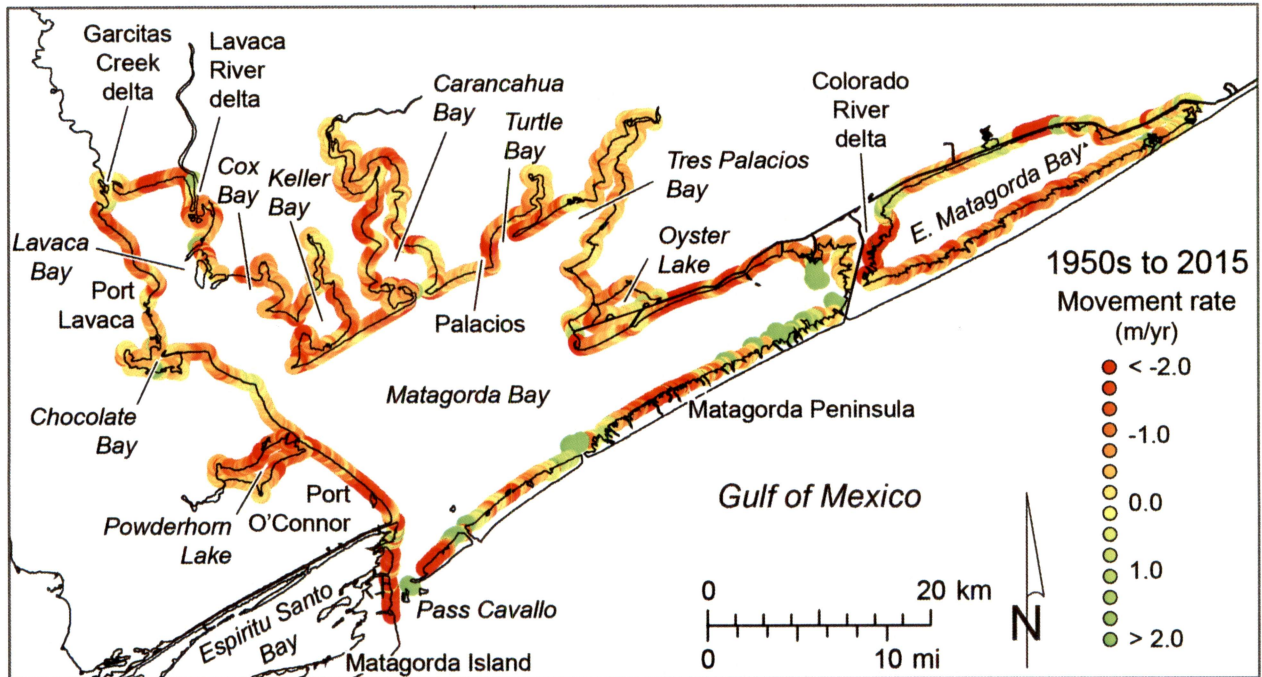


Figure 35. Net recent shoreline movement rates in the Matagorda Bay system, 1950s to 2015.

Distributions of shoreline change rates show a significant shift from long-term rates, primarily as a result of the end of the major progradation phase of the Colorado River delta. For the three largest bays by shoreline length, the most common rates of shoreline movement were between -0.3 and -0.7 m/yr for Matagorda, East Matagorda, and Lavaca Bays (fig. 33b,d,f). The highest average retreat rates were measured along the Colorado delta shore in East Matagorda Bay (-2.84 m/yr), the western shore of Matagorda Bay (-1.70 m/yr), and the northern shore of Matagorda Bay (-1.21 m/yr). The Colorado River delta shore continued to advance into Matagorda Bay at the mouth of the diversion ($+6.03$ m/yr). Shorelines on most other bay segments retreated at average rates of -0.26 to -1.03 m/yr (fig. 35; table 6). Considering shoreline length and average rates of movement, East Matagorda Bay had the highest rate of land loss (6.4 ha/yr), followed by the northern shore of Matagorda Bay (5.6 ha/yr) and Lavaca Bay (5.1 ha/yr). Greatest land gain was along the deltaic marshes of the Colorado River delta in Matagorda Bay (5.5 ha/yr).

Although areas of shoreline advance are less extensive than they were during the long-term period, limited areas of advance remained along the deltaic marsh on the western side of the Colorado River delta and the bay-margin marshes, tidal flats, and spits on the Matagorda Bay shore of Matagorda Peninsula (fig. 35). Areas of advance on Matagorda Peninsula were located at breaches in the peninsula where storm-surge flood currents transport sand from the Gulf beaches toward the bays and deposit some of it there to advance the shoreline into the bay while the Gulf shoreline retreats. Advance was also measured on Matagorda Peninsula near the Matagorda Ship Channel and at the migrating terminus of the peninsula at Pass Cavallo.

Notable areas of erosion include the deltaic marshes of the Colorado delta in East Matagorda Bay; back-barrier marshes, tidal flats, and spits on Matagorda Peninsula in most of East Matagorda Bay and segments along Matagorda Bay between the storm-breached areas; sandy slopes, spits, flood-tidal delta marshes, tidal flats, and tidal-pass shorelines along western Matagorda Bay; bay-margin marshes in Powderhorn Lake and several other bays; spits along Matagorda Bay at Oyster Lake, Lavaca Bay, and Carancahua Bay; and bluffs and deltaic marshes on Lavaca Bay (fig. 35).

Shoreline Movement by Shoreline Type

We used properties such as elevation, slope, substrate material and consolidation, depositional environment, and vegetation characteristics to classify shorelines by type, which resulted in 11 shoreline-type categories (table 3) that are each represented in the Copano Bay (fig. 12), San Antonio Bay (fig. 13), and Matagorda Bay (fig. 14) systems. Each of the nearly 10,000 measurement sites was classified according to shoreline type, allowing a determination of relative abundance (fig. 10) and an analysis of shoreline movement among the types and across the bay systems. The determination of susceptibility to erosion was based on physical properties of the shoreline and did not consider external factors that affect erosion rate, such as shoreline orientation and wave fetch. We examined shoreline movement for both the long-term (1930s to 2010s) and more recent (1950s/74/82 to 2010s) periods.

Long-term Shoreline Movement by Shoreline Type

Average rates of net shoreline movement for the long-term period were erosional for all shoreline types except deltaic marsh (fig. 36a). Retreat rates were highest for shorelines along tidal passes (-0.79 m/yr), sandy and shelly spits (-0.72 m/yr), and high bluffs (-0.54 m/yr). Lowest rates of net retreat were measured along the fan delta (-0.18 m/yr) and bay-margin marsh and tidal-flat shorelines (-0.05 m/yr). Highest net rates of movement were measured for deltaic marsh shorelines, a fact that highlights the extensive progradation of the Colorado River delta across the eastern part of Matagorda Bay beginning in 1929.

Combining the net shoreline movement rates with the total shoreline length classified as a particular type yields an estimate of land loss or gain for that shoreline type (fig. 37). High rates of land loss occurred along sandy and shelly spits (10.6 ha/yr), high and low Pleistocene bluffs (7.9 ha/yr combined), and back-barrier marshes and tidal flats (5.5 ha/yr). These land losses were offset by large land-area gains at the Colorado River delta in Matagorda Bay (30.5 ha/yr).

Short-term Shoreline Movement by Shoreline Type

Generally similar relative movement trends are seen in the comparison of more recent shoreline positions (fig. 36b), although all shoreline types retreated at higher average rates over the more recent period. Highest rates of net retreat were measured for shorelines along tidal passes (-1.67 m/yr), high Pleistocene bluffs (-0.86 m/yr), and sandy and shelly spits (-0.84 m/yr). Deltaic marsh advanced at very low rates (+0.02 m/yr) over the more recent period, largely because the rapid deltaic progradation across eastern Matagorda Bay ended. All other shoreline types retreated at average rates of -0.52 m/yr or more.

The increases in movement rates in the more recent period, along with relative changes in average rates among shoreline types, changed the total land-loss contributions among the types (fig. 37b). Highest rates of land loss were measured at shorelines along bay-margin marsh or tidal flats (17.3 ha/yr, a tenfold increase over the long-term land-loss rate), sandy and shelly spits

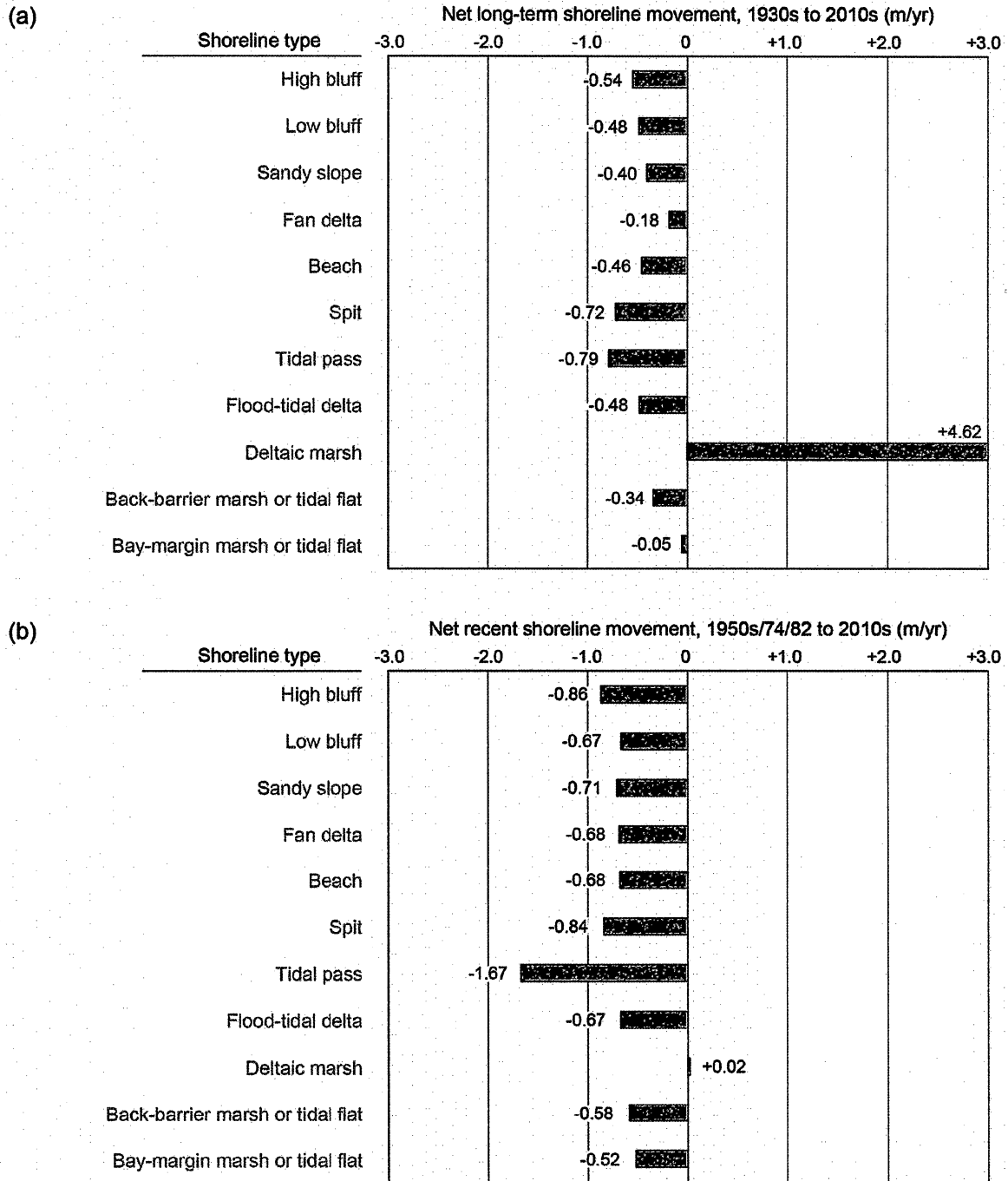


Figure 36. Average (a) long-term (1930s to 2010s) and (b) more recent (1950s/74/82 to 2010s) net shoreline movement rates for common bay shoreline types (table 3) in the Copano, San Antonio, and Matagorda Bay systems.

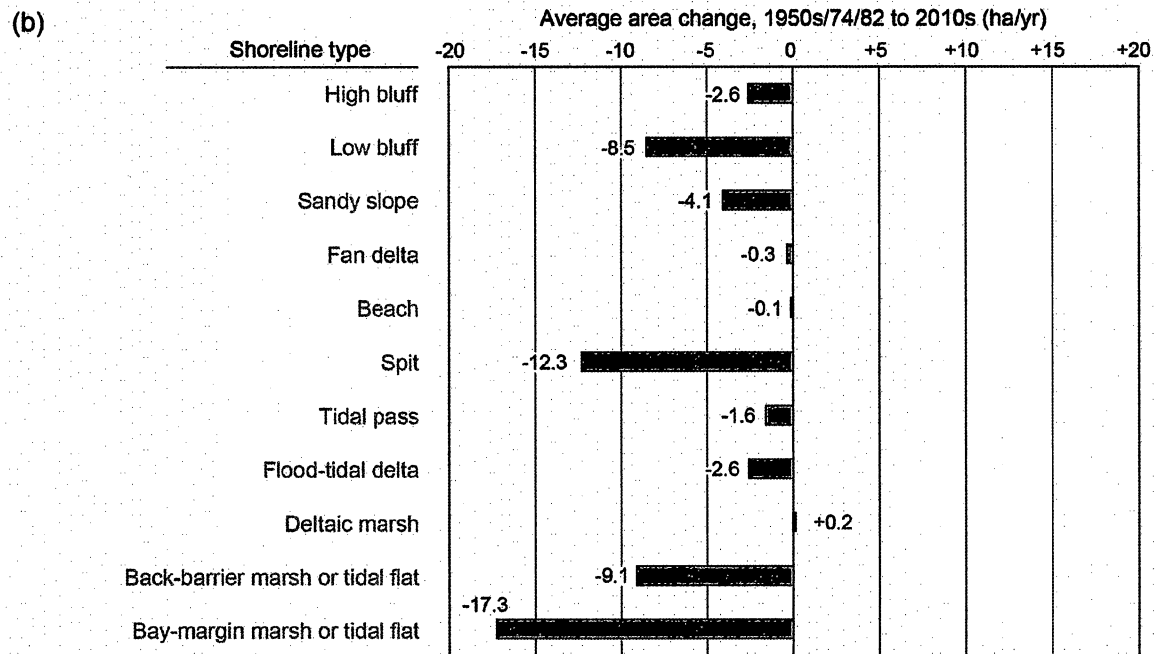
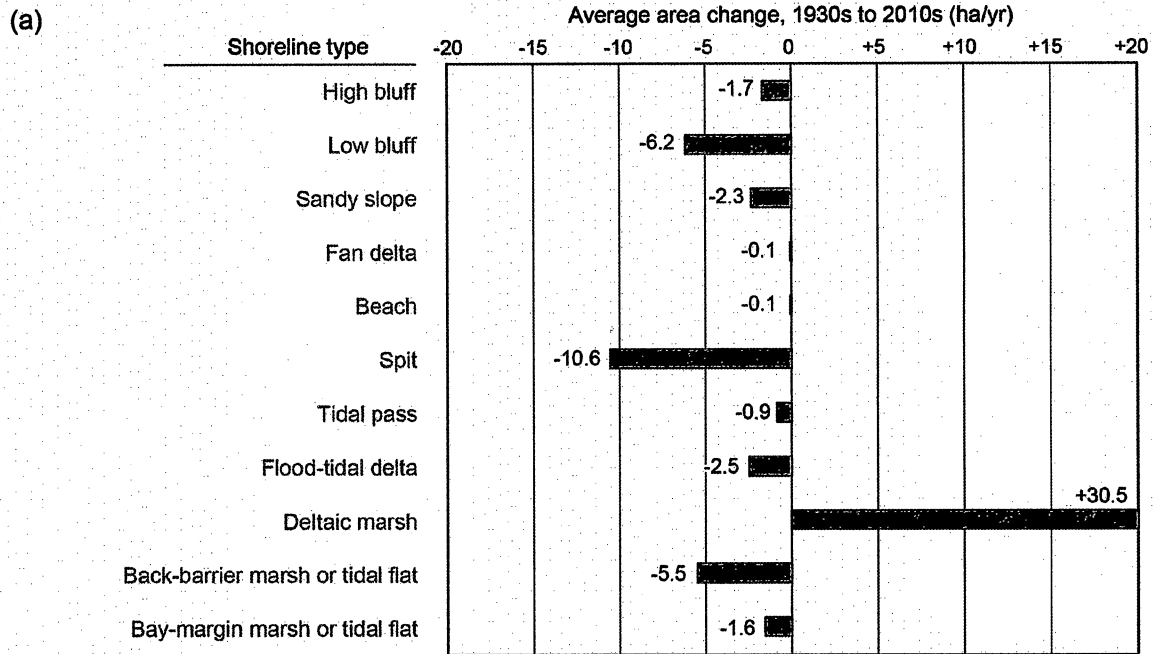


Figure 37. Average (a) long-term (1930s to 2010s) and (b) more recent (1950s/74/82 to 2010s) area change rate for common bay shoreline types (table 3) in the Copano, San Antonio, and Matagorda Bay systems.

(12.3 ha/yr, a nearly 20 percent increase), back-barrier marsh or tidal flats (9.1 ha/yr, a nearly 50 percent increase), and low bluffs (8.5 ha/yr, a more than 30 percent increase).

SHORELINE CLASSIFICATION BY EROSION SUSCEPTIBILITY

As discussed in the shoreline types and movement sections, the physical and environmental characteristics of the shorelines can be used to classify them by type (table 3) and to assess the relative susceptibility of the shoreline types to common causes of shoreline retreat in Texas bays, including relative sea-level rise, storm surge and storm waves, and non-storm wave activity.

Relative sea-level rise, which combines sea-level rise caused by ocean-water volume increases as well as land-surface subsidence, is in the range of a few millimeters per year. Shoreline types along low-elevation coastal lands, including along tidal passes, flood-tidal deltas, deltaic marshes, and back-barrier and bay-margin marsh and tidal flats, are most susceptible to retreat caused by relative sea-level rise (table 4, fig. 38). Shoreline types with slightly higher elevations landward of the shoreline (fan deltas, beaches, and spits) are moderately susceptible to potential retreat associated with relative sea-level rise. Shoreline types with relatively high elevations adjacent to the shoreline (high and low Pleistocene bluffs and sandy slopes) are relatively insensitive to short-term relative sea-level rise.

Elevated water levels and strong, storm-driven waves accompany the passage of tropical cyclones. Except near washover channels, rising water levels tend to flood low-elevation shoreline types before the storm makes landfall, which can reduce the impact of storm-driven waves on those bay shoreline types. Shorelines along deltaic marshes and back-barrier and bay-margin marshes and tidal flats have lower susceptibility to storm-related erosion than do shoreline along types with higher near-shoreline elevations. Shorelines along fan deltas, beaches, and spits are classified as moderately susceptible to storm surge and storm-driven waves.

Shorelines with higher elevations along the shoreline, including low and high bluffs and sandy slopes, are highly susceptible to erosion during tropical cyclone passage because storm-driven

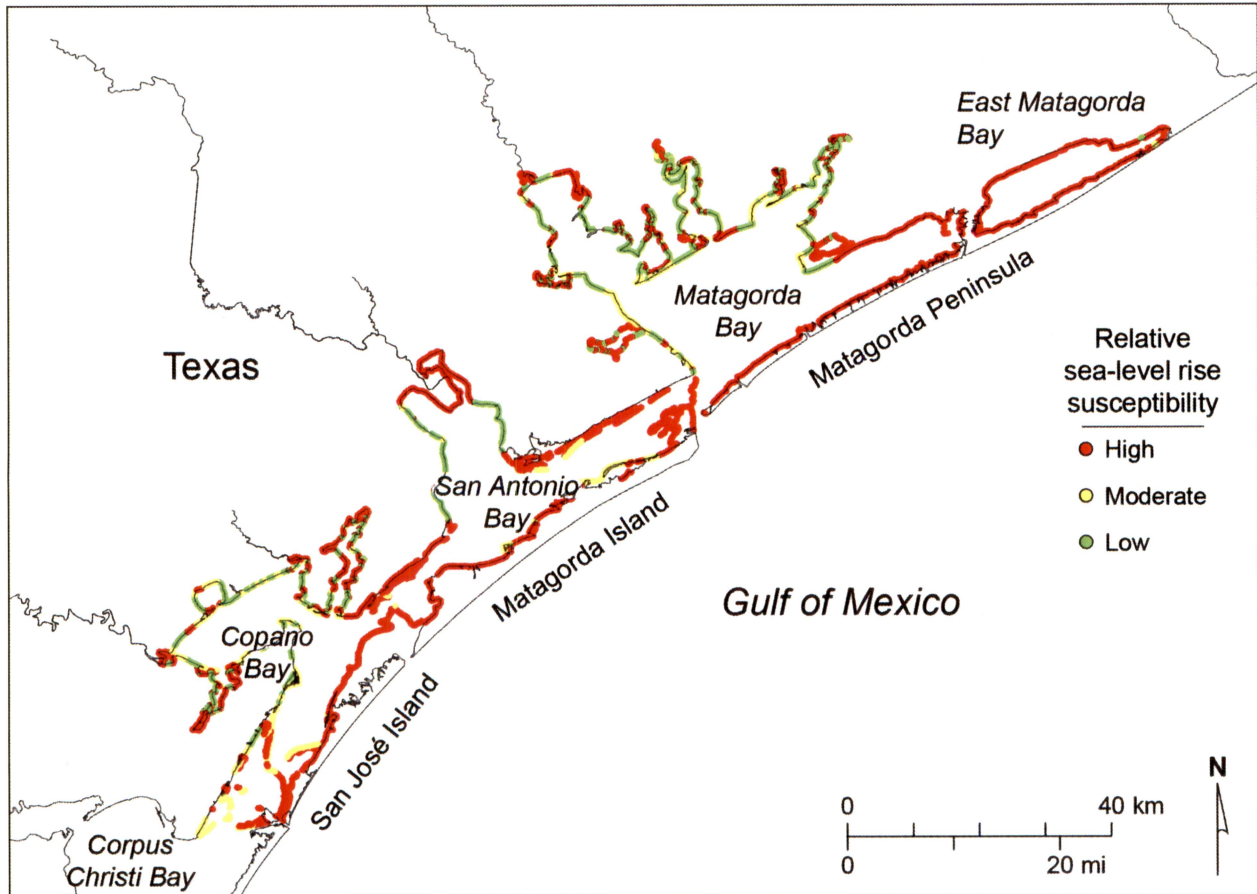


Figure 38. Shoreline types classified by susceptibility to retreat associated with relative sea-level rise.

waves can directly attack the higher-elevation bluffs and slopes and increase the likelihood of erosion and slope failure (table 4; fig. 39). Tidal passes and flood-tidal deltas are highly susceptible to reshaping during flood and ebb currents associated with storm passage.

Normal wave activity is probably the most significant agent of erosion along bay shorelines. All shoreline types are susceptible to wave action, but the higher-elevation shoreline types (high and low bluffs and sandy slopes) may be only moderately and indirectly susceptible to normal waves because the toe of the bluffs and slopes may be protected by narrow beaches, marshes, or tidal flats that absorb direct wave action. All shoreline types with lower elevations (fan delta, beach spit, tidal pass, flood-tidal delta, deltaic marsh, and back-barrier and bay-margin marsh and tidal flats) are highly susceptible to erosion from wave action (table 4; fig. 40).

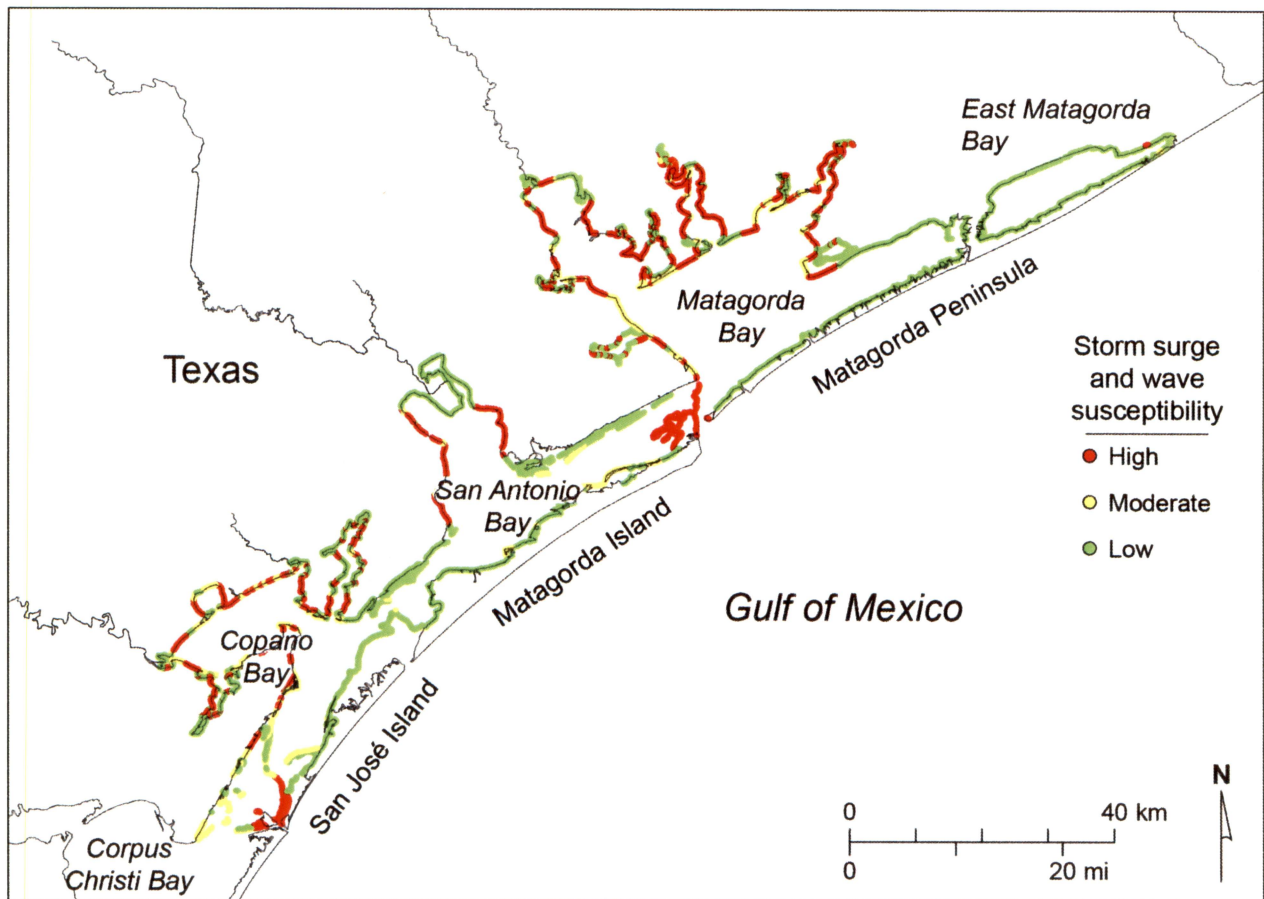


Figure 39. Shoreline types classified by susceptibility to erosion associated with storm surge and storm wave action.

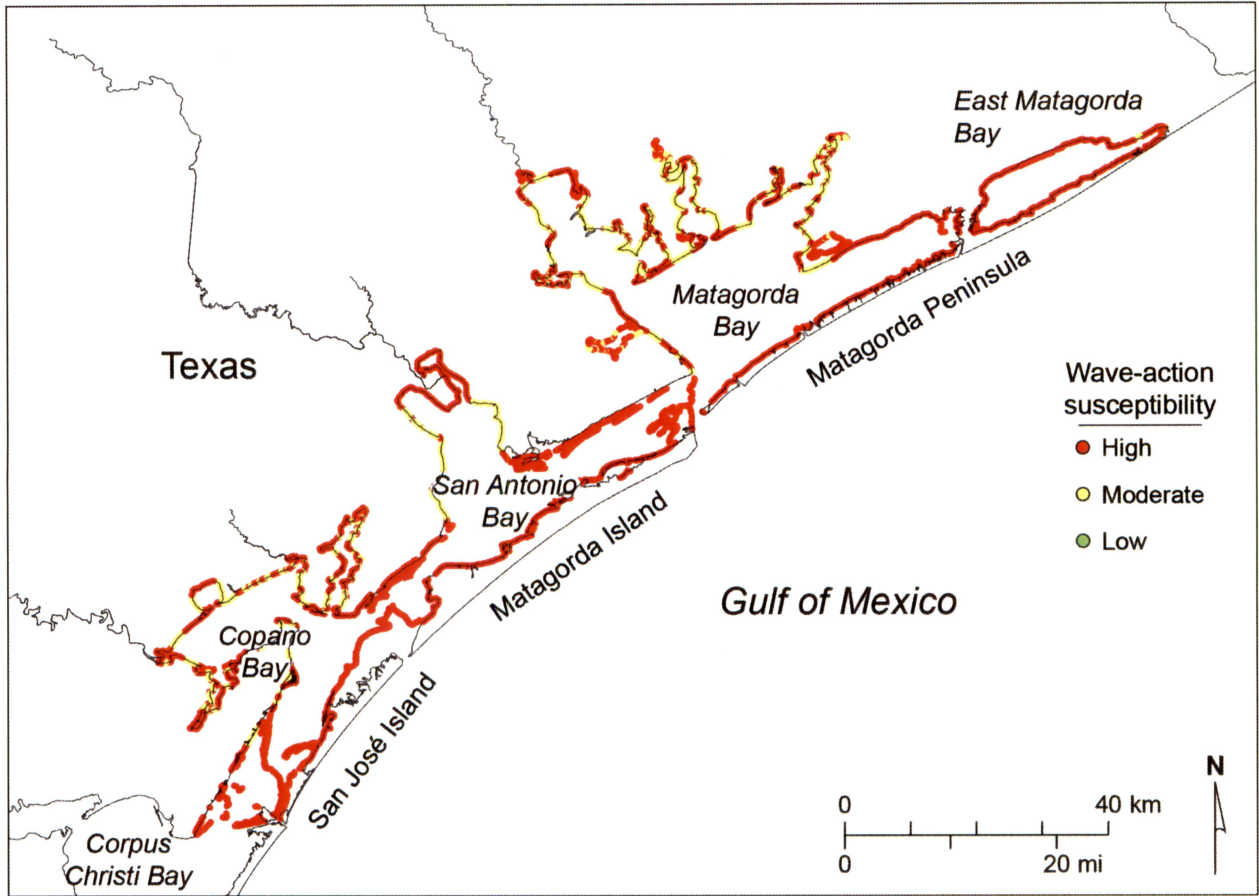


Figure 40. Shoreline types classified by susceptibility to retreat associated with wave action.

CONCLUSIONS

Airborne lidar surveys were flown over the Copano, San Antonio, and Matagorda Bay systems on the central Texas coast between 2013 and 2015 to characterize bay shoreline morphology and determine long-term (1930s to 2010s) and more recent (1950s or 1982 to 2010s) bay shoreline change rates. Shoreline proxies extracted from lidar DEMs at an elevation of 0.29 m NAVD88 were compared to past shoreline positions mapped on aerial photographs taken in 1930s, 1950s, and 1982. These comparisons indicated that long-term bay shoreline movement is dominantly erosional; nearly 80 percent of 9,696 measurement sites recorded shoreline retreat between the 1930s and the 2010s. Nevertheless, net land loss during this period was nearly zero owing to significant growth of the Colorado delta across eastern Matagorda Bay after a logjam on the river was cleared in 1929. Delta growth served to offset ubiquitous shoreline retreat elsewhere in the bay systems. More recently (1950s or 1982 to 2010s), shorelines in the central Texas coastal bays retreated at 82 percent of 9,845 measurement sites at an overall average rate of -0.6 m/yr. This rate yields a land-loss rate averaging 63.5 ha/yr. Average rates of retreat are similar for the bay systems, ranging from -0.49 to -0.64 m/yr.

Lidar data were used to identify and characterize 11 common shoreline types represented in each bay system and examine their relative susceptibility to shoreline retreat related to relative sea-level rise, storm surge and storm waves, and wave action. High and low bluffs and sandy slopes have low susceptibility to retreat related to short-term relative sea-level rise, moderate susceptibility to non-storm wave action, and high susceptibility to storm surge and waves. Fan deltas, sandy and shelly beaches, and sandy and shelly spits have high susceptibility to retreat by non-storm wave action and moderate susceptibility to storm surge and waves and relative sea-level rise. Shorelines along tidal passes, flood-tidal deltas, and back-barrier and bay-margin marshes and tidal flats are highly susceptible to retreat associated with relative sea-level rise and non-storm wave action. Susceptibility to retreat associated with storm waves is generally low for these types, but tidal-pass and flood-tidal delta shorelines are highly susceptible to movement

caused by flood and ebb currents associated with storm passage. Recent average rates of retreat along all shoreline types ranged from -0.52 to -1.67 m/yr. Shorelines along tidal passes, high bluffs, and spits retreated at the highest average rates.

ACKNOWLEDGMENTS

This project was supported in part by a financial assistance award from the U.S. Department of the Interior, U.S. Fish and Wildlife Service, Coastal Impact Assistance Program under CIAP award no. F12AF01039. The award was administered through grant no. 13-258-000-7485 from the General Land Office of Texas to the Bureau of Economic Geology, The University of Texas at Austin. Carly Vaughn and Carla Kartman (General Land Office) served as project managers. Thomas R. Calnan (U.S. Fish and Wildlife Service) served as project liaison. Jeffrey G. Paine and Tiffany Caudle (BEG) served as the principal and co-principal investigators. The views and conclusions contained in this document are those of the authors and should not be interpreted as representing the opinions or policies of the U.S. Government or the State of Texas. Mention of trade names or commercial products does not constitute their endorsement by the U.S. Government or the State of Texas.

REFERENCES

- Berg, R., 2015, Tropical Storm Bill (AL022015): National Oceanic and Atmospheric Administration, National Hurricane Center Tropical Cyclone Report, 31 p.
- Bureau of Economic Geology, 1992, Geology of Texas Map: The University of Texas at Austin, Bureau of Economic Geology, Map SM0002.
- McGowen, J. H., and Brewton, J. L., 1975, Historical changes and related coastal processes, Gulf and mainland shorelines, Matagorda Bay area, Texas: The University of Texas at Austin, Bureau of Economic Geology, 72 p.
- Morton, R. A., and Paine, J. G., 1984, Historical shoreline changes in Corpus Christi, Oso, and Nueces Bays, Texas Gulf Coast: The University of Texas at Austin, Bureau of Economic Geology Geological Circular 84-6, 66 p.
- Paine, J. G., and Morton, R. A., 1986, Historical shoreline changes in Trinity, Galveston, West, and East Bays, Texas Gulf Coast: The University of Texas at Austin, Bureau of Economic Geology Geological Circular 86-3, 58 p.
- Paine, J. G., and Morton, R. A., 1991, Historical shoreline changes in the Galveston Bay system,

in Shipley, F. S., and Kiesling, R. W., eds., Proceedings: Galveston Bay Characterization Workshop: The Galveston Bay National Estuary Program, Publication GBNEP-6, p. 165–167.

Paine, J. G., and Morton, R. A., 1993, Historical shoreline changes in Copano, Aransas, and Redfish Bays, Texas Gulf Coast: The University of Texas at Austin, Bureau of Economic Geology Geological Circular 93-1, 66 p.

Thieler, E. R., Himmelstoss, E. A., Zichichi, J. L., and Ergul, Ayhan, 2009, Digital Shoreline Analysis System (DSAS) version 4.0 — An ArcGIS extension for calculating shoreline change: U.S. Geological Survey Open-File Report 2008-1278.

White, W. A., and Morton, R. A., 1987, Historical shoreline changes in San Antonio, Espiritu Santo, and Mesquite Bays, Texas Gulf Coast: The University of Texas at Austin, Bureau of Economic Geology Geological Circular 87-1, 41 p.

Page intentionally blank

APPENDIX A: DATA SOURCES

Topographic surveys that were used to determine shoreline position.

Date	Map	Source
1856-1859	Matagorda Bay area maps	National Oceanic and Atmospheric Administration
1857	#644, Matagorda Island and the Shore of the SW End of Mataroda Bay	National Oceanic and Atmospheric Administration
1859	#766, Part of Espiritu Santo and San Antonio Bays and Vicinity	National Oceanic and Atmospheric Administration
1859	# 767, Part of San Antonio Bay and Vicinity	National Oceanic and Atmospheric Administration
1859	#1030, Part of Matagorda Island	National Oceanic and Atmospheric Administration
1860	#787, Second Chain to Long Reef	National Oceanic and Atmospheric Administration
1860	#828, St. Charles Bay/ San Antonio Bay	National Oceanic and Atmospheric Administration
1860-66	#823, From Aransas Pass eastward	National Oceanic and Atmospheric Administration
1861	#827, West end of Copano Bay and town of St. Mary's	National Oceanic and Atmospheric Administration
1861	#838, North part of Aransas Bay	National Oceanic and Atmospheric Administration

Aerial photographs that were used to determine shoreline position.

Date	Type	Source
November 1929 to April 1937	Black-and-white mosaics, 1:24,000	Tobin Research, Inc.
1956 to December 1957; January and December 1958	Black-and-white mosaics, 1:24,000	Tobin Research, Inc.
1974	Black-and-white mosaics, 1:24,000	Texas General Land Office
June and November 1974	Black-and-white stereo pair, 1:24,000	Texas General Land Office
November 1979	Color-infrared, 1:66,000	Environmental Protection Agency
June and July 1982	Color infrared mosaics, 1:24,000	Texas General Land Office
June to September 1982	Color infrared stereo pair, 1:24,000	Texas General Land Office

U.S. Geological Survey 7.5-minute quadrangle maps that were used to construct base maps.

Allyns Bight	Long Island	Port Lavaca East
Aransas Pass	Matagorda	Port Lavaca West
Austwell	Matagorda SW	Port O'Connor
Bayside	Mesquite Bay	Rockport
Blessing	Mission Bay	Sargent
Brown Cedar Cut	Mosquito Point	Seadrift
Caranchahua Pass	Olivia	Seadrift NE
Decros Point	Palacios	South of Palacios Point
Dressing Point	Palacios NE	St. Charles Bay
Estes	Palacios Point	St. Charles Bay SE
Kamey	Panther Point	St. Charles Bay SW
Keller Bay	Pass Cavallo SW	Tivoli SE
La Ward	Point Comfort	Tivoli SW
Lamar	Port Aransas	Turtle Bay
Lolita	Port Ingleside	

APPENDIX B: LIDAR DATA AND GIS FILES

Lidar Data

The CIAP Bays survey data are organized on a hard drive as follows:

2013_guad_delta	The Guadalupe Delta portion of San Antonio Bay
2013_sabay	San Antonio Bay
2014_copbay	Copano Bay
2015_mata14	Matagorda Bay (portion within UTM Zone 14)
2015_mata15	Matagorda Bay (portion within UTM Zone 15)
2016_matapranch	Powderhorn Ranch area west of Port O'Connor
index_maps	Index maps in shapefile format for the 6 survey areas listed above
merged_rasters	Merged 4-m-resolution rasters for each of the 6 survey areas listed above, and a single 10-m-resolution raster of all 3 bays.

Each of the folders—excluding `index_maps` and `merged_rasters`—contains 3 subfolders:

01_las: lidar point data in 1 x 1 km tiles in LAS 1.2 format

02_raster: bare earth DEMs in 1 x 1 km tiles in BIL format

03_metadata: metadata files for both LAS and BIL formatted data, above

The folder `merged_rasters` also contains a metadata subfolder.

GIS Files

Two ArcGIS shapefiles and one ArcGIS geodatabase are within a Map Package file called `gis_ciapBay_final.mpk`. Unpacking the document will extract the files listed below as well as open an ArcGIS project (`gis_ciapBay_final.mxd`) displaying the data.

rates_bays_1930s_2010s.shp and **rates_bays_1982_2010s.shp**

These files include measurement points (NAD83 decimal degrees), net movement and rates (in feet and meters), shoreline type, and susceptibility to retreat. We determined long-term net shoreline movement rate by comparing shoreline positions from the 1930s to those from the lidar surveys. We determined recent net shoreline movement rate by comparing shoreline positions from 1982 (1950s or 1974 in some cases) to those from the lidar surveys. The files contain ArcGIS point data that present long-term or recent shoreline change rates and associated

characteristics. Each point is located at the intersection of the lidar extracted shoreline and a shore-perpendicular transect that passes through the other shorelines included in the rate calculation. The key fields in this file are:

site: unique identifier indicating bay system, baseline number, and transect id for which a change rate has been calculated.

rate m/yr: the calculated rate of change determined from the 1930s (long-term) or 1982 (recent) and 2010s shoreline position in meters, averaged over the elapsed time. Negative values indicate shoreline retreat.

rate ft/yr: the calculated rate of change determined from the 1930s (long-term) or 1982 (recent) and 2010s shoreline position in feet, averaged over the elapsed time. Negative values indicate shoreline retreat.

change m: the total distance between the 1930s (long-term) or 1982 (recent) and 2010s shoreline position in meters. Negative values indicate shoreline retreat.

change ft: the total distance between the 1930s (long-term) or 1982 (recent) and 2010s shoreline position in feet. Negative values indicate shoreline retreat.

waterBody: the name of the water body adjacent to the shoreline

shoreType: shoreline type characterized by elevation, slope, depositional environment, material and consolidation level, and vegetation or habitat. The 11 types include: high bluff, low bluff, sandy slope, fan delta, beach, spit, tidal pass, flood-tidal delta, deltaic marsh, backbarrier marsh or tidal flat, and bay-margin marsh or tidal flat.

modType: type of human modification along the shoreline. These include: bulkhead, riprap, dredged, bridge, jetty, breakwater, groins, made land, and multiple combinations of the different modification types.

sus_rsl: shoreline type susceptibility to relative sea-level rise (low, moderate, or high).

sus_storm: shoreline type susceptibility to storm surge and waves (low, moderate, or high).

sus_waves: shoreline type susceptibility to non-storm wave action (low, moderate, or high).

Shorelines_web.gdb

Historical shoreline positions have been mapped from mid- to late-1800s topographic charts produced by the U.S. Coast Survey and mapped on 1:24,000-scale aerial photographs taken in the 1930s, 1950s, 1974, and 1982. A lidar-derived shoreline position (0.29 m above NAVD88) is extracted from the digital elevation models to represent the bay shoreline position. These shoreline positions for the three bay systems are provided in this geodatabase.

The geodatabase (shoreline_web.gdb) contains ArcGIS polyline data representing shoreline position from historical sources and lidar surveys. The key fields in this file are:

date: date of topographic chart, aerial photograph/ photomosaic, or lidar acquisition.

source: map=1800s topographic charts, aerial = photo or photomosaic, and lidar.